THESIS APPROVAL

GRADUATE SCHOOL, KASETSART UNIVERSITY

Master of Engineering (Civil Engineering)

DEGREE

Civil Engineering	Civil Engineering
FIELD	**DEPARTMENT**

TITLE: Effects of Water to Binder Ratio and Slag Fineness on the Properties of Slag Mortar

NAME: Mr. Muhammad Ilyas

THIS THESIS HAS BEEN ACCEPTED BY

THESIS ADVISOR

(Associate Professor Prasert Suwanvitaya, Ph.D.)

THESIS CO-ADVISOR

(Associate Professor Trakool Aramraks, Ph.D.)

DEPARTMENT HEAD

(Associate Professor Korchoke Chantawarangul, Ph.D.)

APPROVED BY THE GRADUATE SCHOOL ON _____

DEAN

(Associate Professor Gunjana Theeragool, D.Agr.)

THESIS

EFFECTS OF WATER TO BINDER RATIO AND SLAG FINENESS ON THE PROPERTIES OF SLAG MORTAR

MUHAMMAD ILYAS

A Thesis Submitted in Partial Fulfillment of

the Requirements for the Degree of

Master of Engineering (Civil Engineering)

Graduate School, Kasetsart University

2011

Muhammad Ilyas 2011: Effects of Water to Binder Ratio and Slag Fineness on the Properties of Slag Mortar. Master of Engineering (Civil Engineering), Major Field: Civil Engineering, Department of Civil Engineering.
Thesis Advisor: Associate Professor Prasert Suwanvitaya, Ph.D. 97 pages.

This research addresses the compressive strength and porosity when granulated blast-furnace slag (GBFS) was used as a supplementary cementitious material (SCM) to make mortar, and discusses in detail the parameters affecting the compressive strength and porosity of mortar cubes and pastes, respectively. The effects of fineness, water-binder ratio, replacement percentage, curing methods and age on the strength and porosity, and hydration products of mortars containing GBFS were studied. The cubes were conventionally-cured and steam-cured to correlate between curing methods and eventually their effects on compressive strength and porosity of mortars. The results showed that finer GBFS had the higher value of compressive strength and lower porosity when steam-cured ones. The increase in water-binder ratio reduced the strength and increased the porosity of mortars as expected.

_____ _____ __ / __ / __

Student's signature Thesis Advisor's signature

ACKNOWLEDGEMENTS

I am greatly indebted and grateful to my supervisor Dr. Prasert Suwanvitaya who provided me with the opportunity to work with him and guide me throughout my whole research. His impeccable guidance, continuous encouragement and great patience constituted into the most essential foundation of this thesis. I am also grateful to Dr. Trakool Aramraks for his useful suggestions and help throughout the development of this research thesis at the International Graduate Program of Civil Engineering, Kasetsart University.

I also appreciate the financial support from the Thailand International Development Cooperation Agency (TICA) who sponsored my research. Sincere thanks to the In-charge Research and Development Department, at the Pakistan Steel for extending all assistance during the procurement of granulated blast-furnace slag. Sincere thanks to the Chairman of Department of Civil Engineering, NED University of Engineering and Technology, Karachi, Pakistan for all of their assistance during the experimental work.

Finally, I owe the most to my family, especially to my parents for being the driving force, support and inspiration during my educational endeavors, continuously providing me their support and kind encouragement. Every small success of me is attributed to them and every compliment from them always adds to my strength for my aspirations.

Muhammad Ilyas

May, 2011

TABLE OF CONTENTS

Page

TABLE OF CONTENTS	i
LIST OF TABLES	ii
LIST OF FIGURES	iv
INTRODUCTION	1
OBJECTIVES	7
LITERATURE REVIEW	9
MATERIALS AND METHODS	26
Materials	26
Methods	29
RESULTS AND DISCUSSIONS	35
CONCLUSION AND RECOMMENDATIONS	54
Conclusion	54
Recommendations	55
LITERATURE CITED	56
APPENDIX	60
CURRICULUM VITAE	97

LIST OF TABLES

Table		Page
1	Suggested slag cement replacement level	2
2	Reduction in embodied energy, CO_2 emissions, and virgin material use in concrete using slag cement	5
3	Chemical composition of mineral phases in Portland cement clinker	10
4	Summery of standard specifications for cements produced in Pakistan	14
5	Effect of steam curing on strength of US Portland BFS cement and OPC	17
6	Categorization of pores in hardened Portland cement paste	21
7	Types of mild steel rods used in grinding on GBFS	27
8	Chemical properties of OPC and two types of GBFS	28
9	Sieve analysis of the selected sand	28
10	Mix proportioning of fresh mortar	30
11	Detail of testing program for the compressive strength of mortars	32
12	Physical properties of OPC and two types of GBFS	36
13	Results of compressive strength tests of control and GBFS-blended mortars	38
14	Porosity parameters for OPC and GBFS-blended pastes	43
15	Results of MIP parameters for OPC and GBFS-blended pastes	43
16	Data of OPC and GBFS-blended pastes with w/b ratio and curing methods	45

LIST OF TABLES (Continued)

Appendix Table		Page
1	Pore size distribution by volume – Intrusion for OPC normal curing	61
2	Pore size distribution by volume – Intrusion for OPC steam curing	67
3	Pore size distribution by volume – Intrusion for GS-30 normal curing	73
4	Pore size distribution by volume – Intrusion for GS-30 steam curing	79
5	Pore size distribution by volume – Intrusion for GS-50/2 normal curing	85
6	Pore size distribution by volume – Intrusion for GS-50/2 steam curing	91

LIST OF FIGURES

Figure		Page
1	Stages of ettringite formaion	11
2	Formation of hydration products in cement paste	12
3	Morphology of plate-like CH and fine bundles of CSH-I, CSH-II and ettringite needles	12
4	Mercury intrusion and extrusion hysteresis for OPC paste in moist curing	20
5	Pore size distribution differential curve	20
6	Types of capillary pores	23
7	Mercury intrusion and extrusion hysteresis	24
8	Gradation curve of sand with ASTM C33 limits	29
9	Steam curing regimes under the atmospheric pressure	32
10	Relationship between slag activity index and percentage replacement for both the fineness	36
11	Relationship between flow spread and water binder ratio of GBFS mortar for type 1 fineness	37
12	Relationship between flow spread and water binder ratio of GBFS mortar for type 2 fineness	37
13	Relationship between replacement percentage and water binder ratio for both the finenesses	38

LIST OF FIGURES (Continued)

Figure		Page
14	Relationship between compressive strength and percentage replacement of GBFS mortar cubes for type 1 fineness	39
15	Relationship between compressive strength and percentage replacement of GBFS mortar cubes for type 2 fineness	40
16	Relationship between compressive strength and age of GBFS mortar cubes for type 1 fineness	41
17	Relationship between compressive strength and age of GBFS mortar cubes for type 2 fineness	41
18	Relationship between pore diameter and incremental pore volume of OPC and GS-30/1 paste in conventional moist curing	46
19	Relationship between pore diameter and incremental pore volume. of OPC and GS-30/1 paste in steam curing	46
20	Relationship between pore diameter and incremental pore volume. of OPC and GS-50/2 paste in steam curing	47
21	Relationship between pore diameter and incremental pore volume. of GS-50/2 paste in normal curing and steam curing	47
22	Relationship between pore diameter and incremental pore volume. of GS-30/1 paste in conventional curing and steam curing	48

LIST OF FIGURES (Continued)

Figure		Page
23	Relationship between pore diameter and incremental pore volume. of OPC and GS-50/2 paste in conventional moist curing	48
24	Relationship between compressive strength and total porosity of all pastes	49
25	XRD pattern of OPC-NC paste at 7-day curing age	50
26	XRD pattern of OPC-AC paste at 7-day curing age	51
27	XRD pattern of GS-30/1-NC paste at 7-day curing age	51
28	XRD pattern of GS-30/1-AC paste at 7-day curing age	52
29	XRD pattern of GS-50/2-NC paste at 7-day curing age	52
30	XRD pattern of GS-50/2-AC paste at 7-day curing age	53

EFFECTS OF WATER TO BINDER RATIO AND SLAG FINENESS ON THE PROPERTIES OF SLAG MORTAR

INTRODUCTION

The dominant role of Portland cement is slowly decreasing in the favor of additives and composite cements. The future lies in the combinations of different binders into more durable and controllable systems thereby trying to making concrete less expensive.

The first recorded production of Portland blast-furnace slag cement dates back to 1892 in Germany and in 1896 in the US. Since its introduction in 1982, the production and marketing of granulated blast furnace slag (GBFS) has grown multifold in the United States. In Pakistan also since 1987, granulated blast furnace slag (GBFS) has been used as a supplementary cementitious material (SCM) in cement concrete (Hussain 1987). Presently there are quite a few cement producers in Karachi who are also producing ASTM Type I plus blast furnace slag (BFSC), alongside other types of cements.

Blast-furnace slag is produced when iron ore is reduced by coke at 1350-1550 °C in a blast-furnace. Main product of blast-furnace is molten iron, which is formed form iron ore, whereas the other components form a liquid slag. Liquid slag flowing on its way to the bottom of the furnace forms a layer above the molten iron, which is then separated and put for cooling by air or by water. 65 % of all the steel manufactured worldwide comes from the blast furnaces/LD converter while the remaining 35 % is produced by the electric furnace process. From three main categories of blast-furnace slag viz., granulated, pelletized and air-cooled, ground GBFS is the most valuable one due to its cementitious properties when mixed with lime, alkalis or Portland cement.

ASTM C 219-94 provides the following definition: ‘the glassy granular material formed when molten blast-furnace slag is rapidly chilled, as by immersion in water—with the following items under the heading of Discussion: Granulation may be achieved by quenching blast-furnace slag from its original molten state or by

quenching air-cooled blast-furnace slag after smelting. Also small percentage of silica and alumina may be added whilst the slag is molten to enhance desired characteristics.'

ASTM C989 provides the specification for granulated blast furnace slag wherein it specifies three grades as specified by their strength: grade 120, grade 100 and grade 80. Grade 120 provides the highest strength among these. ASTM C595 provides specification for the use of granulated blast furnace slag in blended cements either by intergrinding with Portland cement clinker or by blending Portland cement with granulated blast furnace slag (GBFS), or a combination of blending and intergrinding. The American Association of State Highway and Transportation Officials equivalent specification of the same name as ASTM is AASHTO M302, and ASTM C595 equivalent is AASHTO M240.

Granulated blast furnace slag (GBFS) typically replaces 25-70% Portland cement in concrete as per ASTM standards. Table 1 shows the replacement levels for various concrete applications suggested by the Slag Cement Association. The percentages basically show the replacement level of Portland cement by mass and are based on the historical performance. This means that a 50% replacement of each ton of Portland cement would result into a reduction of nearly 0.5 million tons of CO_2.

Table 1 Suggested slag cement replacement level.

Concrete Application	Slag Cement
Concrete Paving	25-50%
Exterior flatwork not exposed to deicer salts	25-50%
Exterior flatwork exposed to deicer salts with w/cm ≤ 0.45	25-50%
Interior flatwork	25-50%
Basement floors	25-50%
Footings	30-65%
Walls and columns	25-50%

Table 1 (Continued)

Concrete Application	Slag Cement
Tilt-up panels	25-50%
Prestressed concrete	20-50%
Precast concrete	20-50%
Concrete blocks	20-50%
Concrete pavers	20-50%
High strength concrete	25-50%
Alkali-silica reaction mitigation	25-70%
Sulfate resistance	
Type II Equivalence	25-50%
Type V Equivalence	50-65%
Lower permeability	25-65%
Marine exposure	25-70%
Mass concrete (heat mitigation)	50-80%

Source: Slag Cement Association (2002)

Ample research has been conducted which concludes that blast furnace slag can be used as a replacement for cement in concrete and mortar. Research conducted shows that up to 65% (by weight) of cement can be replaced by granulated blast furnace slag; thereby the construction industry can further benefit from its utility on a commercial scale in developing countries.

Blast furnace slag comprises of silicates, the alumina silicate of lime, a minor percentage of ferric and manganese oxide and sulfur. In terms of chemical composition, slag has the same oxides as Portland cement such as lime, silica and alumina but with different proportions. The typical percentage of blast furnace slag is as follows:

1. Calcium Oxide 36 - 40%
2. Silica 36 - 39%
3. Alumina 14 - 16%
4. Magnesium Oxide 9% max
5. Manganese Oxide 1.3% max
6. Sulfur 1.5% max

These days the cement along with other construction materials are becoming more and more expensive, out of the buying power of poor and middle-class citizens in Pakistan, and elsewhere in the world. As cement is the main expensive component of concrete and mortar generally, its partial replacement with pozzolan becomes reasonable for the low-cost housing schemes in the developing countries.

Prusinski *et al.* (2004) reported as part of a study that comparing the energy utilized in the production of a ton of Portland cement with a ton of slag cement (at least 70 % GBFS as replacement) showed 86 % reduction in energy when slag cement is to be produced. Similarly, 98 % reduction in CO_2 emissions and 93 % reduction in the utilization of virgin materials were reported. Table 2 shows the achievable percentage reductions on usage of 35 and 50% slag cement in all kinds of concrete from 3000 psi to 7500 psi strength, with virgin material reduced up to 15 %, energy up to 37 %, and CO_2 emissions up to 46 %.

From the environmental sustainability point of view, cement manufacturing is the next largest industrial producer of CO_2 after vehicle and utility emissions, and 50% of all industrial CO_2 emissions. In fact, 7.7 billion metric tonnes per year i.e., 88% of the carbon emissions come from fossil-fuels and cement industry combined. For every ton of cement manufactured in the industry, 1 to 1.25 tons of CO_2 are produced through the cement manufacturing. One of the solutions for minimizing the environmental effects of cement production is to use a supplementary cementitious material (SCM) in concrete.

Table 2 Reductions in embodied energy, CO_2 emissions, and virgin material use in concrete using slag cement.

Item	3000 psi ready mixed concrete		5000 psi ready mixed concrete		7500 psi ready mixed concrete		Concrete Block	
	35 % Slag	50 % Slag	35 % Slag	50 % Slag	35 % Slag	50 % Slag	35 % Slag	50 % Slag
Virgin material	4.80	6.80	6.80	9.80	10.30	14.60	4.30	6.30
Energy	21.10	30.20	23.50	33.70	25.70	36.50	19.90	28.60
CO_2 emissions	30.10	42.90	31.20	44.70	32.30	46.10	29.20	42.00

Source: Prusinski (2006)

The calcinations process has the following reaction:

$$CaCO_3 \text{ (limestone)} + \text{heat} \rightarrow CaO + CO_2 \text{ (gas)} \quad (1)$$

Statement of Problem

Roy et al. (1986), Binici et al. (2007) and Oner et al. (2007) have reported that the early-age compressive strength values of GBFS-blended concrete mixes are lower than the control mixes, but the long-term compressive strength of GBFS-blended cement concretes is higher than the control mixes. Slag cement is being used in private and state-owned massive construction projects across Pakistan like in the canals of Ghazi Barotha Hydropower Project, mainly due to its low heat of hydration property. However, in recent times its production has slowed down almost to a halt due to its lack of durability in aggressive environment (Khan, 2009). Therefore, the long-term strength parameter needs to be studied to check the ASTM C 989 criteria for strength activity index.

Temperature is a significant factor during a curing regime which enormously effects the strength development of mortar. In precast construction, sometimes the acceleration of strength development is intentionally desired so that the structural elements gain ample strength in order to sustain their self weight. Consequently formwork can be shifted to another location thereby improving the construction management. One of the ways of making this possible is by raising the temperature of the curing regime (Neville, 1997).

OBJECTIVES

The objectives of this study are as follows:

1. To determine the effect of grinding of GBFS on the strength and porosity of mortar.
2. To determine the effect of water-binder ratio on GBFS mortar for fixed workability.
3. To investigate the effect of partial replacement of cement with GBFS (20, 40, 60%) on the compressive strength of cubes with time.
4. To correlate between accelerated strength and strength gained at later age from conventional curing method.
5. To investigate the porosity parameters of pastes with and without GBFS using Mercury Intrusion Porosimetry (MIP).
6. To study the phase composition of the GBFS-blended cement mortar, and compare with control mix using the X-ray Diffraction (XRD) analysis.

Scope

Variables for fineness of GBFS were two i.e., two different fineness of GBFS achieved through grinding and measuring by ASTM C204 “Standard Test Method for Fineness of Hydraulic Cement by Air-Permeability Apparatus”, to study their individual effect on parameters of mortar. The workability of GBFS mortar was fixed as per ASTM C1437 “Standard Test Method for Flow of Hydraulic Cement Mortar” and ASTM C109/C 109M “Test Method for Compressive Strength of Hydraulic Cement Mortars (Using 2-in or [50-mm] Cube Specimens)” and the variable were water content. A relationship was made between flow value and water content to achieve the required workability. The number of mortar cubes was 135 in to two groups of curing method. The accelerated temperature curing and the conventional curing were applied to mortar cubes. Variables for the compressive strength is the partial replacement of GBFS and the cubes were tested for compressive strength on 3-

, 7-, 28- and 90-days. The porosity of pastes was studied using mercury intrusion porosimetry (MIP) method. A relationship was also developed between porosity and strength parameters showing the correlation of porosity with the strength of mortar with and without GBFS. X-ray diffraction method is used to study the phase composition of control mix and GBFS-blended mixes.

LITERATURE REVIEW

1. Hydration of Portland cement and slag

The chemical reactions of pure cement compounds have been mentioned clearly before by researchers (Odler *et al.,* 1981). Hydration of tricalcium silicate (C_3S) and dicalcium silicate (C_2S) produces calcium silicate hydrates, calcium hydroxide (CH) and heat:

$$2\,C_3S + 5.6H \rightarrow C_3S_2H_3 + 2.6CH \quad (2.1)$$

$$2\,C_2S + 3.6H \rightarrow C_3S_2H_3 + 0.6CH \quad (2.2)$$

Calcium silicate hydrate gel, the main hydration product, does not have a well-defined composition. The formula $C_3S_2H_3$ is denoted as C-S-H (C=CaO, A=Al_2O_3, S=Si_2O_3, H=H_2O). Tricalcium aluminate reacts with gypsum ($CaSO_4.2H_2O$; $C\bar{S}H_2$) in the presence of water to produce ettringite (AFt; $C_3A.3CaSO_4.32H_20$; $C_6A\bar{S}_3H_{32}$) and heat.

$$C_3A + 3C\bar{S}H_2 + 26H \rightarrow C_6A\bar{S}_3H_{32} \quad (2.3)$$

Ettringite (AFt) and monosulfate (AFm) are two groups of minerals that occur in cement. Ettringite crystallizes into hexagonal shape, as slender needles with a length up to 10 μm and 0.25 μm in diameter (Stutzman *et al.,* 2001). Once all the gypsum is consumed in reaction (2.3), the ettringite becomes unstable and reacts with the remaining tricalcium aluminate to form monosulfate aluminate hydrate.

$$2C_3A + C_6A\bar{S}_3H_{32} + 4H \rightarrow 3C_4A\bar{S}H_{12} \quad (2.4)$$

Monosulfate crystals are stable only in sulfate-deficient solution.

Ferrite reacts in two different reactions with gypsum. Firstly, ferrite reacts with gypsum and water to form ettringite, lime and alumina hydroxides.

$$C_4AF + 3C\bar{S}H_2 + 30H \rightarrow 3C_6(A,F)\bar{S}_3H_{32} + (A,F)H_3 + CH \quad (2.5)$$

Secondly, ferrite reacts with ettringite to form garnets.

$$C_4AF + C_6(A,F)\bar{S}_3H_{32} + 2CH + 23H \rightarrow 3C_4(A,F)\bar{S}H_{18} + (A,F)H_3 \qquad (2.6)$$

The GBFS when bended with ordinary Portland cement, after ground to the fineness comparable to Portland cement, the two ingredients hydrate at different rates. When water is added, Portland cement in the blended cement hydrates immediately, whereas a small amount of GBFS reacts may be due to gypsum in cement. The hydration of slag is greatly activated by alkalis and later by the Portlandite (CH) released by the hydration of Portland cement. Generally, GBFS hydration is far too low than clinker. After one year, the clinker hydrates about 90-100% whereas the GBFS has hydrated around only 45-75%. Reasons for GBFS's low reactivity are related to hydraulic modulus and fineness (Lumley *et al.,* 1996).

Table 3 Chemical composition of mineral phases in Portland cement clinker.

Formula	***Mass fraction (%)***	***Name***
C_3S	50-70	Alite
C_2S	15-30	Belite
C_3A	5-10	Aluminate
C_4AF	5-15	Ferrite

Source: Taylor (1997)

The main hydration products of pure slags consist of CSH, hydrotalcite (M_5AH_{13}; M=MgO), an iron-containing hydrogarnet, ettringite and some AFm phases. The composition of hydrotalcite is that of natural mineral M_6ACH_{12}. Pure hydrotalcite is difficult to distinguish in hardened cement paste as it is attached to CSH. AFm phases comprises of tetracalcium aluminate hydrate (C_4AH_{13}) and stratlingite (C_2ASH_8). If the aluminum content in slag is relatively low or the magnesium content is high, the AFm phases are not formed.

Hydration of GBFS-blended cement is much more complex than ordinary Portland cement due to the fact that two components hydrate simultaneously and interfere with each other. GBFS is activated by the alkalis and CH produced by the hydration of ordinary Portland cement and consumes a large amount of CH as well. The main hydration products of GBFS-blended cement consists of CSH, CH, hydrotalcite, ettringite, and tetracalcium aluminate hydrate.

Figure 1 Stages of ettringite formation (a) First stage: thin layer of ettringite is formed on C_3A grain, (b) second stage: Ettringite is directly formed on C_3A grain, (c) third stage: bursting of ettringite layer caused by pressure of crystallization, (d) fourth stage: bursting section is sealed by newly formed ettringite, (e) fifth stage: insufficient sulfate ions to allow formation of ettringite; on further hydration of the C_3A, ettringite converts to monosulfate.

Source: Soroka (1979).

CSH is the most plentiful hydration product whereas CH comes from the hydration of clinker and works together with GBFS hydration to increase the C/S ratio in CSH. The quantity of CH participating in GBFS hydration depends upon the blending proportions of GBFS in the cement. Increasing the GBFS proportions in the cement increases the proportions of CSH in the hydration products (Chen *et al.,* 2006).

$$\mathrm{OPC} + \mathrm{water} \rightarrow \mathrm{CSH} + \mathrm{CH\{NaOH|KOH\}} \qquad (2.7)$$

$$\text{GBFS} + \text{water} + \text{CH}\{\text{NaOH}|\text{KOH}\} \rightarrow \text{C} - \{\text{NaOH}|\text{KOH}\} - \text{S} - \text{H} \quad (2.8)$$

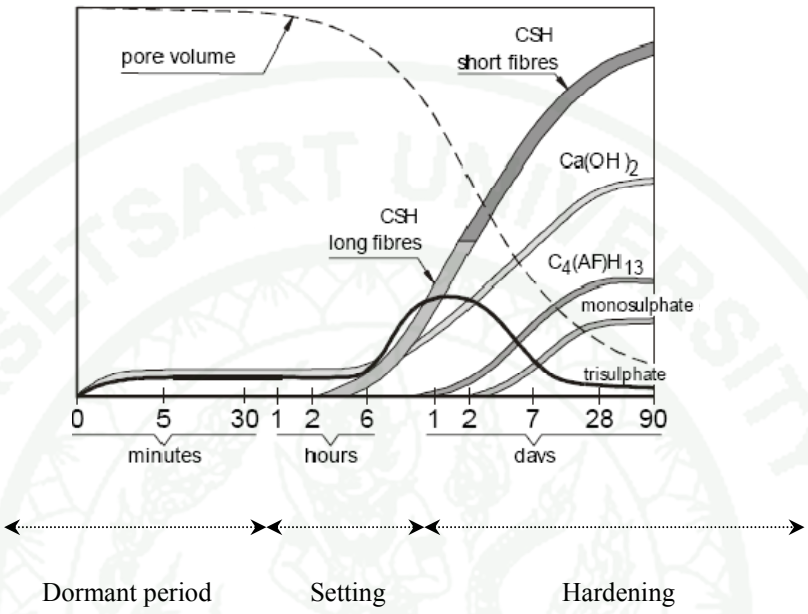

Figure 2 Formation of hydration products in cement paste

Source: Soroka (1979).

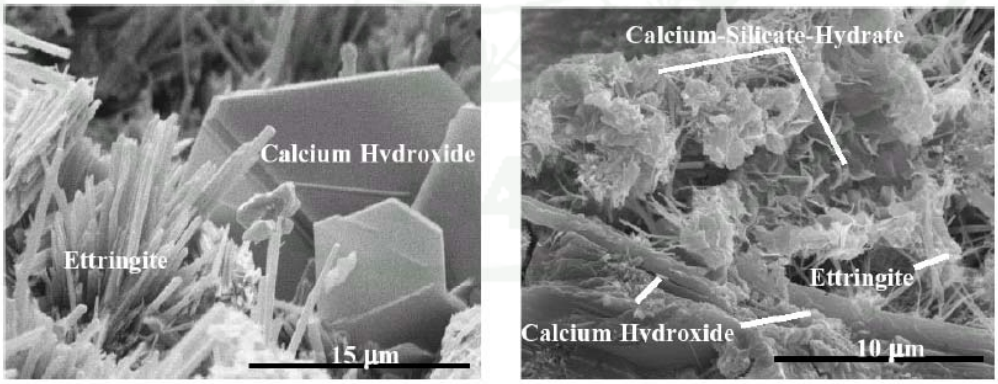

Figure 3 Morphology of plate-like CH and fine bundles of type I CSH, type II CSH, and ettringite needles.

Source: Stutzman (2001).

2. Chemical Analysis

The composition of slag for a wider range of steel-producing countries is: Silica (SiO_2), 27-42%; alumina (Al_2O_3), 5-33%; CaO, 30-50%; MgO, 0-21%. SiO_2 and Al_2O_3 in GBFS are associated with the ore or present in ash from the coke. The effect of Al_2O_3 content was reported to be very complex (Taylor 1997), and so from the analysis of western European GBFSs (Smolczyk 1978), showed that Al_2O_3 content above 13% has increased early-strength-effect but lower late strengths. MgO content up to 11% was quantitatively equivalent to CaO. The research from Wang et al. (2004) concluded that 15 % of Al_2O_3 content has a positive effect on the reactivity of GBFS, but should not be lower than 10.5% and CaO content at the same time should not be lower than 40% by mass. BS 6699 states a term 'chemical modulus' or 'reactivity index' $(CaO+MgO)/SiO_2$ should be greater than 1.0, which is also reported by Pal et al. (2003) at a maximum of 1.4. Chojnacki *et al.,* (1981) performed tests in Ontario, Canada which showed that low-alumina (7-8%) GBFS with 50:50 combination by mass with ASTM Type I Portland cement is equivalent in sulfate resistance to the ASTM Type V cement.

Loss on Ignition, or LOI, is the percentage of weight that is lost when cementitious material is heated at 950 ºC. The main sources of LOI in cement are water from gypsum ($CaSO_4.2H_2O$), and CO_2 from limestone ($CaCO_3$). LOI for ordinary Portland cement (ASTM Type I) is set at a maximum of 3%.

3. Grinding

GBFS varies widely in its grindability but usually it's harder to grind than Portland cement clinker. Ehrenberg (2003) investigated the grinding resistance of GBFS and compared with Portland cement clinker. The study comprises of various factors affecting the grindability of GBFS and reported the variability over a wide range, resulting into effects from the microstructure, the chemical composition and the storage and testing conditions. The factors that partly influence are melt history and the granulation conditions of the blast-furnace slag. GBFS is usually considered

to be hard during grinding procedure thereby utilizes more resources than other cements. Some consider the possibility of intergrinding the clinker with slag which produces cement which has coarser slag and finer clinker. Therefore separate grinding can be a better option over intergrinding. It is said by Swamy *et al.,* (1998) that grinding the GBFS in concrete two to three times finer than ordinary Portland cement would benefit in preserving the engineering properties such as bleeding, setting-time, heat evolution, high strength and excellent durability.

4. Compressive strength

The standard specification details shown in Table 4 describes the composition of all cement produced in Pakistan.

Table 4 Summary of Standard specifications for cements produced in Pakistan.

Description		Composition			Performance requirement	
Type	Symbol	Clinker + calcium sulfate	Slag %	Fly ash %	Vicat set, minutes	
					IST	FST
Ordinary Portland	P	100			45	600
High strength Portland	HSP	100			45	600
Rapid hardening	RHP	100			45	600
Sulfate resistant	SR-P (A)	100			45	600
	SR-P (B)	100			45	600
White cement	WC	100			45	600
Blast furnace slag	PBLF	≥35	≤65		45	600

Source: Young *et al,*. (2004).

The compressive strength of GGBFS initially was slow at 3-days but after 28-days curing, the strength increased and higher long-term strength was obtained as compared to normal PC concrete (Roy *et al.,* 1986). 20% finely granulated blast furnace slag can significantly increase the compressive strength of concrete after 3 days. Whereas combination of 10% finely ground fly ash and 10% finely granulated blast furnace slag can increase the compressive strength of concrete at all ages (Tan *et al.,* 1998).

The compressive strength of all mixes decrease with an increase in water-to-binder ratio at all ages. The mix with 30% GBFS achieve higher strength than the Portland cement concrete and 70% GBFS mix at all ages. The reason is that sufficient quantities of alkalies rapidly hydrated the relatively small quantity of the GBFS (Olorunsogo *et al.,* 1998).

The strength development of mortars incorporating GGBFS and Portland cement has variables such as replacement level of GGBFS in binder, water-binder ratio and curing temperature. The early age strength development of mortars containing GGBFS is highly dependent on curing temperature. Therefore GGBFS mortars usually gain strength more slowly than Portland cement mortars. But at higher temperatures, the gain in strength is much more rapid and significant (Barnett *et al.,* 2006).

It was observed that by increasing the GGBFS content, the water-binder ratio decreases for the same workability, thus GBFS has positive effects on workability. Also the early strength of GGBFS concretes is lower than the control concretes with the same binder content. But if the curing time is extended, the strength increase for the GGBFS concretes compared to control concretes was higher. The reason explained is the pozzolanic reaction is slow and the formation of calcium hydroxide requires time. The compressive strength of GGBFS concrete increases with increase in the GGBFS content up to an optimum level of 55-59 % (Oner *et al.,* 2007).The finer ground blended cements yield superior compressive strength and sulfate resistance than other cement types. The rate of increase of compressive strength of

blended cement is lower than Portland cement in the early ages but increases to higher level at later ages (Binici *et al.,* 2007).

5. Accelerated curing

The rise in the curing temperature accelerates the hydration process of concrete and increases the early strength without any adverse effects on its later strength. However, very high temperature may increase the early strength but introduces adverse effects on the later age strength (Neville, 1997).

The rate of increase of strength of concrete under the normal conditions are lethargic and slow therefore to avoid the production rate of concrete plants, it is beneficial to accelerate the hardening process using various methods available at hand. Accelerated curing by temperature has adverse effects on the chloride penetration resistance of concrete; therefore these negative effects can be mitigated using supplementary cementitious materials (SCM) in concrete (Hooton *et al.,* 2004).

Heat treatment cycle is a process of accelerated curing (steam curing) through temperature rise up to a benchmark temperature (60 ±5 °C) and then cooled down. The total duration of a usual heat cycle is 12-13 hours. The cycle starts with pretreatment of 2h at around room temperature (23 °C), which is called as the *delay period*, the aim of it is to allow the concrete to achieve the maximum early age strength. It is the time from the casting of concrete to its exposure to steam. After delay period, there is a gradual rise of temperature for 2h. Heating rate of this steam curing stage was 20 °C/h. Then there is a constant temperature zone which is named as treatment with duration of 8h. Afterwards cooling phase follows with one hour duration completing the heat cycle procedure. The relative humidity of the steam-curing box is above 90 % (Lui *et al.,* 2005). Another method of steam curing was adopted by Yazici *et al.,* (2009) for the investigation of mechanical properties of reactive powder concrete containing supplementary cementitious materials such as class-C fly ash and GGBFS. The heating rate for steam curing was 11 °C/h until reached to a maximum temperature of 100 °C for total duration of 3 days. Steam-curing does not affect the physical and chemical properties of the hydration products

of concrete. But some physical causes such as the coefficient of thermal expansion do affect the later-age strength of concrete causing micro-cracking in the paste and at the aggregate-paste interface. Therefore it is said that supplementary wet-curing can avoid these deficiencies and would enhance the later-age strength (Soroka *et al.,* 1978).

Comparison between OPC concrete and Portland BFS cement manufactured in the US shows the values for early-age and 28-days compressive strength in Table 5. Strength values from accelerated curing are similar to that of OPC for concrete w/c ratio of 0.42.

Table 5 Effect of steam curing on strength of US Portland BFS cement and OPC.

Curing	Cement	Compressive strength (MPa)		
		1 day	3 day	28 day
4h at 23 °C 16 h in steam at 71 °C, then at 23 °C	Portland BFS Cement	27.6	30.7	42.7
	OPC	25.5	27.9	39.3
23 °C	Portland BFS Cement	9.0	18.6	44.8
	OPC	10.0	23.1	44.8

Source: Lea (2003).

6. Porosity

Different parameters are used to characterize the pore structure of a cementitious material, of which some are elaborated below:

- Porosity
- Hydraulic radius

- Specific surface area
- Threshold diameter
- Pore size distribution (PSD).

Porosity is also a major component of microstructure study. Porosity is further subdivided into two classes: total porosity, and effective porosity as shown in figure 4. Total porosity is the ratio between the volume of pores and bulk volume of the material expressed as percentage.

$$\varepsilon = \frac{Vp}{Vb} \times 100$$

Where ε is the total porosity (%), Vp is the total volume of pores, Vb is the bilk volume of the material. For the case of MIP method, mercury density (ρHg) and helium density (ρHe) values are used to find porosity of a material.

$$\varepsilon = \left[1 - \frac{\rho Hg}{\rho He}\right] \times 100$$

In finer materials such as powders, interparticle porosity and intraparticle porosity constitute to the total porosity which can be as follows (Quantachrome 2009):

$$Interparticle\ porosity\ (\%) = \frac{Vv}{Vb} \times 100$$

$$Intraparticle\ porosity\ (\%) = \frac{Vt - Vv}{Vb} \times 100$$

$$Total\ (mercury\ intrusion)\ porosity\ (\%) = \frac{Vt}{Vb} \times 100$$

Where Vv is the volume of the mercury intruded up to the Interparticle Filling Limit, Vt is the volume of mercury intruded up to the maximum experimental pressure and Vb is the volume of the bulk sample.

Effective porosity is the fraction of pores with respect to the bulk volume of the material constituted only by open and interconnecting pores. Ye *et al.,* (2003) defined effective porosity as the volume of the mercury removed during the extrusion

process. If the mercury is pressurized second time after the extrusion, effective porosity can be obtained from the second intrusion curve of the pore size distribution. Effective porosity is always going to be less than or equal to the total porosity.

Porosity parameters by Mercury Intrusion Porosimetry (MIP):

Washburn equation (Washburn, 1921) is responsible for the elaboration of the relationship between pressure p (MPa) and the pore diameter d (μm) based on the assumption of cylindrical pores,

$$p = -\frac{4\gamma \times \cos\theta}{d}$$

Where γ is the surface tension of the mercury (mN/m) and θ (-) is the contact angle between the mercury and the pore surface of the cement. For cementitious material, Cook (1991) proposed the contact angle of 139º and the surface tension of 480 (N/m) for mercury for the intrusion process. These values were used in this study like many other studies.

The pore size distribution differential curve is obtained by taking the slope of the pore size distribution curve $dV/dlogd$ againstlog d as shown in the Figure 5. For cement paste, several peaks can be found from this curve, where these peaks represent the pore diameters corresponding to the higher rate of mercury intrusion per change in pressure.

Mode radius or mode diameter is the value where the greatest volume intruded/extruded occurred (Quantachrome operating manual 2009).

Cook et al. refers to these peaks as ‘threshold’, ‘critical’ or ‘percolation’ pore diameters. In cement pastes, the first peak corresponds to capillary porosity, 0.01 μm to 10 μm, whereas the second peak corresponds to the gel pore, 0.001 μm to 0.01 μm. These parameters are considered to be important and essential for the transport properties, such as permeability properties of the cement pastes.

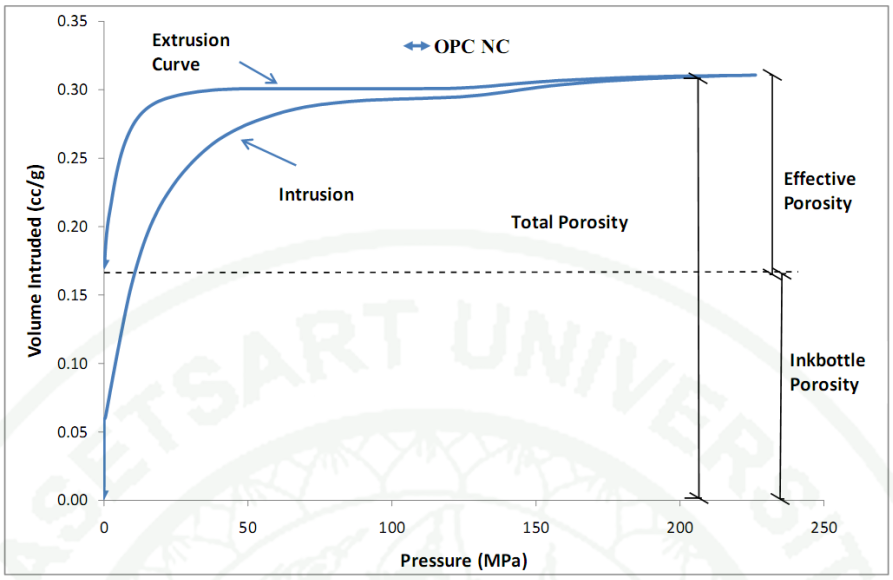

Figure 4 Mercury intrusion and extrusion hysteresis for OPC paste for moist curing.

Source: Ye (2003).

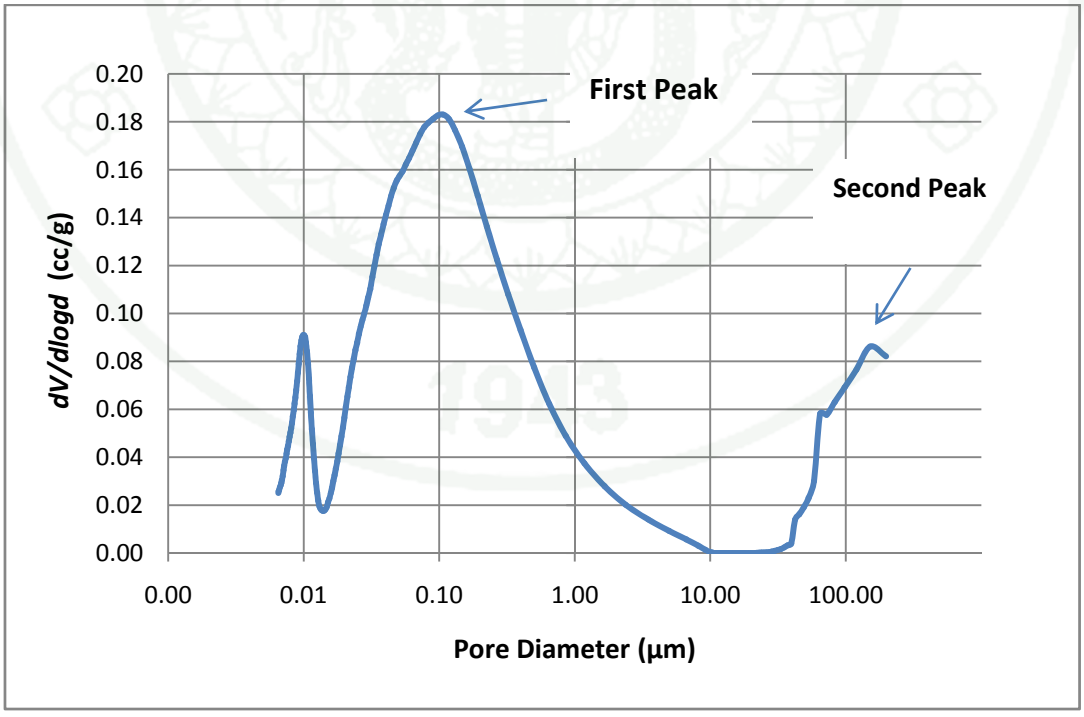

Figure 5 Pore size distribution differential curve.

Source: Ye (2003).

Generally it is accepted that capillary pores are the pores with diameter larger than 0.01 μm, and gel pores are the one with diameter smaller than 0.01 μm. As a matter of fact, in the early hydration stage, the capillary pores are well-connected and they are larger in diameter than the CSH gel pores.

With the advent of hydration, the capillary pores decrease in size and become partially connected. The second peak corresponds to the gel pores within the hydration products. With the increase in curing age, the hydration products blocks the capillary pores, therefore the mercury now has to flow through gel pores to reach the capillary pores. Threshold pore diameter was also explained by Winslow *et al.,* (1970) which said that threshold pore diameter is minimum diameter of channels that are continuous through the paste at a specific age.

Table 6 Categorization of pores in hardened Portland cement paste.

Categories	Sizes	Name	Role of water	Effect on concrete
Capillary pores	50nm – 10μm	Macropores	Behaves as bulk water	Permeability, diffusivity
	10 – 50 nm	Large mesopores	Small surface tension generated	Permeability in the absence of macropores, shrinkage above 80% RH
Gel pores	2.5 – 10 nm	Small mesopores	Large surface tension generated	Shrinkage between 80% RH and 50% RH
	0.5 – 2.5 nm	Micropores	Strongly adsorbed water	Shrinkage at all RH, creep
	Smaller than 0.5 nm	Interlayer spaces		

Source: Mindess *et al.,* (2003).

After the completion of hydration process in cement concrete, this “stone-like”, solid and porous material contains different aforementioned phases which are intermixed having structure to a micro-level (or nano-level) scale. This structure is generally called microstructure, and the time-dependent variation in microstructure due to continuous cement hydration is called microstructure development. The microstructure of cement paste develops when hydration products are formed, which is the solid phase, and pore structure is distributed as network, which is the pore phase.

C_3A is the most active phase during the first stage of hydration of cement paste. The volume of the pore phase decreases with the increase in the volume of the solid phase. The pore phase is classified in to two categories according to their sizes: gel pores and capillary pores. Table 6 shows the classification of pores as given by Mindess *et al.*, (2003) which lays down the vast ranges for different categories of pores.

This categorization is used in concrete technology but for a more general classification of pores in solids, International Union of Pure and Applied Chemistry (IUPAC) is officially referred which classifies as follows:

- Macropore have size larger than 50 nm
- Mesopore has size ranging from 2 to 50 nm
- Micropore has size less than 2 nm.

From the proposed terminologies and size ranges in various literatures, apparently there is no distinct terminology applied to the different sizes of the pores in cement paste. Furthermore, the division of sizes between capillary pores and gel pores are arbitrary due to the spectrum of pore sizes in cement paste is continues. Normally, it is assumed that the capillary pores are those remaining water-filled pores in saturated paste between the cement particles. Gel pores are those still existing in the hydration product CSH, thereby gel porosity being the part of CSH gel itself.

The interconnectivity of pores in cementitious material paste is important due to the fact that they contribute to the transport properties. Capillary pores are

classified by Ye *et al.,* (2003) into a continuous pore, continuous pore with inkbottle, dead-end pore with inkbottle or an isolated pore as shown in the Figure 6.

Isolated pores do not contribute to the transport properties and cannot be detected by mercury intrusion porosimetry. There are certain limitations to MIP measurements which can eventually affect the data interpretation, therefore needs caution. Pore shape which was said to be cylindrical are actually irregular, thereby pore volume becomes an important factor. Ink-bottle effect is that mercury must pass through the narrowest pores connecting the pore network.

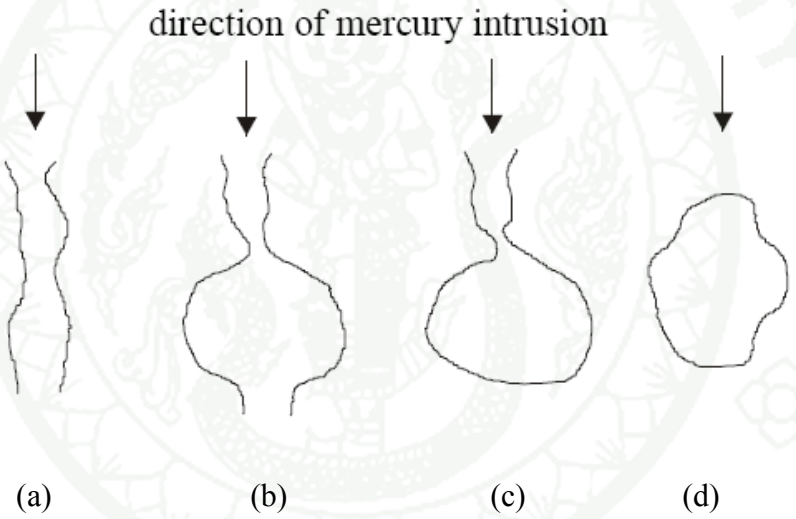

Figure 6 Types of capillary pores (a) Continuous pore, (b) continuous pore with inkbottle, (c) dead-end pore with ink-bottle, and (d) isolated pore.

Source: Ye (2003).

This irregular pore shape pattern causes an overestimation of pore volume due to different mercury intrusion pressure. Figure 7 shows the hysteresis for the whole MIP testing procedure, including first intrusion, extrusion and the second intrusion. Ye *et al.,* (2003) has reported that continuous pores and the inkbottle pores can be detected from the first intrusion curve and extrusion curve. Water must be removed from the samples before mercury pressure is applied during the MIP testing. The

reason for this is that water being present in the pores during mercury intrusion would provide inaccurate results on the porosity parameters. Prior to the MIP testing, the samples are treated with various drying procedures to remove water from the pores.

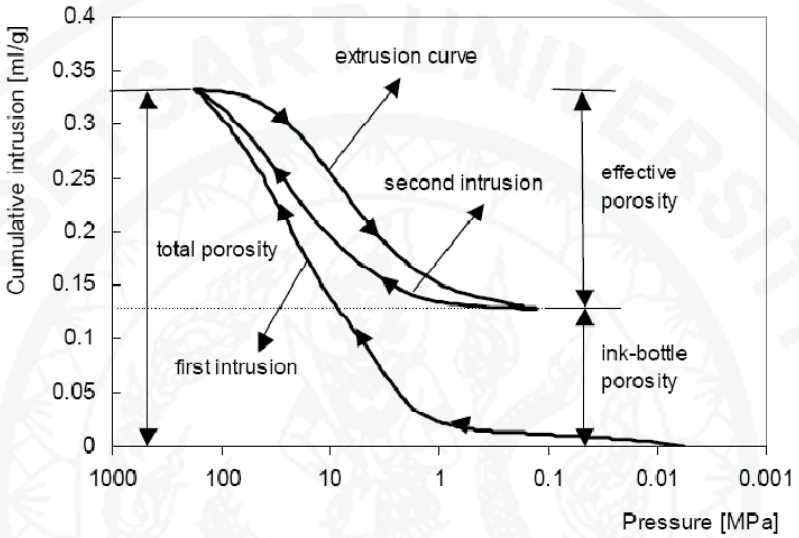

Figure 7 Mercury intrusion and extrusion hysteresis.

Source: (Ye, 2003).

One of the methods is oven-drying, in which the samples are oven-dried at 105 °C for 2-3 days. It is reported that a total porosity of 21% increase has been found by oven-drying, compared to vacuum-drying and freeze-drying for a cement paste with water cement ratio of 0.40 at a curing age of 28 days (Ye 2003). For freeze-drying, the samples are immersed in liquid nitrogen for 5 minutes at -195 °C. The low freezing process produces small ice microcrystals and prevents the growth of large ice microcrystals. After freezing, the samples are introduced in freeze-dryer in which the temperature is -40 °C and vacuum pressure is 10^{-1} Pa (Gale 2001).

Li *et al.,* (2006) performed a study on the relationship between porosity of cement paste with mineral additives and compressive strength of mortar based on this paste. It was accomplished that mineral additives delayed the process that the

micropore structure of the OPC paste developed. The porosity of OPC paste with GGBFS decreased after 28-days whereas the strength increased.

Pandey *et al.*, (2000) investigated the influence of mineral additives on the strength and porosity of Ordinary Portland Cement mortars. It was accomplished that the addition of GGBFS in OPC increased the total porosity of mortars during the early hydration period. The strength of mortars containing GGBFS decreased with the increase in porosity. At the age of 7 days, the pore size greater than 2000 A seems to affect the strength of mortars with fly ash and slag. Whereas 28- and 90-days strength depended on pores greater than 1000 A and 500 A, respectively. The total volume of pores smaller than 200 A at 90-days of hydration increased, indicating improvement in the hydration and strength of mortars incorporating GGBFS.

MATERIALS AND METHODS

Materials

1. Granulated Blast Furnace Slag

Granular Blast Furnace Slag (GBFS) was procured from Pakistan Steel Mills Corporation (PVT) LTD., Karachi, Pakistan which is the sole manufacturer of steel products in the country. Pakistan Steel comes under the Ministry of Industries and Production. It is located at 40 kilometers south east of Karachi and spreads over 75 square kilometers of main plant, township for employees and water reservoirs. It is Pakistan's largest industrial complex of the country with component units of more than 20. Pakistan Steel' production capacity is 1.10 million tonnes of steel expandable up to 3.0 million tonnes per year.

2. Preparation of GBFS

Grinding was done by using Los Angeles abrasion machine as per ASTM C131 – 03 "Standard Test Method for Resistance to Degradation of Small-Size Coarse Aggregate by Abrasion and Impact in the Los Angeles Machine" rotated at 35 rpm to get two different fineness of blast furnace slag, as fineness being a parameter in terms of cycles. Zain *et al.,* (2011) experimented with two types of rods (10 and 20-mm) for grinding burnt rice husk ash in Los Angeles machine. 5.0 kg specimen was placed in the drum of Los Angeles machine along with mild steel rods type D as shown in Table 7.

3. Chemical properties

Table 8 shows the chemical properties of ordinary Portland cement type-I and GBFS.

4. Fine Aggregate

Natural river sand (Malir Sand) was procured from the local market, washed, cleaned from the impurities, sieved for sieve analysis (ASTM C136) and used as fine aggregate for the mortar. The specific gravity of sand was 2.60; its fineness modulus

was 1.98, unit weight of 1511.98 kg/m^3 and water absorption of 1.01%. Table 9 and Figure 8 shows that the sand that was about to be used for mortar was finer than the upper limit of the ASTM C33. Therefore graded sand complying with the limits of ASTM C778 “Standard Specification for Standard Sand” was used in mortar.

5. Portland cement

Ordinary Portland cement (ASTM Type 1) was used throughout this study. The cement was manufactured by the Lucky Cement Company conforming to ASTM C150 – 04 “Standard Specification for Portland Cement”, and available in the local market.

6. Water

Water for the mixing and curing purpose was obtained from ordinary tap which was usually used for drinking and domestic purpose, free from the organic matters and acidic matter.

Table 7 Types of MS rods used in grinding GBFS.

	Types of rod used			
	A	B	C	D
Number	5	5	5	
Diameter (mm)	12	16	25	Combination of A, B and C.
Length (mm)	500	500	500	

Table 8 Chemical properties of OPC Type I and GBFS.

Chemical Properties	Ordinary Portland Cement Type I	GBFS
Major Components:		
Silica (SiO_2)	16.35	30.58
Alumina (Al_2O_3)	3.03	12.07
Lime (CaO)	67.42	38.10
Ferric Oxide (Fe_2O_3)	4.00	0.62
Magnesia (MgO)	1.94	5.79
Sulfur Trioxide (SO_3)	2.64	0.99
Loss on Ignition (LOI)	2.58	7.50
Minor Components:		
Potassium Oxide (K_2O)	0.85	0.59
Titanium oxide (TiO_2)	0.26	1.86
Sodium oxide(Na_2O)	0.15	0.42
Phosphorus pentaoxide(P_2O_5)	0.56	--

Table 9 Sieve analysis of the selected sand as per ASTM specification.

Sieve Size		Cumulative Passing (%)			Cumulative Retained (%)
No	(mm)	Lower Limit	Upper Limit	Malir Sand	
4	4.75	95	100	98.6	1.5
8	2.36	80	100	97.5	2.5
16	1.18	50	85	95	5
30	0.6	25	60	88.5	11.4
50	0.3	10	30	51.3	48.7
100	0.15	0	10	7.2	92.8

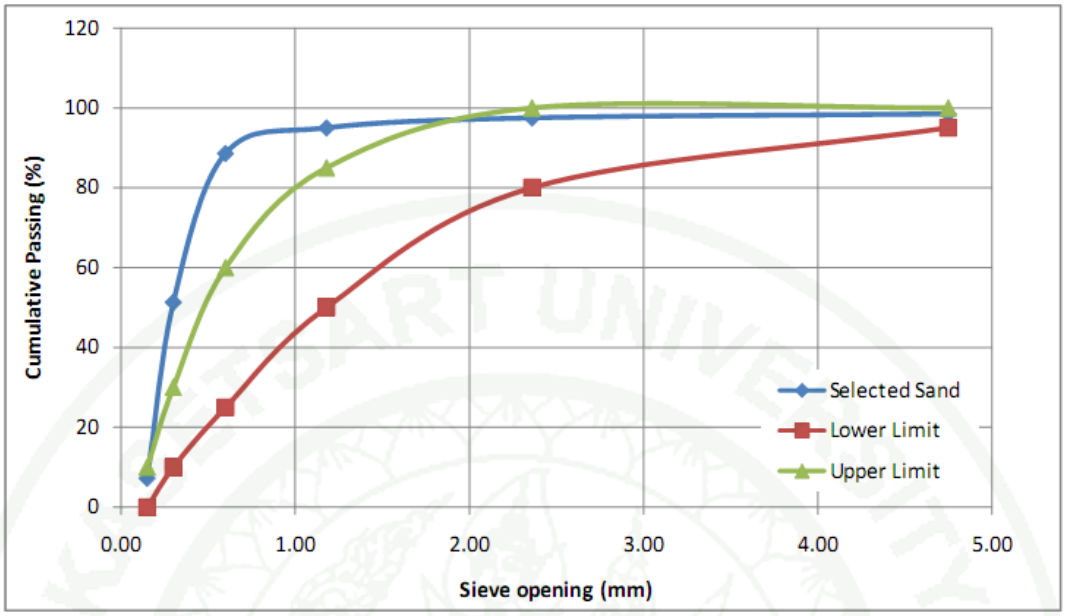

Figure 8 Gradation curve of sand with ASTM C33 limits.

Methods

Experimental Procedures

An experimental investigation was carried out to study the effects of several parameters on the strength and porosity of GBFS-blended mortars and pastes. The main parameters were fineness, water-binder ratio, percentage replacements of GBFS and curing methods. GBFS was used to partially replace with 30%, 40%, 50% and 60% by weight of cementitious materials. The replacement was achieved by blending GBFS together with ordinary Portland cement while mixing. All compressive strength tests were conducted as per ASTM C109/C 109M "Test Method for Compressive Strength of Hydraulic Cement Mortars (Using 2-in or [50-mm] Cube Specimens)". All specimens consisted of 1 part cementitious material and 2.75 parts of graded sand proportioned by weight. Water content for the mixes was varied to achieve constant flow ability at 110±5%. Trial mixes were made with varying dosage of water until the specified flow was achieved. The details of mix proportions are shown in Table 10.

Table 10 Mix proportioning of fresh mortar.

Symbol	Water (liters)	Cement (g)	GBFS (g)	Sand (g)	S/B (%)	W/B (%)
OPC	120	248	0	691	2.75	0.484
GS-30/1	155	174	74	691	2.75	0.625
GS-40/1	170	149	99	691	2.75	0.685
GS-50/1	170	124	124	691	2.75	0.685
GS-60/1	188	99	149	691	2.75	0.758
GS-30/2	146	174	74	691	2.75	0.589
GS-40/2	151	149	99	691	2.75	0.609
GS-50/2	153	124	124	691	2.75	0.617
GS-60/2	156	99	149	691	2.75	0.629

Two-inch or 50-mm specimen cubes were compacted by tamping in two layers and were casted for 24 hours, after which they were subjected to curing methods.

Determinations of the few physical and chemical requirements of GBFS were conducted in material laboratories of NED University of Engineering and Technology, Karachi, Pakistan. These included Blaine's fineness for GBFS. X-ray fluorescence spectrometry (XRF) for the chemical analysis of GBFS was conducted at the Pakistan Council for Scientific and Industrial Research (PCSIR) Laboratories Complex, Karachi. Physical requirement tests were conducted in accordance with ASTM C989-04 "Standard Specification for Ground Granulated Blast-Furnace Slag for Use in Concrete and Mortars". The X-ray diffraction (XRD) analysis and mercury intrusion porosimetry (MIP) for GBFS and pure cement pastes were conducted at the Thailand Institute of Scientific and Technological Research (TISTR), Bangkok, Thailand.

1. Flow Table

Water content of mortar containing granulated blast furnace slag was adjusted to give a flow of 110±5% determined by using flow table test as recommended in ASTM C230 "Specification for Flow Table for Use in Tests of

Hydraulic Cement". The flow of 110±5% is recommended in ASTM C109/C 109M "Test Method for Compressive Strength of Hydraulic Cement Mortars (Using 2-in or [50-mm] Cube Specimens)" for cements other than Portland or air-entraining Portland cements. Sand-binder ratio was fixed at 1:2.75 by weight. First the table was wiped clean and flow mold was placed at center. Then a layer of 1 inch mortar was placed in mold and tamped 20 times. Similarly successive layers were placed till mold was full and then the mold top was flushed with a trowel. The table was then dropped 25 times in 15 seconds and afterwards the diameter of mortar spread was measured from four scribed lines to record the flow value. The flowability of the mortar was expressed as a flow percentage of the spread diameter over the original bottom diameter of the sample.

2. Compressive Strength Tests

For compressive strength tests of mortars, Universal Testing Machine was used. GBFS was used to replace 30%, 40%, 50% and 60% by weight of the total cementitious materials. Mortars of size 50x50x50 mm molds were cast and covered with polyurethane sheet and damped cloth in 23 ± 2 °C chamber for 24 hours. Two curing conditions were used i.e., conventional moist curing (NC) and accelerated curing (AC - steam curing) with delay period of seven hours and three regimes i.e., initial curing with increasing temperature, constant regime and decreasing temperature. The compressive strength tests (ASTM C 109) were conducted at the age of 3-, 7-, 28- and 90-days for conventional moist-curing, whereas for accelerated curing, the compressive strength test was performed after the specified period for accelerated curing.

3. Accelerated Curing/Steam Curing

Specimens were exposed to accelerated curing conditions to develop a significant portion of their ultimate strength. The delay period of seven (07) hours was applied before the specimens were de-molded from their molds. Time period for initial curing with gradual increasing temperature for 3 hours (25 °C/h); to a maximum 100 °C temperature was kept constant for 4 hours; then there was gradual

decrease in temperature to 23 °C temperature within 3 hours (Figure 9). Relative humidity was held constant at 100% throughout the procedure.

Table 11 Detail of Testing Program for the Compressive Strength of Mortars.

Type	Blaine's fineness (m^2/kg)	Replacement level (%)	Number of 50 mm cube specimens				Steam Cured at 100 °C
			Normal Curing Conditions 23 °C				
			3 days	7 days	28 days	90 days	
OPC	304	0	3	3	3	3	3
	217	30	3	3	3	3	3
		40	3	3	3	3	3
		50	3	3	3	3	3
GBFS		60	3	3	3	3	3
	386	30	3	3	3	3	3
		40	3	3	3	3	3
		50	3	3	3	3	3
		60	3	3	3	3	3

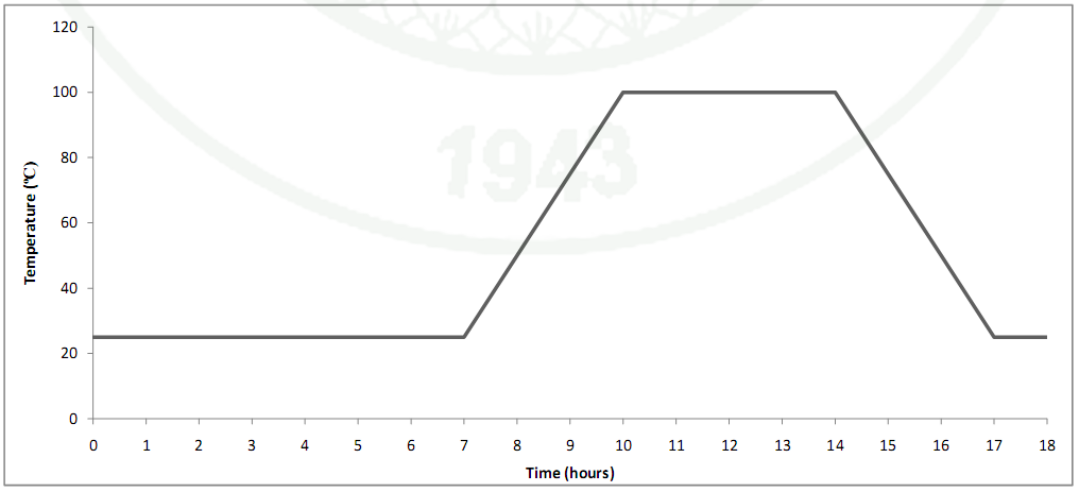

Figure 9 Steam-curing regimes under the atmospheric pressure.

Source: Soroka (1979).

4. Mercury Intrusion Porosimetry (MIP)

The control and GBFS-blended pastes were prepared from the same water binder ratio as in the case of cementitious mortars for the compressive strength tests. For the measurement of pore size distribution (PSD) of paste, mercury intrusion porosimetry (MIP) was carried out with a low pressure range from 1.5 to 55 psi (for large pore size), and high pressure range from 55 to 33,000 psi (for small pore size), capable of measuring pore diameter down to 0.0065 micron. The contact angle of 140º and surface tension of 485 mN/m were assumed. The hardened pastes moist-cured up to 7 days were carefully broken with a clean hammer, taking representative sample of 5mm pieces from the middle of the specimen. The samples were dried at 110 ºC for 1 hour in the oven before being introduced into porosimeter. MIP study is expressed by Washburn equation (Washburn 1921).

The weight of the sample usually varies according to the machine, 60-90% of penetrometer stem volume is proposed by Ye (2003) whereas 50-80% of penetrometer stem volume is suggested in the Quantachrome PoreMaster-33 Operating Manual. The sample was introduced in to the chamber where the sample was surrounded by mercury, and the pressure was applied and increased gradually on the mercury. Mercury was forced to enter the pores of the sample as the pressure was increased, and if there were continuous pores, a pressure would be achieved at which the mercury can penetrate the whole pore-network of the sample. On the other hand, if there were inkbottle pores or isolated pores, mercury might penetrate through the pore walls of the sample volume.

5. X-ray Diffraction

X-ray diffraction was performed on the cementitious pastes for the structural and phase composition studies. XRD analysis was also used to study the hydration of GBFS-blended cement mortar with two curing methods as described in the scope of the study. XRD analysis of the pastes where carried out with Shimadzu XRD-6000 for the investigation of hydration process in both control and GBFS-blended pastes. After the samples were prepared in the same manner as MIP

investigation, except after crushing, the samples were passed from sieve No. 50. XRD was performed on the pastes containing various partial replacement levels of GBFS at 7-days conventional curing and steam curing. The samples were broken from the paste with the help of clean hammer and their size was not exceeding 1 cm^3.

RESULTS AND DISCUSSIONS

The experimental results are organized and presented in the subsequent sections as follows. All the tests were conducted in accordance with the relevant ASTM standards as mentioned in the previous section.

1. Slag Activity Index

Few physical requirements of OPC and two types of GBFS are shown in the Table 12. Type-2 GBFS is finer than the OPC whereas the OPC is finer than the type-I GBFS. The coarser type-1 GBFS eventually shows more water requirement which caused the strength to reduce and porosity to increase. On the contrary, type 2 GBFS is finer which means the water requirement reduces and thus increases the strength. Slag Activity Indexes as:

$$Slag\ activity\ index, \% = \left(\frac{SP}{P}\right) X\ 100$$

Where,

SP = average compressive strength of slag-reference cement mortar cubes at designated ages, MPa (psi),

P = average compressive strength of reference cement mortar cubes at designated age, MPa (psi).

Slag activity indexes of both types of GBFS are tabulated in Figure 10 and Table 12, and compared with the limits of ASTM specification. The slag activity indexes of both GBFS were lower than the ASTM limits, and therefore failed to meet the requirements. The reference cement used to test slag activity has 28-day strength of 25 MPa which was lower than 35 MPa, the requirement of ASTM C 989 specification.

2. Workability

Figure 11 shows the relationship between flow spread (%) from the Flow Table Test against the water-binder ratio for the GBFS-blended mortars of type 1 fineness. Figure 11 and Figure 12 show that by increasing the water-binder ratio, the flow spread (%) increased.

Table 12 Physical requirements of OPC and two types of GBFS as per ASTM C989.

Physical Properties	Ordinary Portland Cement Type I	GBFS-1	GBFS-2	ASTM C 989
Blaine's Fineness (m^2/kg)	304	217	386	--
Slag Activity Index with Portland Cement, at 7 days (%)	--	24	24	--
Grade 80				70
Grade 100				90
Grade 120				
At 28 days (%)	--	34	53	
Grade 80				70
Grade 100				90
Grade 120				110

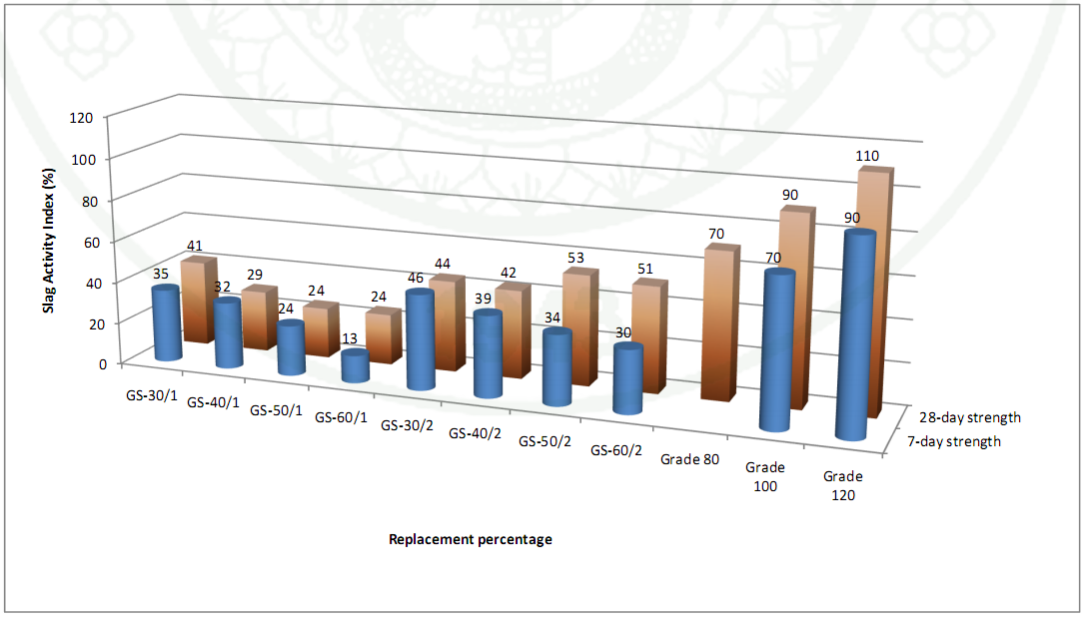

Figure 10 Relationship between Slag activity index and replacement percentage for both the finenesses.

Also it was observed that on increasing the replacement level the water demand increased thereby consequently affected the strength and porosity parameters.

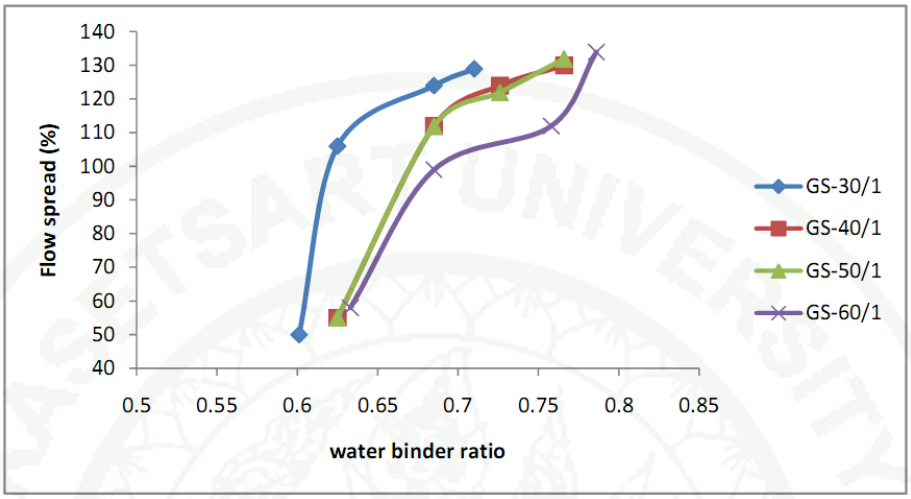

Figure 11 Relationship between flow spread and. water-binder ratio of GBFS mortar for type 1 finenesses.

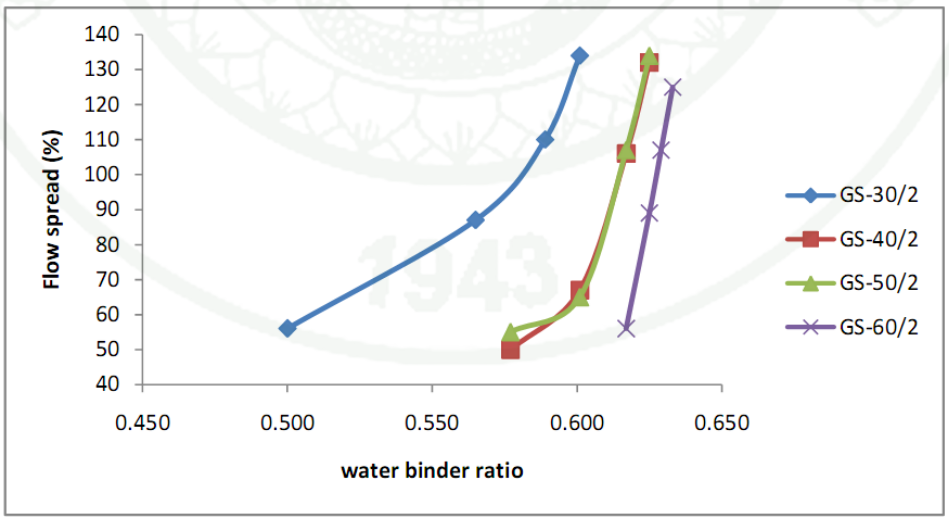

Figure 12 Relationship between flow spread and. water-binder ratio of GBFS mortar for type 2 finenesses.

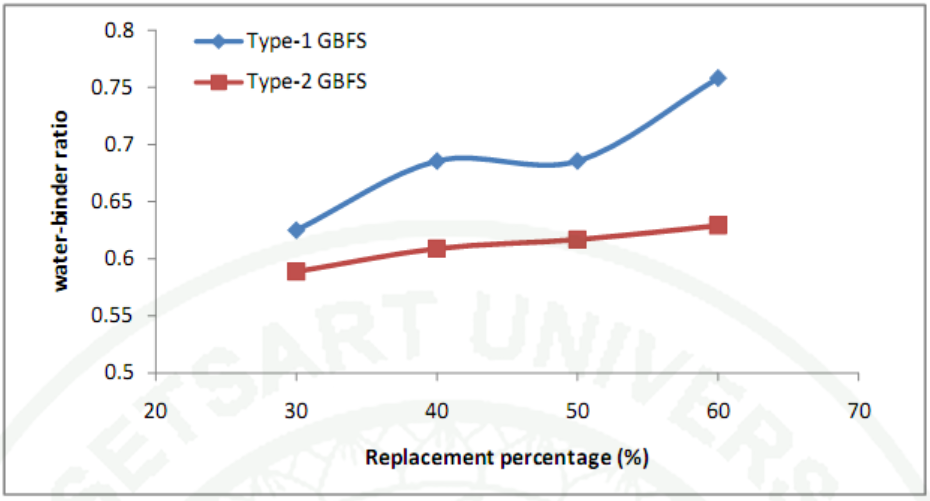

Figure 13 Relationship between replacement percentage and water-binder ratio for both the finenesses.

3. Compressive Strength

The results of the compressive strength tests of conventional curing and accelerated curing (steam curing) GBFS are presented in Table 13, Figure 14 and Figure 15. The unexpected increase in the 90-day strength of OPC specimen was observed. It was observed that the finer the cementitious material, the higher the compressive strength of mortars.

Table 13 Results of compressive strength tests of control and GBFS-blended mortars.

Symbol	W/B	Conventional Curing (23 ºC) (MPa)				Steam Curing (100 ºC) (MPa)
		3 days	7 days	28 days	90 days	
OPC	0.485	19.24	21.48	24.88	57.28	6.38
GS-30/1	0.625	6.92	7.58	10.23	27.58	3.97
GS-40/1	0.685	6.59	6.89	7.30	25.13	4.90
GS-50/1	0.685	4.87	5.18	6.03	23.95	4.91
GS-60/1	0.758	2.32	2.82	6.07	13.08	2.03
GS-30/2	0.588	9.31	9.79	10.89	39.12	8.54
GS-40/2	0.600	8.08	8.38	10.56	42.38	12.04

Table 13 (Continued)

Symbol	W/B	Conventional Curing (23 ºC) (MPa)				Steam Curing (100 ºC) (MPa)
		3 days	7 days	28 days	90 days	
GS-50/2	0.617	6.14	7.21	13.18	39.14	13.49
GS-60/2	0.629	5.73	6.47	12.62	41.58	13.90

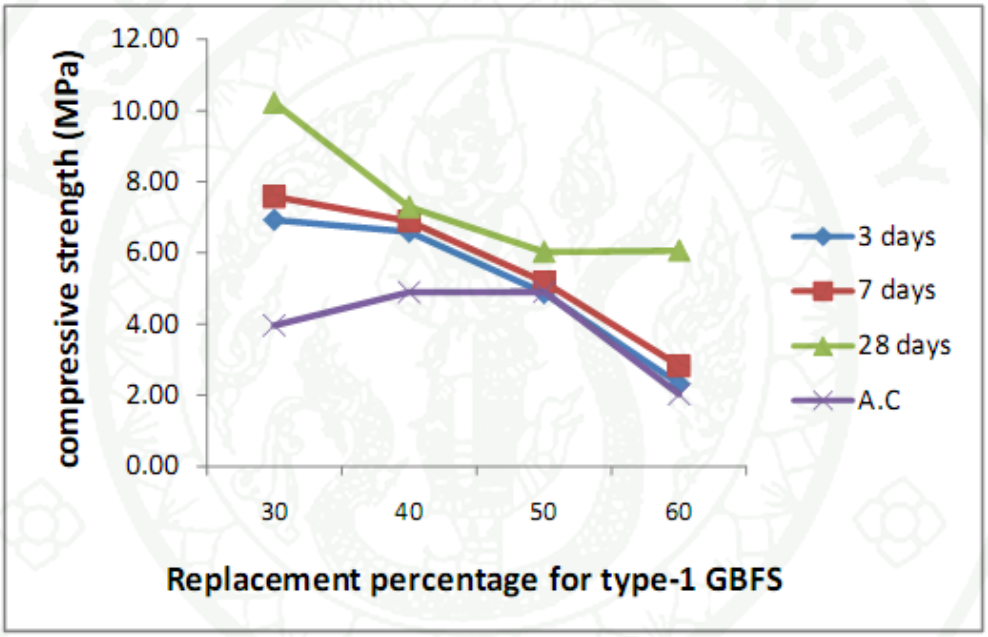

Figure 14 Relationship between compressive strength and % replacement of GBFS mortar cubes for type 1 finenesses.

As the replacement level was increased, the compressive strength gradually decreased for the conventional curing method. But in case of steam curing method for type 2 fineness, the compressive strength was shown to increase with the increase in replacement level.

.It was reported by Neville et al. (1995) that steam curing of concrete containing GBFS could be used at higher temperature to avoid the harmful effects of long-term strength and permeability. Steam curing was also useful where early

strength gain in concrete was essential or in cold weather where additional heat was required to achieve the hydration process. Figure 15 indicated that the steam curing in the case of finer GBFS (386 m^2/kg) accelerated the hydration process and helped in the completion of hydration reaction and gain in early strength.

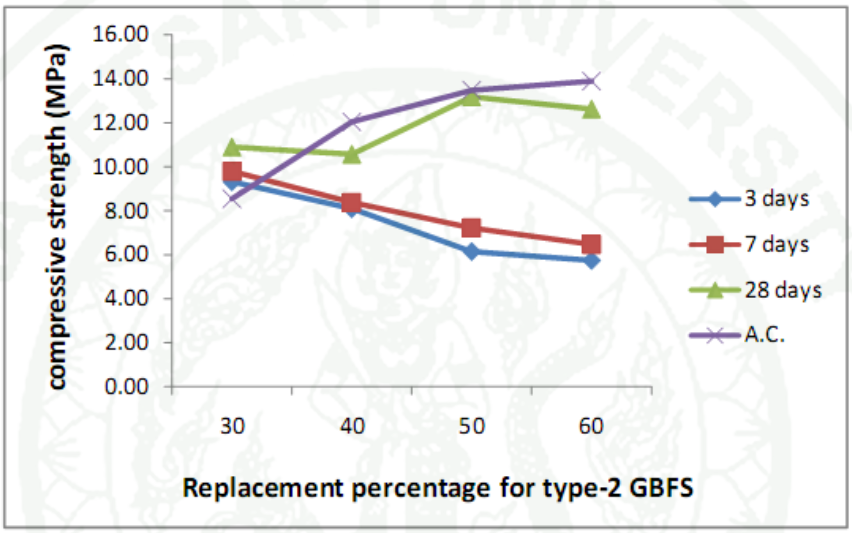

Figure 15 Relationship between compressive strength and % replacement of GBFS mortar cubes for type 2 fineness.

In Figure 16 and 17 the relationships between compressive strength and age of the control and GBFS-blended mortar were shown. The compressive strength of control mix at 28-day was 25 MPa which should be a minimum of 35 MPa as per ASTM C989, whereas the compressive strength of various GBFS-blended mortars at 28-day varied from 6.03 MPa for GS-50/1 being a minimum to a maximum of 13.18 MPa for GS-50/2. Similarly, in the case of 90-days compressive strength, the values had increased substantially but the compressive strength of control mix was still much higher than any of the GBFS-blended mortar, which was unexpected. For 90-day strength, the maximum value was 27.58 MPa for GS-30/1 for type 1 fineness and 42.38 MPa for type 2 fineness.

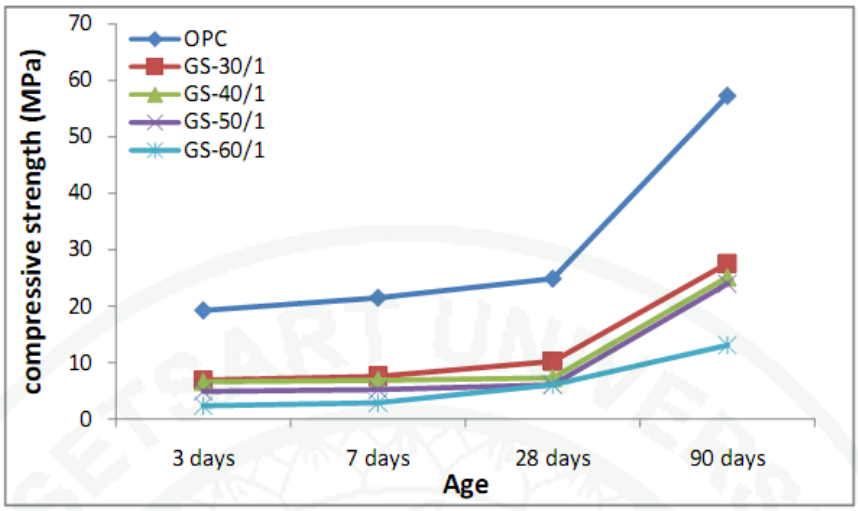

Figure 16 Compressive strength vs. Age of GBFS mortar cubes for type 1 fineness.

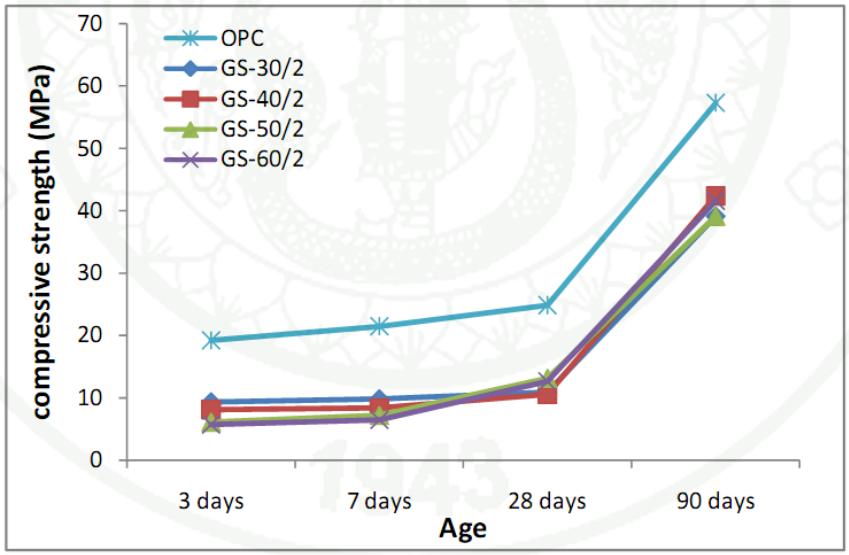

Figure 17 Compressive strength vs. Age of GBFS mortar cubes for type 2 fineness.

For control mix, the compressive strength value was 57.28 MPa which showed the unexpected result of long-term strength for OPC being higher than the GBFS-blended mortars even after increased fineness in excess to the fineness of cement (Lea 2003, Neville 1995)

4. Mercury Intrusion Porosimetry (MIP)

There are several terminologies that are used to explain the pore structure of a material, like capillary pores, gel pores, total porosity, effective porosity and threshold pore diameter as explained extensively in the Literature Review section. Effective porosity is a very important parameter when used for water permeability. Inkbottle porosity can be measured by subtracting effective porosity from total porosity.

4.1 Total Porosity and Effective Porosity

Table 14, 15 and 16 showed some of the parameters of pore structure or microstructure using MIP measurements. The first peak and second peak were the threshold pore diameters for the control and GBFS-blended pastes for the conventional curing and steam curing methods. In the same table, threshold pore diameters of first peak showed the capillary porosity, and second peak showed the gel porosity.

Aligizaki (2009) classified capillary pores into two categories of small and large capillary pores due to the influence of mineral admixtures on the microstructure of cement paste. Large amount of pores in the range between 2 to 50 nm were formed by the addition of mineral admixture with cement paste. First peak for GS-30/1 is 143.20 nm which was the maximum value of among the three samples. This showed that GS-30/1 had most capillary pores than others and OPC had the least capillary pores for the conventional curing method. When comparing the conventional curing with steam curing, the reduction in the values of total porosity was due to the gel pores changed into inkbottle pores or isolated pores during the hydration process (Ye *et al.,* 2003). The second threshold pore diameters, in the Table 16, had the sizes between 7-13 nm in all samples regardless of the w/b ratio, which classified them in gel pores.

4.2 Effect of replacement level and curing methods on pore size distribution of pastes.

Table 14 Porosity parameters for OPC and GBFS-blended pastes for 7-days.

Symbol	W/B (%)	Conventional Curing (23 ºC) at 7-day			Steam Curing (100 ºC)		
		Total Porosity (%)	Eff. Porosity (%)	Eff./total (%)	Total Porosity (%)	Eff. Porosity (%)	Eff./total (%)
OPC	0.485	44.37	24.08	0.54	37.26	18.05	0.48
GS-30/1	0.625	48.64	20.55	0.42	44.20	15.47	0.35
GS-50/2	0.617	43.24	20.29	0.47	36.19	19.91	0.55

Table 15 Results of MIP parameters of OPC and GBFS-blended pastes .

Symbol	Conventional Curing (23 ºC) at 7-day			Steam Curing (100 ºC)		
	Total Porosity (%)	Interparticle porosity (%)	Intraparticle porosity (%)	Total Porosity (%)	Interparticle porosity (%)	Intraparticle porosity (%)
OPC	44.36	8.53	35.83	37.26	1.69	35.57
GS-30/1	48.63	0.17	48.46	44.20	1.29	42.90
GS-50/2	43.24	1.14	42.09	36.18	0.67	35.15

Relationship between pore diameter and incremental pore volume of OPC and GS-30 pastes moist-cured at 7-day were shown in the Figure 18. The peaks of capillary pores (mode pore diameter) of OPC and GS-30 were at 0.1071 micron and 0.1163 micron respectively; with incremental pore volume of 0.183 cc/g and

0.1726 cc/g, respectively. This result suggested that the replacement of OPC with GBFS increased the porosity. Similarly Figure 23 also showed the same behavior pore diameter and incremental pore volume of OPC and GS-50/2 pastes in moist curing condition at 7-day. The increase in porosity was due to the higher water binder ratio when cement was partially replaced.

In Figure 19, the peaks of capillary pores (mode pore diameter) of OPC and GS-30 were at 0.07484 micron and 0.0672 micron respectively; with incremental pore volume of the two were 0.1972 cc/g and 0.1889 cc/g, respectively. This result suggested that accelerated curing reduced the pore size and consequently porosity. These results also suggested that inclusion of finer GBFS reduced the capillary pores which were also reported elsewhere with fly ash as a partial replacement (Chindaprasirt *et al.,* 2007). Similarly Figure 20 also showed the same behavior pore diameter and incremental pore volume of OPC and GS-50/2 pastes in steam curing condition at 7-day.

Table 16 Data of OPC and GBFS-blended pastes with w/b ratio and curing methods.

Symbol	W/B ratio (%)	Conventional Curing (23 ºC) on 7-day					Steam Curing at 100 ºC				
		Total Porosity (%)	threshold pore diameter (nm)		Mode pore diameter (nm)	Bulk density (cc/g)	Total Porosity (%)	threshold pore diameter (nm)		Mode pore diameter (nm)	Bulk density (cc/g)
			1st Peak	2nd Peak				1st Peak	2nd Peak		
OPC	0.485	44.37	107.1	9.92	107.10	1.427	37.26	74.84	8.11	74.84	1.465
GS-30/1	0.625	48.64	143.2	10.90	116.30	1.367	44.20	67.20	13.0	67.20	1.356
GS-50/2	0.617	43.24	116.3	10.25	143.20	1.487	36.19	41.31	7.14	41.31	1.480

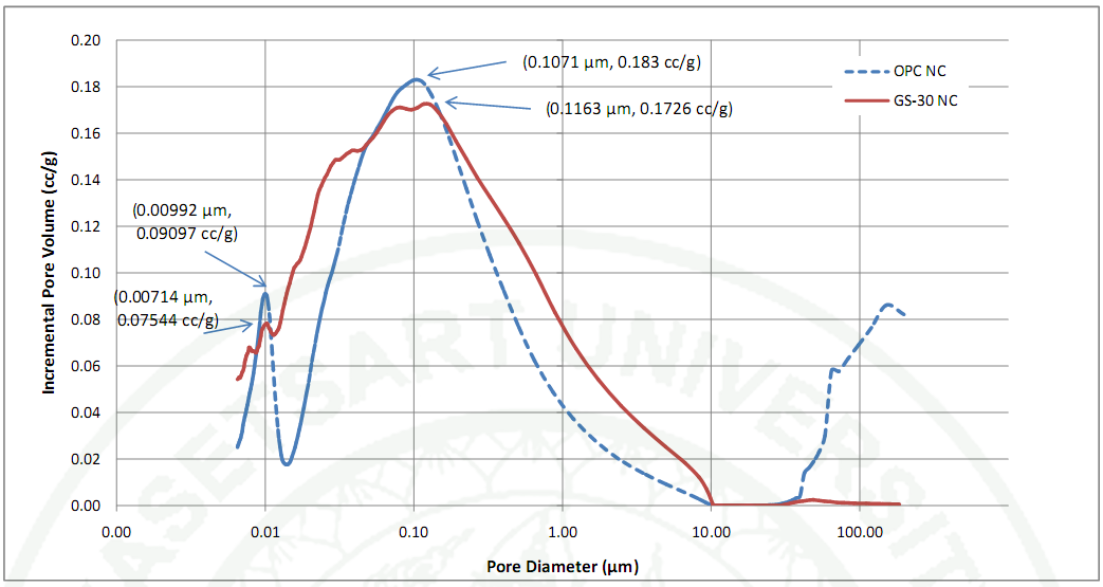

Figure 18 Relationship between pore diameter and incremental pore volume of OPC & GS-30 pastes in conventional moist curing.

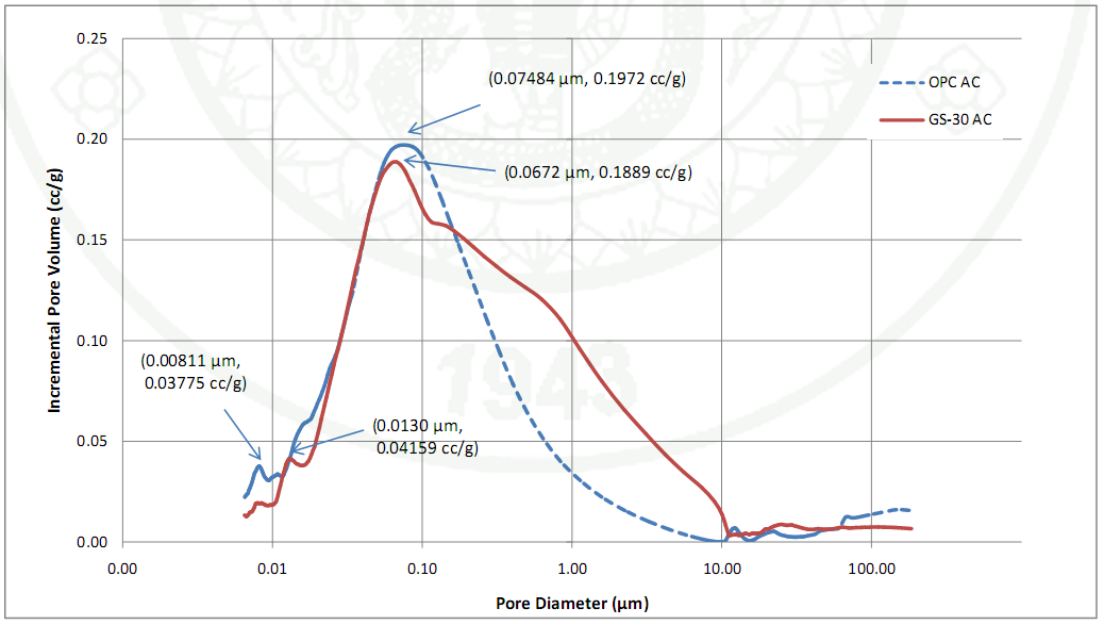

Figure 19 Relationship between pore diameter and incremental pore volume of OPC & GS-30 pastes in steam curing

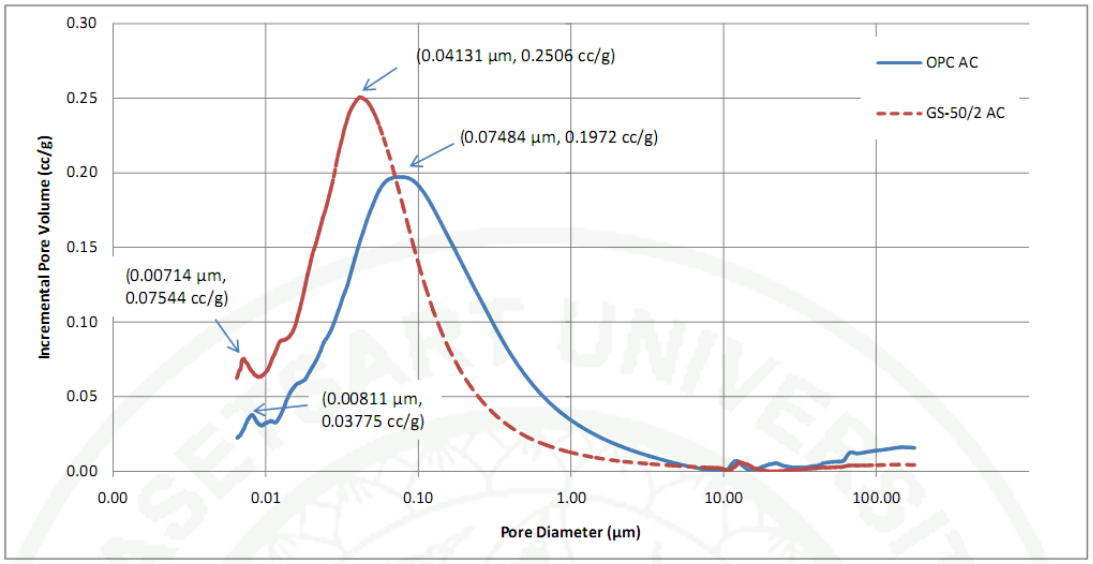

Figure 20 Relationship between pore diameter and incremental pore volume of OPC & GS-50/2 pastes in steam curing

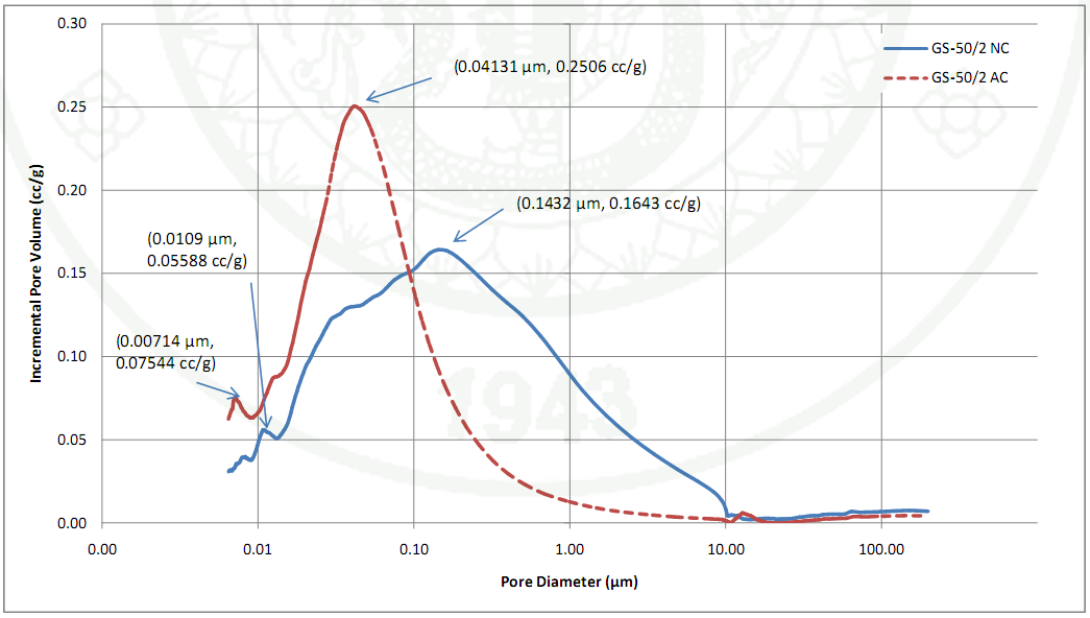

Figure 21 Relationship between pore diameter and incremental pore volume of GS-50/2 pastes in steam curing and normal curing.

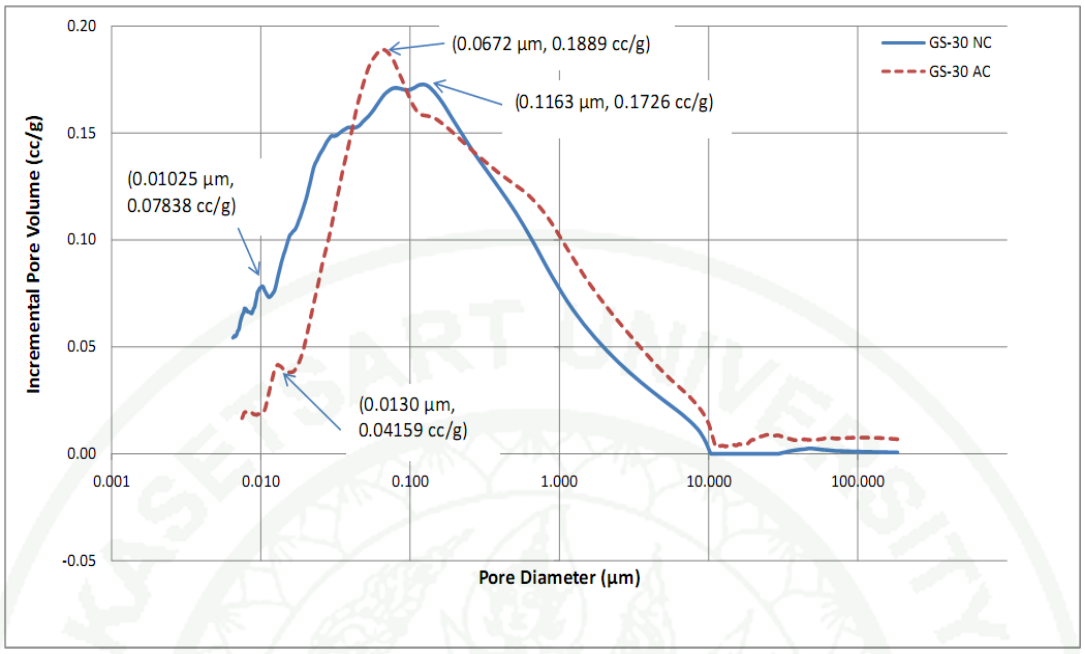

Figure 22 Relationship between pore diameter and incremental pore volume of GS-30/1 pastes in steam curing and normal curing.

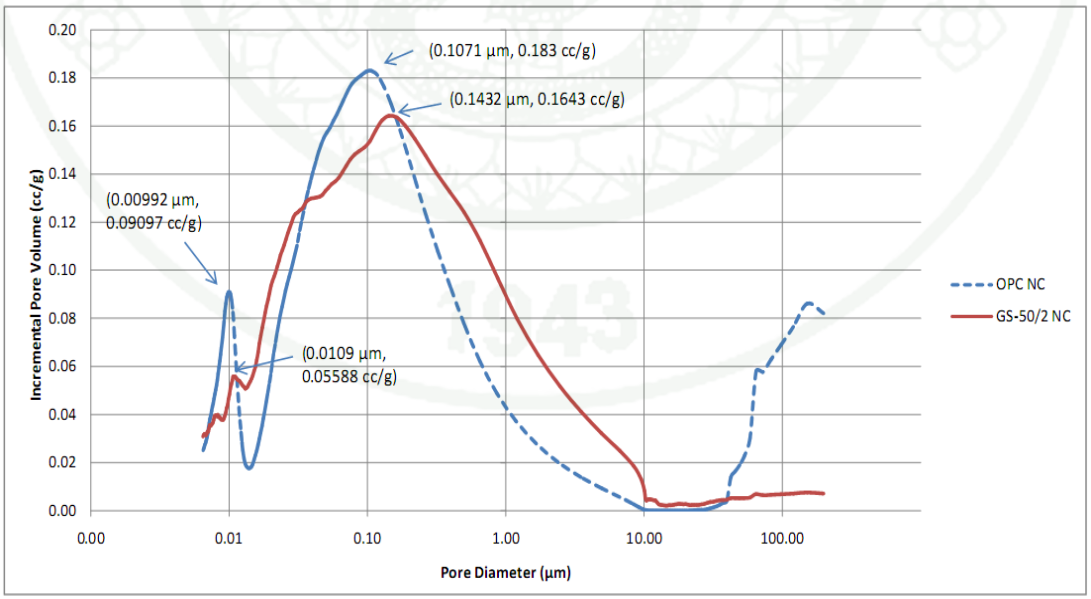

Figure 23 Relationship between pore diameter and incremental pore volume of OPC & GS-50/2 pastes in conventional moist curing.

Figure 24 shows the relationship between compressive strength and total porosity of OPC, GS-30/1, and GS-50/2 with comparison on their curing methods respectively. The maximum compressive strength of 21.48 MPa was of OPC with 7-day moist curing and total porosity of 44 %. Then GS-50/2 with steam curing had the next highest compressive strength of 13.49 MPa and total porosity of 36 %.

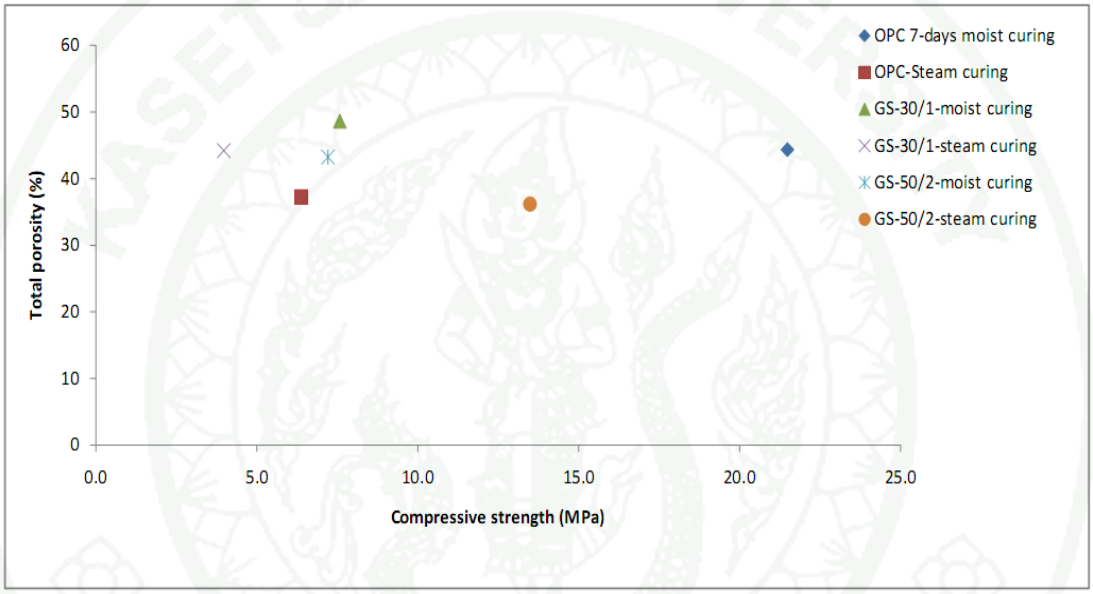

Figure 24 Relationship between compressive strength and total porosity of all pastes.

5. XRD analysis

When hydration of GBFS-blended cement paste takes place, both Portland cement and GBFS hydrations comprise of the hydration products, except the CH phase formed by the Portland cement is influenced by the GBFS hydration. The hydration of GBFS is very slow in pure water. Figure 25 and 26 shows the XRD patterns of OPC pastes both in normal curing at 7 days and accelerated curing, and bore close similarity i.e., accelerated curing had little effect on OPC. Steam curing had unremarkable effect on the hydration of Portland cement paste. Figure 27 to 30 shows that the hydration products of OPC when mixed with GBFS and water, yield

CSH and CH same as when OPC hydrate. When GBFS was replaced with OPC, peaks of CSH increased as compared to CH, which suggested that the hydration of GBFS consumed CH to produce more CSH as expected. In other words, CH encouraged the growth of CSH. Same results were reported elsewhere (Pal et al. 2003). The CH produced during the hydration of Portland cement acted as an activator or catalyst to the GBFS hydration. Figure 27 to 30 shows the XRD patterns of GS-30 and GS-50 with moist curing and steam curing. In these figures, on the increase of GBFS content, the sharp peaks decreased, indicating that with higher GBFS content resulted in an increase in hydration process of Portland cement.

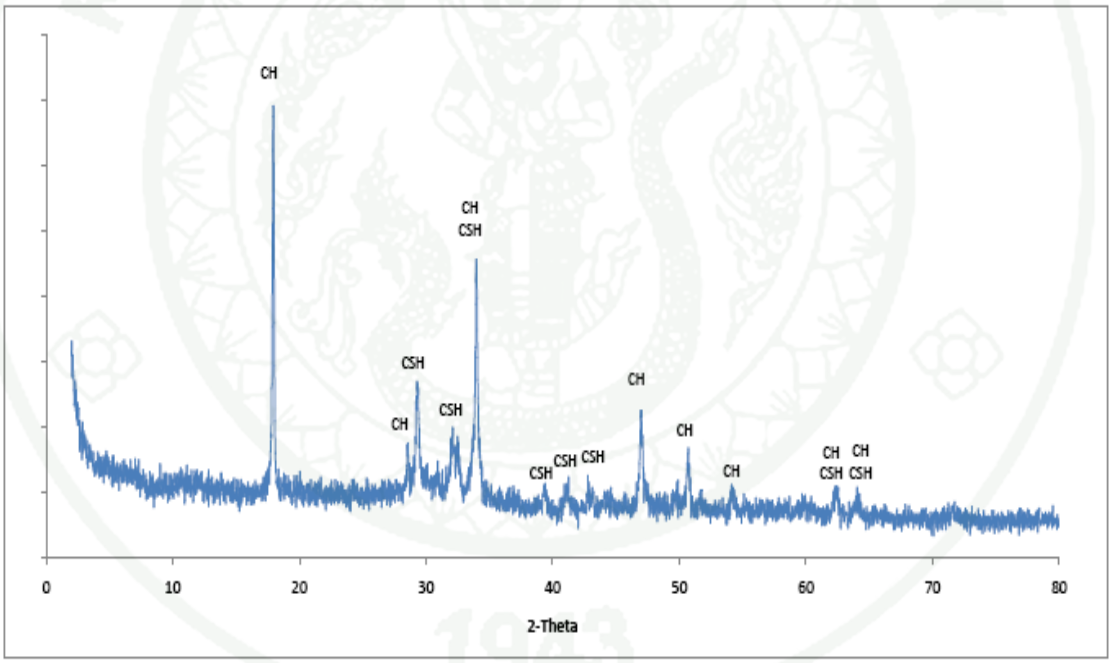

Figure 25 XRD pattern of OPC-NC paste at 7 days curing age

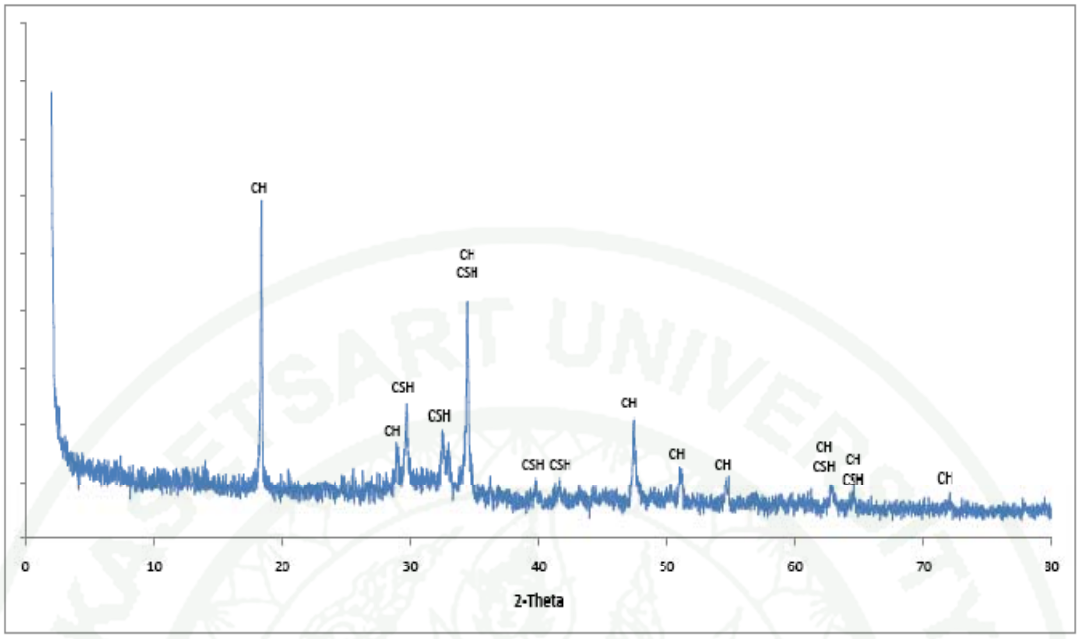

Figure 26 XRD pattern of OPC-AC paste at 7 days curing age

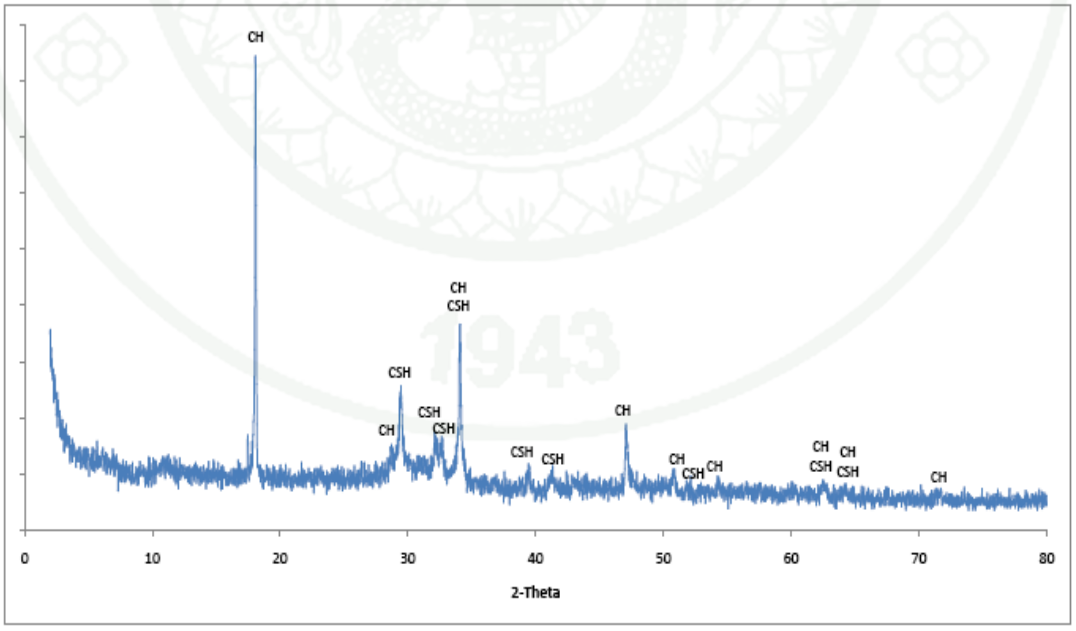

Figure 27 XRD pattern of GS-30/1-NC paste at 7 days curing age

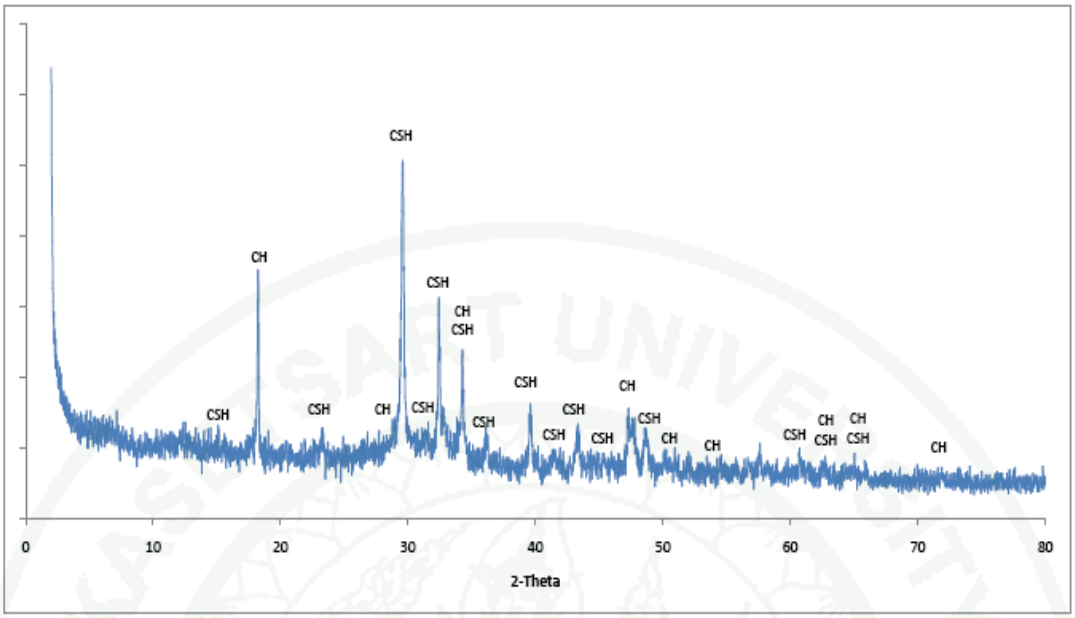

Figure 28 XRD pattern of GS-30/1-AC paste at 7 days curing age

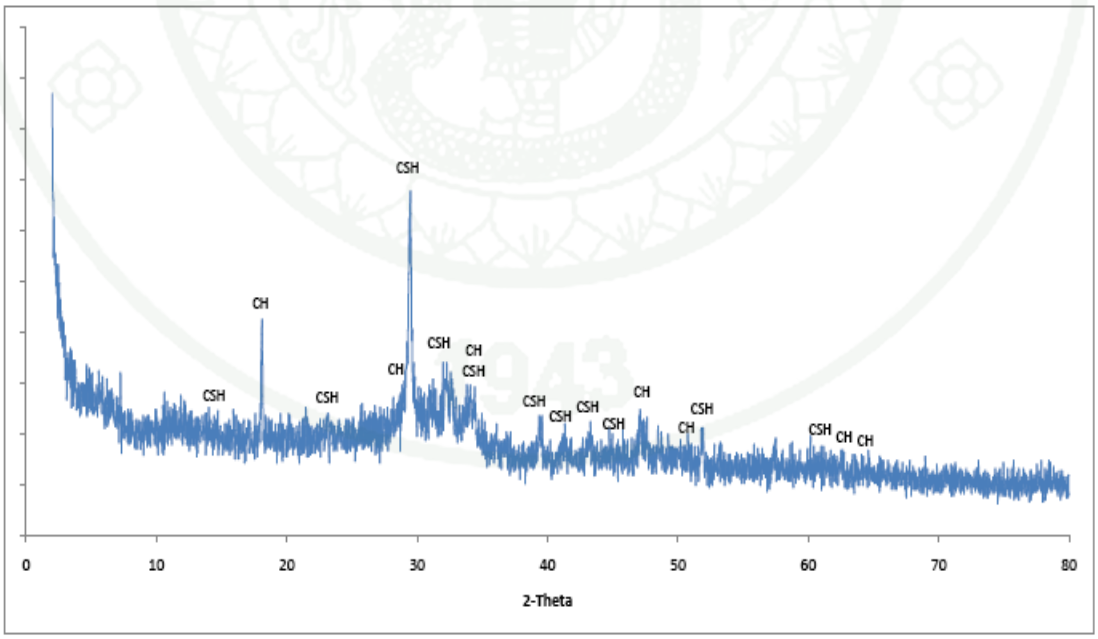

Figure 29 XRD pattern of GS-50/2-NC paste at 7 days curing age

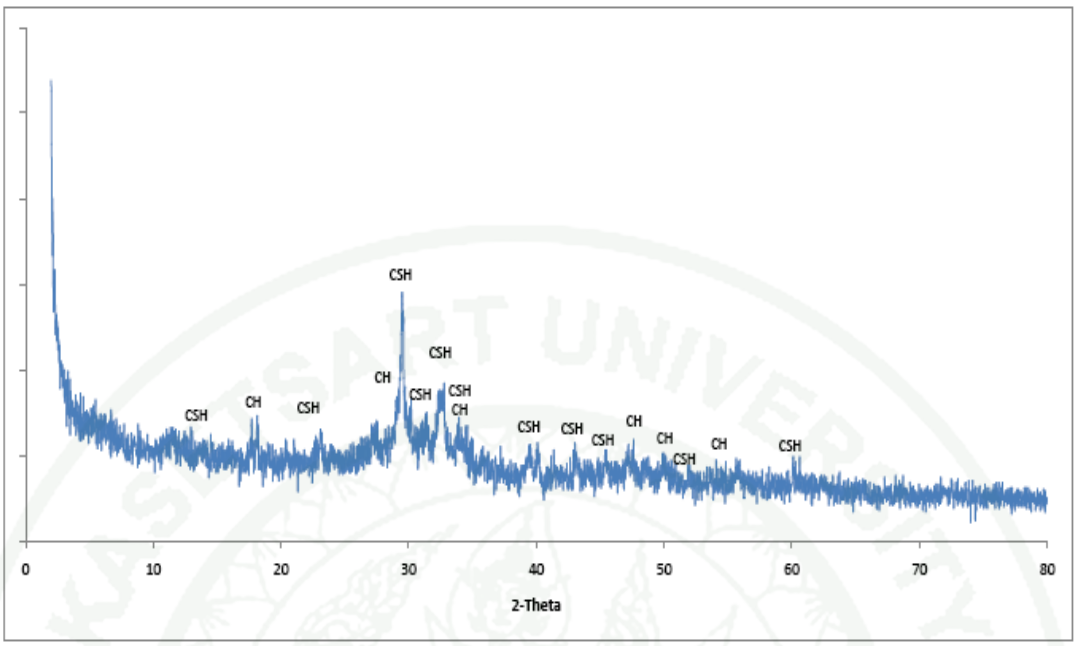

Figure 30 XRD pattern of GS-50/2-AC paste at 7 days curing age

CONCLUSION AND RECOMMENDATIONS

Conclusion

The following conclusions are drawn from the experimental study of the tests:

1. Increasing the fineness of GBFS reduced the water binder ratio for the required flowability.
2. Increase in the fineness of GBFS increased compressive strength and reduced total porosity.
3. Increase in the percentage replacement of GBFS increased water-to-binder ratio, thereby decreased the compressive strength, and increased the total porosity.
4. GBFS partial replacement caused initial low-strength as expected but showed trend towards increase in long-term strength. The long-term strength for GBFS-blended cement increased but did not go higher than the value of compressive strength of control mix.
5. The optimum percentage replacement of GBFS was 30% to 50%.
6. Accelerated curing (steam curing) significantly increased early compressive strength of GBSF mortar, and decreased pore size.
7. The hydration of Portland cement produced CH and CSH. GBFS decreased the pore sizes, and eventually deceased total porosity.

Recommendations

- The use of grinding aid in grinding of GBFS can be investigated.
- The use of workability admixture can be investigated so as to reduce the water content in the mix thereby increasing the strength, and reducing the total porosity.
- The effect of TiO_2 nanoparticles in GBFS on the abrasive resistance, strength and porosity of GBFS mortar can be investigated.
- Same materials used in this study can be investigated for aggressive environment in order to compare with the results of Khan et al (2009).
- For mercury intrusion porosimetry measurement, samples can also be dried by freezing method, consequently comparing the results with other methods.
- An extensive study is recommended in the engineering properties of the GBFS procured from Pakistan Steel.

LITERATURE CITED

Zain, M. F. M., M.N. Islam, F. Mahmud and M. Jamil. 2011. Production of rice husk ash for use in concrete as a supplementary cementitious material. **Construction and Building Materials** 25(2): 798-805.

Khan, A.R. and N.S. Zafar. 2009. Performance of different types of Pakistani cements exposed to aggressive environments, 17-24. **SBEIDO – 1st International Conference on Sustainable Built Environment Infrastructures in Developing Countries ENSET**, Oran, Algeria.

Quantachrome Instruments. 2009. **POREMASTER & POREMASTER GT, Operating Manual**.

Oner, A. and S. Akyuz. 2007. An experimental study on optimum usage of ground granulated blast furnace slag for the compressive strength of concrete. **Cement and Concrete Composites** 29(6): 505-514.

Binici, H., H. Temiz and M.M. Kose. 2007. The effect of fineness on the properties of the blended cements incorporating ground granulated blast furnace slag and ground basaltic pumice. **Construction and Building Materials**, 21(5): 1122-1128.

Chindaprasirt, P., C. Jaturapitakkul and T. Sinsiri. 2007. Effect of fly ash fineness on microstructure of blended cement paste. **Construction and Building Materials**, 21(7): 1534-1541.

Barnett, S.J., M.N. Soutsos, S.G. Millard and J.H. Bungey. 2006. Strength development of mortars containing ground granulated blast furnace slag: Effect of curing temperature and determination of apparent activation energies. **Cement and Concrete Research**, 36(3): 434-440.

Li, Y.X., Y.M. Chen, J.X. Wei, H.T. Zhang and W.S. Zhang. 2006. A study on the relationship between porosity of the cement paste with mineral additives and compressive strength of mortar based on this paste. **Cement and Concrete Research**, 36 (9): 1740-1743.

Chen, W. 2006. **Hydration of slag cement: theory, modeling and application**. PhD Thesis, University of Twente, Enschede, The Netherlands.

Aligizaki, K.K. 2006. **Pore structure of cement-based materials: testing, interpretation and requirements**. Taylor & Francis, Abingdon, Oxon.

Prusinski, J.R. 2006. **Slag as a cementitious material, Significance of tests and properties of concrete and concrete-making materials (ASTM-STP 169D).** ASTM International, West Conshohocken, P.A.

Wang, P. Z., R. Trettin, V. Rudert and T. Spaniol. 2004. Influence of Al_2O_3 content on hydraulic reactivity of granulated blast-furnace slag, and the interaction between Al_2O_3 and CaO. **Advances in Cement Research**, 16 (1): 1-7.

Liu, B., Y. Xie and J. Li. 2005. Influence of steam curing on the compressive strength of concrete containing supplementary cementing materials. **Cement and Concrete Research**, 35(5): 994-998.

Pal, S.C., A. Mukherjee and S.R. Pathak. 2003. Investigation of hydraulic activity of ground granulated blast furnace slag in concrete**. Cement and Concrete Research**, 33(9): 1481-1486.

Ye, G. 2003. **Experimental study and numerical simulation of the development of the microstructure and permeability of cementitious materials**. PhD Thesis, Delft university press, Delft, The Netherlands.

Li, G. and X. Zhao. 2003. Properties of concrete incorporating fly ash and ground granulated blast furnace slag. **Cement and Concrete Composites**, 25(3): 293-299.

Hewlett, P. C. 2003. **Lea's Chemistry of Cement and Concrete**. Fourth Edition. Elsevier Science & Technology, USA.

Mindess, S., Young, J.F., Darwin, D. 2003. **Concrete**. Second Edition. Prentice Hall, Englewood Cliffs, NJ, USA.

Chatterji, A. 2001. **X-ray diffraction, Handbook of analytical techniques in concrete science and technology**. Noyes Publications / William Andrew Publishing, LLC, NY, USA.

American Concrete Institute. 2003. **Slag Cement in Concrete and Mortar.** ACI 233-R.

Ehrenberg, A. 2003. Investigation into the grinding resistance of granulated blast-furnace slag. **ZKG International,** 56(3): 70-81.

Slag Cement Association. 2002. **Concrete Proportioning.** SCIC No.2.

Olorunsogo, F.T. and P.J. Wainwright. 1998. Effect of GGBFS particle-size distribution on mortar compressive strength. **Journal of Materials in Civil Engineering, ASCE**, 10(3): 180-187.

Tan, K., and X. Pu. 1998. Strengthening effect of finely ground fly ash, granulated blast furnace slag, and their combination. **Cement and Concrete Research**, 28 (12): 1819-1825.

Swamy, R.N. 1998. Design for durability and strength through the use of fly ash and slag in concrete, 1-72. **CANMET/ACI International Workshop on Supplementary Cementitious Material, Superplasticizers and Other Chemical Admixtures in Concrete.** ACI, Toronto, Canada.

Taylor, H.F.W. 1997. **Cement Chemistry**. Second Edition. Thomas Telford Publishing, London, U.K.

Lumley, J.S., R.S. Gollop, G.K. Moir and H.F.W. Taylor. 1996. Degree of reaction of the slag in some blends with Portland cement. **Cement and Concrete Research**, 26 (1): 139-151.

Neville, A.M. 1995. **Properties of concrete**. Fourth Edition. Pearson Education Limited, Essex, England

Smolczyk, H.G. 1978. The effect of the chemistry of slag on the strength of blast-furnace cements. **Zement-Kalk-Gips**, 31(6): 294-296.

Soroka, I. 1979. **Portland cement paste and concrete**. Macmillan Press Ltd., London, U.K.

Washburn, E.W. 1921. Note on method of determining the distribution of pore size in porous materials. **P Natl Acad Sci USA**, 7, 115-6.

APPENDIX

Appendix Table 1 Pore Size Distribution By Volume - Intrusion for OPC - Normal curing

Pressure	Pore Diameter	Volume Intruded	Delta Volume	% Volume Intruded	Dv(d)	-dV/d(log d)
[PSI]	[μm]	[cc/g]	[cc/g]	%	[cc/(μm-g)]	[cc/g]
1.076	198.200	0.000	0.000	0.000	0.00014	0.08216
1.413	151.000	0.037	0.037	11.830	0.00017	0.08619
1.783	119.600	0.045	0.008	14.440	0.00025	0.07650
2.175	98.060	0.049	0.004	15.680	0.00034	0.06910
2.573	82.900	0.051	0.002	16.420	0.00045	0.06301
2.952	72.260	0.053	0.002	16.910	0.00055	0.05772
3.304	64.560	0.058	0.005	18.650	0.00071	0.05811
3.662	58.250	0.058	0.000	18.770	0.00032	0.03007
4.006	53.240	0.059	0.000	18.900	0.00025	0.02308
4.352	49.010	0.059	0.000	18.990	0.00022	0.01906
4.698	45.410	0.059	0.000	19.040	0.00021	0.01625
5.041	42.310	0.059	0.000	19.090	0.00020	0.01398
5.384	39.620	0.059	0.000	19.110	0.00005	0.00400
5.725	37.260	0.060	0.000	19.140	0.00005	0.00327
6.065	35.170	0.060	0.000	19.140	0.00004	0.00242
6.405	33.310	0.060	0.000	19.150	0.00003	0.00175
7	31.550	0.060	0.000	19.150	0.00002	0.00131
7	29.900	0.060	0.000	19.150	0.00002	0.00091
7	28.470	0.060	0.000	19.160	0.00001	0.00066
8	27.180	0.060	0.000	19.160	0.00001	0.00038
8	26.000	0.060	0.000	19.170	0.00001	0.00034
9	24.910	0.060	0.000	19.170	0.00001	0.00028
9	23.920	0.060	0.000	19.170	0.00000	0.00023
9	22.990	0.060	0.000	19.170	0.00000	0.00018
10	22.180	0.060	0.000	19.170	0.00000	0.00012
10	21.460	0.060	0.000	19.170	0.00000	0.00006
10	20.820	0.060	0.000	19.170	0.00000	0.00000
11	20.220	0.060	0.000	19.170	0.00000	0.00000
11	19.640	0.060	0.000	19.170	0.00000	0.00000
11	19.070	0.060	0.000	19.170	0.00000	0.00000
12	18.500	0.060	0.000	19.170	0.00000	0.00000
12	17.970	0.060	0.000	19.170	0.00000	0.00000
12	17.470	0.060	0.000	19.170	0.00000	0.00000
13	17.000	0.060	0.000	19.170	0.00000	0.00000

Appendix Table 1 (Continued)

Pressure [PSI]	Pore Diameter [µm]	Volume Intruded [cc/g]	Delta Volume [cc/g]	% Volume Intruded %	Dv(d) [cc/(µm-g)]	-dV/d(log d) [cc/g]
13	16.550	0.060	0.000	19.170	0.00000	0.00000
13	16.100	0.060	0.000	19.170	0.00000	0.00000
14	15.660	0.060	0.000	19.170	0.00000	0.00000
14	15.230	0.060	0.000	19.170	0.00000	0.00000
14	14.820	0.060	0.000	19.170	0.00000	0.00000
15	14.430	0.060	0.000	19.170	0.00000	0.00000
15	14.070	0.060	0.000	19.170	0.00000	0.00000
16	13.730	0.060	0.000	19.170	0.00000	0.00000
16	13.400	0.060	0.000	19.170	0.00000	0.00000
16	13.090	0.060	0.000	19.170	0.00000	0.00000
17	12.790	0.060	0.000	19.170	0.00000	0.00000
17	12.520	0.060	0.000	19.170	0.00000	0.00000
17	12.260	0.060	0.000	19.170	0.00000	0.00000
18	12.030	0.060	0.000	19.170	0.00000	0.00000
18	11.810	0.060	0.000	19.170	0.00000	0.00000
18	11.620	0.060	0.000	19.170	0.00000	0.00000
19	11.440	0.060	0.000	19.170	0.00000	0.00000
19	11.260	0.060	0.000	19.170	0.00000	0.00000
19	11.100	0.060	0.000	19.170	0.00000	0.00000
20	10.930	0.060	0.000	19.170	0.00000	0.00000
20	10.780	0.060	0.000	19.170	0.00000	0.00000
20	10.620	0.060	0.000	19.170	0.00000	0.00004
20	10.480	0.060	0.000	19.170	0.00000	0.00011
21	10.330	0.060	0.000	19.170	0.00001	0.00024
22	9.895	0.060	0.000	19.170	0.00001	0.00052
23	9.193	0.060	0.000	19.170	0.00003	0.00139
26	8.133	0.060	0.000	19.180	0.00005	0.00314
32	6.649	0.060	0.000	19.200	0.00010	0.00571
43	4.968	0.060	0.000	19.250	0.00021	0.00926
61	3.489	0.060	0.001	19.410	0.00050	0.01400
90	2.383	0.062	0.002	19.910	0.00124	0.02015
129	1.660	0.065	0.003	20.890	0.00299	0.02791
181	1.179	0.069	0.004	22.240	0.00672	0.03747
248	0.862	0.074	0.005	23.950	0.01415	0.04884
329	0.649	0.081	0.006	26.020	0.02764	0.06228
425	0.502	0.088	0.008	28.440	0.05002	0.07745
536	0.398	0.097	0.009	31.200	0.08228	0.09312

Appendix Table 1 (Continued)

Pressure [PSI]	Pore Diameter [μm]	Volume Intruded [cc/g]	Delta Volume [cc/g]	% Volume Intruded %	Dv(d) [cc/(μm-g)]	-dV/d(log d) [cc/g]
661	0.323	0.107	0.010	34.300	0.12470	0.10790
799	0.267	0.117	0.010	37.650	0.17950	0.12240
949	0.225	0.128	0.011	41.240	0.24730	0.13630
1109	0.192	0.140	0.012	44.930	0.32690	0.14920
1275	0.167	0.151	0.011	48.490	0.41540	0.16040
1449	0.147	0.161	0.010	51.740	0.50950	0.16970
1627	0.131	0.170	0.009	54.770	0.60380	0.17650
1808	0.118	0.179	0.009	57.600	0.69530	0.18120
1992	0.107	0.187	0.008	60.240	0.77640	0.18300
2179	0.098	0.195	0.007	62.630	0.84620	0.18270
2369	0.090	0.201	0.007	64.810	0.90810	0.18120
2561	0.083	0.208	0.006	66.780	0.97020	0.17960
2755	0.077	0.213	0.006	68.600	1.02800	0.17770
2952	0.072	0.218	0.005	70.230	1.07900	0.17480
3151	0.068	0.223	0.005	71.750	1.12300	0.17130
3353	0.064	0.227	0.004	73.180	1.16700	0.16800
3557	0.060	0.232	0.004	74.550	1.21000	0.16490
3763	0.057	0.236	0.004	75.850	1.25600	0.16220
3971	0.054	0.239	0.004	77.050	1.29900	0.15940
4181	0.051	0.243	0.004	78.170	1.34800	0.15740
4394	0.049	0.246	0.003	79.250	1.39800	0.15540
4610	0.046	0.250	0.003	80.270	1.44000	0.15250
4827	0.044	0.253	0.003	81.250	1.47400	0.14900
5048	0.042	0.255	0.003	82.170	1.50100	0.14500
5271	0.040	0.258	0.003	83.050	1.52500	0.14110
5495	0.039	0.261	0.003	83.900	1.54800	0.13720
5722	0.037	0.263	0.002	84.650	1.56400	0.13300
5950	0.036	0.265	0.002	85.340	1.57700	0.12900
6181	0.035	0.267	0.002	85.990	1.58000	0.12440
6415	0.033	0.269	0.002	86.600	1.58000	0.11990
6650	0.032	0.271	0.002	87.160	1.57300	0.11520
6887	0.031	0.273	0.002	87.700	1.55700	0.11030
7126	0.030	0.274	0.002	88.220	1.55500	0.10670
7368	0.029	0.276	0.001	88.680	1.55400	0.10320
7611	0.028	0.277	0.001	89.130	1.55600	0.10010
7857	0.027	0.278	0.001	89.550	1.56000	0.09732
8104	0.026	0.280	0.001	89.950	1.56200	0.09450

Appendix Table 1 (Continued)

Pressure [PSI]	Pore Diameter [μm]	Volume Intruded [cc/g]	Delta Volume [cc/g]	% Volume Intruded %	Dv(d) [cc/(μm-g)]	-dV/d(log d) [cc/g]
8354	0.026	0.281	0.001	90.340	1.55800	0.09143
8605	0.025	0.282	0.001	90.710	1.54200	0.08785
8859	0.024	0.283	0.001	91.060	1.53200	0.08466
9114	0.023	0.284	0.001	91.400	1.51200	0.08105
9371	0.023	0.285	0.001	91.720	1.48600	0.07733
9631	0.022	0.286	0.001	92.010	1.45500	0.07348
9893	0.022	0.287	0.001	92.270	1.40900	0.06916
10156	0.021	0.288	0.001	92.510	1.36500	0.06524
10422	0.020	0.288	0.001	92.720	1.30900	0.06092
10689	0.020	0.289	0.001	92.910	1.24600	0.05653
10959	0.019	0.289	0.001	93.080	1.18000	0.05226
11230	0.019	0.290	0.001	93.240	1.12400	0.04868
11503	0.019	0.290	0.001	93.390	1.06700	0.04510
11779	0.018	0.291	0.000	93.520	1.00700	0.04157
12056	0.018	0.291	0.000	93.650	0.94920	0.03826
12336	0.017	0.291	0.000	93.760	0.89510	0.03523
12617	0.017	0.292	0.000	93.870	0.84550	0.03250
12900	0.017	0.292	0.000	93.960	0.79930	0.03002
13185	0.016	0.292	0.000	94.040	0.74170	0.02727
13478	0.016	0.293	0.000	94.110	0.69520	0.02499
13780	0.015	0.293	0.000	94.170	0.65120	0.02291
14091	0.015	0.293	0.000	94.230	0.61660	0.02125
14404	0.015	0.293	0.000	94.290	0.57070	0.01932
14719	0.014	0.293	0.000	94.340	0.55010	0.01831
15036	0.014	0.293	0.000	94.380	0.54230	0.01776
15354	0.014	0.293	0.000	94.430	0.54790	0.01765
15675	0.014	0.294	0.000	94.470	0.56380	0.01787
15998	0.013	0.294	0.000	94.520	0.59110	0.01844
16323	0.013	0.294	0.000	94.570	0.63690	0.01955
16650	0.013	0.294	0.000	94.620	0.72110	0.02180
16973	0.013	0.294	0.000	94.680	0.84740	0.02524
17292	0.012	0.294	0.000	94.740	0.99980	0.02931
17605	0.012	0.295	0.000	94.800	1.18500	0.03421
17920	0.012	0.295	0.000	94.880	1.40200	0.03975
18237	0.012	0.295	0.000	94.980	1.63600	0.04555
18557	0.012	0.296	0.000	95.100	1.89500	0.05176
18878	0.011	0.296	0.000	95.250	2.18600	0.05858

Appendix Table 1 (Continued)

Pressure [PSI]	Pore Diameter [μm]	Volume Intruded [cc/g]	Delta Volume [cc/g]	% Volume Intruded %	Dv(d) [cc/(μm-g)]	-dV/d(log d) [cc/g]
19201	0.011	0.297	0.001	95.410	2.49900	0.06563
19526	0.011	0.297	0.001	95.590	2.83100	0.07288
19852	0.011	0.298	0.001	95.780	3.14300	0.07928
20181	0.011	0.298	0.001	95.990	3.41200	0.08434
20507	0.010	0.299	0.001	96.200	3.62500	0.08789
20835	0.010	0.300	0.001	96.420	3.79100	0.09020
21164	0.010	0.300	0.001	96.650	3.89200	0.09091
21495	0.010	0.301	0.001	96.870	3.96600	0.09097
21828	0.010	0.302	0.001	97.080	4.00200	0.09020
22163	0.010	0.302	0.001	97.270	4.00500	0.08877
22499	0.009	0.303	0.001	97.450	3.95700	0.08630
22837	0.009	0.303	0.001	97.620	3.86900	0.08307
23177	0.009	0.304	0.001	97.780	3.73100	0.07894
23519	0.009	0.304	0.001	97.930	3.60800	0.07525
23863	0.009	0.305	0.001	98.070	3.48500	0.07167
24212	0.009	0.305	0.000	98.210	3.35400	0.06799
24563	0.009	0.306	0.000	98.340	3.25000	0.06494
24917	0.009	0.306	0.000	98.460	3.16600	0.06235
25272	0.008	0.306	0.000	98.580	3.06700	0.05954
25630	0.008	0.307	0.000	98.690	2.98000	0.05705
25989	0.008	0.307	0.000	98.790	2.87700	0.05432
26351	0.008	0.307	0.000	98.890	2.80000	0.05217
26714	0.008	0.308	0.000	98.990	2.72900	0.05019
27080	0.008	0.308	0.000	99.070	2.67400	0.04852
27447	0.008	0.308	0.000	99.160	2.60300	0.04664
27817	0.008	0.308	0.000	99.240	2.52900	0.04469
28189	0.008	0.309	0.000	99.330	2.48300	0.04329
28562	0.007	0.309	0.000	99.400	2.41100	0.04147
28938	0.007	0.309	0.000	99.480	2.33500	0.03962
29316	0.007	0.309	0.000	99.550	2.28100	0.03818
29695	0.007	0.310	0.000	99.620	2.20800	0.03647
30077	0.007	0.310	0.000	99.680	2.12300	0.03456
30460	0.007	0.310	0.000	99.730	2.00000	0.03211
30845	0.007	0.310	0.000	99.790	1.92500	0.03054
31198	0.007	0.310	0.000	99.830	1.86500	0.02927
31576	0.007	0.310	0.000	99.880	1.82800	0.02826
31952	0.007	0.311	0.000	99.920	1.80700	0.02747

Appendix Table 1 (Continued)

Pressure	Pore Diameter	Volume Intruded	Delta Volume	% Volume Intruded	Dv(d)	-dV/d(log d)
[PSI]	[µm]	[cc/g]	[cc/g]	%	[cc/(µm-g)]	[cc/g]
32322	0.007	0.311	0.000	99.940	1.76800	0.02644
32664	0.007	0.311	0.000	99.980	1.74600	0.02573
32807	0.007	0.3108	0.000	100.000	1.71800	0.02511

Appendix Table 2 Pore Size Distribution By Volume – Intrusion for OPC-Steam curing

Pressure	Pore Diameter	Volume Intruded	Delta Volume	% Volume Intruded	Dv(d)	-dV/d(log d)
[PSI]	[μm]	[cc/g]	[cc/g]	%	[cc/(μm-g)]	[cc/g]
1.198	178.000	0	0	0	3.09E-05	0.016
1.454	146.700	0.0054	0.0054	2.1	3.56E-05	0.016
1.843	115.700	0.0065	0.0011	2.54	4.90E-05	0.015
2.228	95.760	0.007	0.0005	2.75	6.76E-05	0.014
2.535	84.150	0.0074	0.0004	2.89	8.46E-05	0.013
2.86	74.600	0.0077	0.0004	3.04	1.00E-04	0.012
3.179	67.100	0.0086	0.0009	3.38	1.28E-04	0.012
3.494	61.050	0.0088	0.0002	3.45	5.85E-05	0.007
3.82	55.840	0.0089	0.0002	3.52	5.60E-05	0.007
4.137	51.560	0.0091	0.0002	3.58	5.92E-05	0.006
4.448	47.960	0.0093	0.0002	3.64	6.07E-05	0.006
4.755	44.860	0.0094	0.0001	3.7	6.05E-05	0.005
5.078	42.010	0.0096	0.0001	3.76	4.29E-05	0.004
5.416	39.390	0.0097	0.0001	3.81	4.24E-05	0.004
5.769	36.980	0.0098	0.0001	3.85	4.11E-05	0.003
6.102	34.960	0.0098	0	3.87	3.86E-05	0.003
6.418	33.240	0.0099	0	3.89	3.79E-05	0.003
6.734	31.680	0.0099	0	3.91	3.76E-05	0.003
7.068	30.180	0.0099	0	3.91	3.72E-05	0.003
7.402	28.820	0.0099	0	3.91	3.85E-05	0.003
7.736	27.580	0.0099	0	3.91	4.06E-05	0.003
8.052	26.490	0.01	0.0001	3.93	4.74E-05	0.003
8.35	25.550	0.0101	0.0001	3.96	5.41E-05	0.003
8.65	24.660	0.0102	0.0001	3.99	6.10E-05	0.004
8.95	23.840	0.0102	0.0001	4.02	7.36E-05	0.004
9.249	23.060	0.0103	0.0001	4.05	8.80E-05	0.005
9.565	22.300	0.0104	0.0001	4.09	1.04E-04	0.005
9.897	21.560	0.0105	0.0001	4.12	1.04E-04	0.005
10.244	20.820	0.0106	0.0001	4.15	1.04E-04	0.005
10.572	20.180	0.0106	0.0001	4.18	1.02E-04	0.005
10.883	19.600	0.0107	0.0001	4.21	9.98E-05	0.004
11.192	19.060	0.0108	0.0001	4.25	9.30E-05	0.004
11.502	18.550	0.0108	0	4.25	8.58E-05	0.004
11.827	18.040	0.0108	0	4.26	7.82E-05	0.003

Appendix Table 2 (Continued)

Pressure	Pore Diameter	Volume Intruded	Delta Volume	% Volume Intruded	Dv(d)	-dV/d(log d)
[PSI]	[µm]	[cc/g]	[cc/g]	%	[cc/(µm-g)]	[cc/g]
12.135	17.580	0.0109	0	4.27	7.00E-05	0.003
12.424	17.170	0.0109	0	4.28	5.95E-05	0.002
12.715	16.780	0.0109	0	4.28	4.67E-05	0.002
13.004	16.400	0.0109	0	4.28	3.24E-05	0.001
13.293	16.050	0.0109	0	4.29	2.95E-05	0.001
13.58	15.710	0.0109	0	4.29	2.65E-05	0.001
13.866	15.380	0.0109	0	4.29	2.29E-05	0.001
14.152	15.070	0.0109	0	4.3	2.13E-05	0.001
14.438	14.780	0.0109	0	4.3	2.80E-05	0.001
14.738	14.470	0.0109	0	4.3	3.81E-05	0.001
15.021	14.200	0.0109	0	4.3	4.90E-05	0.002
15.303	13.940	0.0109	0	4.3	6.71E-05	0.002
15.585	13.690	0.0109	0	4.3	8.64E-05	0.003
15.866	13.440	0.011	0	4.31	1.07E-04	0.003
16.146	13.210	0.011	0	4.33	1.29E-04	0.004
16.424	12.990	0.011	0	4.34	1.56E-04	0.005
16.701	12.770	0.0111	0.0001	4.37	1.85E-04	0.006
16.978	12.560	0.0112	0.0001	4.39	2.16E-04	0.006
17.254	12.360	0.0112	0.0001	4.41	2.40E-04	0.007
17.529	12.170	0.0113	0.0001	4.43	2.49E-04	0.007
17.802	11.980	0.0113	0.0001	4.45	2.49E-04	0.007
18.075	11.800	0.0114	0.0001	4.47	2.50E-04	0.007
18.347	11.630	0.0114	0.0001	4.49	2.30E-04	0.006
18.62	11.460	0.0115	0	4.51	2.08E-04	0.005
18.874	11.300	0.0115	0	4.52	1.84E-04	0.005
19.114	11.160	0.0115	0	4.53	1.58E-04	0.004
19.353	11.020	0.0115	0	4.54	1.31E-04	0.003
19.577	10.900	0.0115	0	4.54	1.01E-04	0.002
19.801	10.770	0.0115	0	4.54	7.06E-05	0.002
20.04	10.640	0.0115	0	4.54	4.39E-05	0.001
20.277	10.520	0.0115	0	4.54	2.64E-05	0.001
20.498	10.410	0.0115	0	4.54	1.35E-05	0.000
20.719	10.300	0.0115	0	4.54	0.00E+00	0.000
20.939	10.190	0.0115	0	4.54	0.00E+00	0.000
21.159	10.080	0.0115	0	4.54	0.00E+00	0.000
21.379	9.978	0.0115	0	4.54	0.00E+00	0.000

Appendix Table 2 (Continued)

Pressure	Pore Diameter	Volume Intruded	Delta Volume	% Volume Intruded	Dv(d)	-dV/d(log d)
[PSI]	[μm]	[cc/g]	[cc/g]	%	[cc/(μm-g)]	[cc/g]
21.613	9.870	0.0115	0	4.54	0.00E+00	0.000
21.845	9.765	0.0115	0	4.54	0.00E+00	0.000
22.09	9.657	0.0115	0	4.54	0.00E+00	0.000
22.334	9.551	0.0115	0	4.54	0.00E+00	0.000
22.562	9.455	0.0115	0	4.54	0.00E+00	0.000
22.789	9.361	0.0115	0	4.54	0.00E+00	0.000
23.017	9.268	0.0115	0	4.54	0.00E+00	0.000
23.244	9.178	0.0115	0	4.54	3.28E-06	0.000
23.457	9.094	0.0115	0	4.54	7.26E-06	0.000
24.553	8.688	0.0115	0	4.54	1.27E-05	0.000
26.58	8.026	0.0115	0	4.54	2.23E-05	0.001
30.324	7.035	0.0115	0	4.54	4.11E-05	0.002
36.782	5.800	0.0116	0.0001	4.57	8.12E-05	0.004
47.801	4.463	0.0118	0.0002	4.65	1.75E-04	0.006
66.091	3.228	0.0122	0.0004	4.79	4.08E-04	0.010
94.793	2.250	0.013	0.0008	5.12	1.00E-03	0.016
135.291	1.577	0.0146	0.0016	5.74	2.43E-03	0.022
188.348	1.133	0.0172	0.0027	6.78	5.54E-03	0.031
253.864	0.840	0.0212	0.0039	8.33	1.14E-02	0.040
332.799	0.641	0.0264	0.0052	10.37	2.17E-02	0.051
425.058	0.502	0.0326	0.0062	12.82	3.89E-02	0.064
531.237	0.402	0.0398	0.0072	15.64	6.51E-02	0.079
651.187	0.328	0.0477	0.008	18.77	1.03E-01	0.094
784.261	0.272	0.0563	0.0085	22.12	1.52E-01	0.110
929.209	0.230	0.0655	0.0092	25.74	2.14E-01	0.124
1083.239	0.197	0.0751	0.0097	29.55	2.86E-01	0.137
1243.406	0.172	0.085	0.0098	33.42	3.66E-01	0.149
1408.014	0.152	0.0948	0.0098	37.26	4.54E-01	0.160
1576.663	0.135	0.1041	0.0093	40.91	5.46E-01	0.170
1750.601	0.122	0.1127	0.0086	44.31	6.43E-01	0.179
1927.733	0.111	0.1205	0.0079	47.4	7.41E-01	0.186
2107.509	0.101	0.1279	0.0074	50.31	8.35E-01	0.191
2290.179	0.093	0.1349	0.0069	53.03	9.23E-01	0.195
2474.795	0.086	0.1415	0.0066	55.64	1.00E+00	0.196
2661.806	0.080	0.1479	0.0064	58.14	1.08E+00	0.197
2850.314	0.075	0.1539	0.006	60.52	1.15E+00	0.197

Appendix Table 2 (Continued)

Pressure	Pore Diameter	Volume Intruded	Delta Volume	% Volume Intruded	Dv(d)	-dV/d(log d)
[PSI]	[μm]	[cc/g]	[cc/g]	%	[cc/(μm-g)]	[cc/g]
3041.067	0.070	0.1596	0.0057	62.78	1.23E+00	0.197
3234.316	0.066	0.1651	0.0055	64.92	1.30E+00	0.196
3430.707	0.062	0.1702	0.0051	66.94	1.37E+00	0.195
3629.694	0.059	0.1751	0.0048	68.84	1.44E+00	0.192
3830.476	0.056	0.1795	0.0045	70.6	1.49E+00	0.189
4034.052	0.053	0.1838	0.0042	72.25	1.53E+00	0.184
4241.022	0.050	0.1877	0.0039	73.8	1.56E+00	0.179
4450.337	0.048	0.1914	0.0037	75.25	1.59E+00	0.173
4662.596	0.046	0.1948	0.0034	76.58	1.61E+00	0.167
4877.1	0.044	0.1979	0.0032	77.83	1.62E+00	0.161
5094.597	0.042	0.2008	0.0029	78.96	1.63E+00	0.155
5314.839	0.040	0.2035	0.0027	80	1.63E+00	0.149
5536.978	0.039	0.206	0.0026	81.01	1.63E+00	0.143
5761.111	0.037	0.2084	0.0023	81.93	1.62E+00	0.137
5987.939	0.036	0.2106	0.0022	82.79	1.61E+00	0.131
6216.714	0.034	0.2126	0.0021	83.61	1.60E+00	0.125
6448.481	0.033	0.2145	0.0019	84.36	1.59E+00	0.120
6681.997	0.032	0.2163	0.0017	85.03	1.59E+00	0.116
6917.906	0.031	0.2179	0.0016	85.67	1.58E+00	0.112
7155.911	0.030	0.2193	0.0015	86.25	1.57E+00	0.107
7395.912	0.029	0.2208	0.0014	86.81	1.56E+00	0.103
7638.109	0.028	0.2222	0.0014	87.37	1.54E+00	0.099
7882.051	0.027	0.2236	0.0014	87.9	1.54E+00	0.095
8128.089	0.026	0.2248	0.0012	88.39	1.54E+00	0.093
8376.223	0.025	0.2259	0.0011	88.84	1.54E+00	0.090
8626.402	0.025	0.227	0.0011	89.27	1.55E+00	0.088
8878.828	0.024	0.2281	0.001	89.67	1.56E+00	0.086
9133.249	0.023	0.2291	0.001	90.07	1.55E+00	0.083
9389.616	0.023	0.2301	0.001	90.46	1.53E+00	0.080
9647.929	0.022	0.231	0.0009	90.83	1.52E+00	0.077
9908.586	0.022	0.2319	0.0009	91.19	1.51E+00	0.075
10171.24	0.021	0.2328	0.0009	91.53	1.51E+00	0.073
10435.54	0.020	0.2335	0.0008	91.83	1.51E+00	0.071
10701.888	0.020	0.2342	0.0007	92.11	1.50E+00	0.069
10970.678	0.019	0.2349	0.0007	92.37	1.49E+00	0.067
11241.515	0.019	0.2356	0.0006	92.62	1.49E+00	0.065

Appendix Table 2 (Continued)

Pressure	Pore Diameter	Volume Intruded	Delta Volume	% Volume Intruded	Dv(d)	-dV/d(log d)
[PSI]	[μm]	[cc/g]	[cc/g]	%	[cc/(μm-g)]	[cc/g]
11513.999	0.019	0.2362	0.0006	92.87	1.48E+00	0.063
11794.864	0.018	0.2368	0.0007	93.13	1.47E+00	0.061
12083.563	0.018	0.2375	0.0007	93.38	1.48E+00	0.061
12380.796	0.017	0.2381	0.0006	93.63	1.50E+00	0.060
12686.709	0.017	0.2387	0.0006	93.88	1.53E+00	0.060
12994.919	0.016	0.2394	0.0006	94.12	1.56E+00	0.059
13305.223	0.016	0.2399	0.0006	94.35	1.58E+00	0.059
13617.574	0.016	0.2405	0.0006	94.58	1.59E+00	0.058
13938.457	0.015	0.2411	0.0006	94.82	1.59E+00	0.056
14267.921	0.015	0.2417	0.0006	95.04	1.60E+00	0.055
14606.416	0.015	0.2423	0.0006	95.27	1.59E+00	0.054
14947.407	0.014	0.2428	0.0005	95.48	1.57E+00	0.052
15284.309	0.014	0.2433	0.0005	95.68	1.55E+00	0.049
15617.066	0.014	0.2438	0.0004	95.85	1.51E+00	0.047
15945.534	0.013	0.2442	0.0004	96.01	1.46E+00	0.044
16269.56	0.013	0.2446	0.0004	96.16	1.41E+00	0.042
16595.031	0.013	0.2449	0.0003	96.29	1.37E+00	0.040
16923.049	0.013	0.2452	0.0003	96.4	1.33E+00	0.038
17253.463	0.012	0.2454	0.0003	96.51	1.29E+00	0.037
17579.533	0.012	0.2457	0.0002	96.61	1.26E+00	0.035
17900.965	0.012	0.2459	0.0002	96.71	1.23E+00	0.034
18217.406	0.012	0.2462	0.0003	96.81	1.22E+00	0.033
18535.795	0.012	0.2465	0.0002	96.91	1.23E+00	0.033
18855.93	0.011	0.2467	0.0002	97	1.26E+00	0.033
19178.109	0.011	0.2469	0.0002	97.09	1.29E+00	0.033
19502.137	0.011	0.2471	0.0002	97.18	1.33E+00	0.034
19827.857	0.011	0.2474	0.0002	97.27	1.36E+00	0.034
20155.377	0.011	0.2476	0.0003	97.37	1.36E+00	0.033
20480.252	0.010	0.2479	0.0003	97.48	1.37E+00	0.033
20806.223	0.010	0.2481	0.0002	97.57	1.38E+00	0.033
21133.992	0.010	0.2484	0.0002	97.67	1.39E+00	0.032
21463.107	0.010	0.2486	0.0002	97.75	1.41E+00	0.032
21794.119	0.010	0.2488	0.0002	97.83	1.41E+00	0.032
22126.877	0.010	0.249	0.0002	97.91	1.41E+00	0.031
22461.633	0.009	0.2492	0.0002	97.98	1.40E+00	0.031
22798.086	0.009	0.2494	0.0002	98.05	1.42E+00	0.031

Appendix Table 2 (Continued)

Pressure	Pore Diameter	Volume Intruded	Delta Volume	% Volume Intruded	Dv(d)	-dV/d(log d)
[PSI]	[µm]	[cc/g]	[cc/g]	%	[cc/(µm-g)]	[cc/g]
23136.33	0.009	0.2495	0.0002	98.12	1.45E+00	0.031
23476.67	0.009	0.2497	0.0002	98.19	1.48E+00	0.031
23819.16	0.009	0.2499	0.0002	98.27	1.54E+00	0.032
24167.482	0.009	0.2501	0.0002	98.35	1.59E+00	0.033
24518.305	0.009	0.2503	0.0002	98.44	1.66E+00	0.034
24870.721	0.009	0.2506	0.0002	98.53	1.74E+00	0.035
25225.533	0.008	0.2508	0.0002	98.62	1.82E+00	0.036
25582.193	0.008	0.251	0.0002	98.7	1.90E+00	0.037
25940.596	0.008	0.2512	0.0002	98.79	1.97E+00	0.038
26301.398	0.008	0.2515	0.0002	98.88	2.01E+00	0.038
26663.943	0.008	0.2517	0.0002	98.98	2.01E+00	0.037
27028.783	0.008	0.252	0.0002	99.07	2.02E+00	0.037
27395.67	0.008	0.2522	0.0002	99.16	1.99E+00	0.036
27764.061	0.008	0.2524	0.0002	99.25	1.97E+00	0.035
28134.637	0.008	0.2526	0.0002	99.33	1.96E+00	0.034
28507.211	0.007	0.2528	0.0002	99.4	1.91E+00	0.033
28882.131	0.007	0.253	0.0002	99.47	1.86E+00	0.032
29258.6	0.007	0.2531	0.0002	99.53	1.78E+00	0.030
29637.158	0.007	0.2533	0.0002	99.58	1.72E+00	0.029
30018.219	0.007	0.2534	0.0002	99.65	1.67E+00	0.027
30400.721	0.007	0.2536	0.0001	99.7	1.64E+00	0.027
30785.273	0.007	0.2537	0.0001	99.75	1.61E+00	0.026
31138.387	0.007	0.2538	0.0001	99.8	1.54E+00	0.024
31515.826	0.007	0.2539	0.0001	99.85	1.55E+00	0.024
31892.219	0.007	0.2541	0.0001	99.9	1.55E+00	0.024
32262.369	0.007	0.2542	0.0001	99.95	1.53E+00	0.023
32606.834	0.007	0.2543	0.0001	99.99	1.54E+00	0.023
32757.2230	0.007	0.2543	0	100.00	1.53E+00	0.022

Appendix Table 3 Pore Size Distribution By Volume – Intrusion for GS-30-Normal curing

Pressure	Pore Diameter	Volume Intruded	Delta Volume	% Volume Intruded	Dv(d)	-dV/d(log d)
[PSI]	[μm]	[cc/g]	[cc/g]	%	[cc/(μm-g)]	[cc/g]
1.076	1.982E+02	0	0	0	1.11E-05	7.121E-03
1.413	1.510E+02	0.0026	0.0026	0.82	1.42E-05	7.580E-03
1.783	1.196E+02	0.0033	0.0008	1.06	2.12E-05	7.167E-03
2.175	9.806E+01	0.0037	0.0004	1.18	2.99E-05	6.837E-03
2.573	8.290E+01	0.0041	0.0003	1.28	4.00E-05	6.609E-03
2.952	7.226E+01	0.0043	0.0003	1.37	5.08E-05	6.456E-03
3.322	6.421E+01	0.0048	0.0005	1.53	6.73E-05	6.901E-03
3.68	5.796E+01	0.005	0.0002	1.59	4.61E-05	5.429E-03
4.024	5.301E+01	0.0052	0.0002	1.64	4.57E-05	5.259E-03
4.37	4.881E+01	0.0054	0.0002	1.7	4.92E-05	5.246E-03
4.715	4.524E+01	0.0055	0.0002	1.75	5.31E-05	5.219E-03
5.059	4.217E+01	0.0057	0.0001	1.79	5.69E-05	5.178E-03
5.402	3.949E+01	0.0058	0.0002	1.85	5.08E-05	4.516E-03
5.743	3.714E+01	0.006	0.0001	1.89	5.31E-05	4.420E-03
6.083	3.507E+01	0.0061	0.0001	1.93	5.56E-05	4.344E-03
6.423	3.321E+01	0.0062	0.0001	1.96	5.56E-05	4.058E-03
6.779	3.147E+01	0.0063	0.0001	1.99	5.46E-05	3.742E-03
7.136	2.990E+01	0.0064	0.0001	2.01	5.48E-05	3.576E-03
7.492	2.847E+01	0.0064	0.0001	2.03	5.14E-05	3.200E-03
7.848	2.718E+01	0.0065	0.0001	2.05	4.75E-05	2.840E-03
8.205	2.600E+01	0.0065	0	2.06	4.54E-05	2.609E-03
8.563	2.491E+01	0.0065	0	2.07	4.48E-05	2.496E-03
8.92	2.392E+01	0.0066	0.0001	2.09	4.38E-05	2.387E-03
9.277	2.299E+01	0.0066	0	2.1	4.49E-05	2.379E-03
9.634	2.214E+01	0.0067	0	2.1	4.56E-05	2.351E-03
9.974	2.139E+01	0.0067	0	2.11	4.56E-05	2.305E-03
10.316	2.068E+01	0.0067	0	2.13	5.18E-05	2.537E-03
10.66	2.001E+01	0.0068	0	2.14	5.86E-05	2.776E-03
11.004	1.939E+01	0.0068	0	2.15	5.85E-05	2.690E-03
11.365	1.877E+01	0.0068	0	2.16	6.22E-05	2.744E-03
11.743	1.817E+01	0.0069	0	2.18	6.62E-05	2.798E-03
12.121	1.760E+01	0.0069	0.0001	2.19	7.00E-05	2.835E-03
12.497	1.707E+01	0.007	0.0001	2.21	6.90E-05	2.686E-03
12.872	1.657E+01	0.007	0	2.22	6.76E-05	2.535E-03
13.246	1.610E+01	0.007	0	2.23	6.56E-05	2.377E-03

Appendix Table 3 (Continued)

Pressure	Pore Diameter	Volume Intruded	Delta Volume	% Volume Intruded	Dv(d)	-dV/d(log d)
[PSI]	[µm]	[cc/g]	[cc/g]	%	[cc/(µm-g)]	[cc/g]
13.619	1.566E+01	0.0071	0	2.24	6.35E-05	2.227E-03
14.009	1.523E+01	0.0071	0	2.25	6.71E-05	2.322E-03
14.396	1.482E+01	0.0071	0	2.25	6.48E-05	2.206E-03
14.779	1.443E+01	0.0071	0	2.25	6.18E-05	2.083E-03
15.161	1.407E+01	0.0071	0	2.26	6.51E-05	2.148E-03
15.542	1.373E+01	0.0072	0	2.26	6.89E-05	2.225E-03
15.921	1.340E+01	0.0072	0	2.28	7.31E-05	2.316E-03
16.298	1.309E+01	0.0072	0	2.28	7.83E-05	2.432E-03
16.672	1.279E+01	0.0073	0	2.29	8.78E-05	2.650E-03
17.045	1.252E+01	0.0073	0	2.3	1.08E-04	3.197E-03
17.401	1.226E+01	0.0073	0	2.31	1.30E-04	3.755E-03
17.739	1.203E+01	0.0073	0	2.32	1.53E-04	4.324E-03
18.06	1.181E+01	0.0074	0	2.33	1.55E-04	4.318E-03
18.381	1.161E+01	0.0074	0	2.34	1.63E-04	4.431E-03
18.703	1.141E+01	0.0074	0.0001	2.35	1.71E-04	4.545E-03
19.023	1.121E+01	0.0075	0.0001	2.37	1.79E-04	4.659E-03
19.343	1.103E+01	0.0076	0.0001	2.39	1.86E-04	4.744E-03
19.66	1.085E+01	0.0076	0	2.4	1.93E-04	4.828E-03
19.976	1.068E+01	0.0076	0	2.4	1.91E-04	4.663E-03
20.291	1.051E+01	0.0076	0	2.41	1.88E-04	4.492E-03
20.605	1.035E+01	0.0077	0	2.42	1.75E-04	4.234E-03
20.932	1.019E+01	0.0077	0	2.43	1.91E-04	5.352E-03
21.248	1.004E+01	0.0077	0	2.44	2.28E-04	8.271E-03
22.445	9.504E+00	0.0078	0	2.45	2.97E-04	1.317E-02
25.403	8.397E+00	0.0078	0.0001	2.48	4.01E-04	1.870E-02
32.02	6.662E+00	0.0083	0.0004	2.62	6.21E-04	2.494E-02
43.493	4.905E+00	0.0109	0.0026	3.44	1.13E-03	3.233E-02
61.071	3.493E+00	0.0167	0.0058	5.29	2.25E-03	4.122E-02
86.8	2.458E+00	0.0256	0.0088	8.08	4.63E-03	5.181E-02
124.671	1.711E+00	0.0357	0.0102	11.3	9.92E-03	6.475E-02
176.931	1.206E+00	0.0468	0.011	14.79	2.11E-02	7.982E-02
244.727	8.717E-01	0.0588	0.012	18.59	4.20E-02	9.682E-02
328.209	6.500E-01	0.0718	0.013	22.69	7.28E-02	1.124E-01
427.552	4.989E-01	0.0856	0.0139	27.07	1.11E-01	1.243E-01
541.965	3.936E-01	0.1005	0.0148	31.76	1.53E-01	1.326E-01

Appendix Table 3 (Continued)

Pressure	Pore Diameter	Volume Intruded	Delta Volume	% Volume Intruded	Dv(d)	-dV/d(log d)
[PSI]	[µm]	[cc/g]	[cc/g]	%	[cc/(µm-g)]	[cc/g]
671.146	3.178E-01	0.116	0.0156	36.67	2.05E-01	1.403E-01
813.5	2.622E-01	0.132	0.016	41.72	2.68E-01	1.479E-01
967.929	2.204E-01	0.1464	0.0144	46.27	3.39E-01	1.547E-01
1133.834	1.881E-01	0.1581	0.0117	49.98	4.16E-01	1.601E-01
1309.219	1.629E-01	0.1674	0.0093	52.93	4.94E-01	1.636E-01
1490.093	1.432E-01	0.1759	0.0084	55.59	5.63E-01	1.643E-01
1675.008	1.274E-01	0.1838	0.0079	58.09	6.18E-01	1.624E-01
1862.319	1.145E-01	0.1912	0.0074	60.42	6.53E-01	1.582E-01
2051.825	1.040E-01	0.1979	0.0068	62.56	6.82E-01	1.537E-01
2244.225	9.505E-02	0.2041	0.0062	64.53	7.21E-01	1.511E-01
2439.718	8.744E-02	0.2096	0.0055	66.26	7.73E-01	1.497E-01
2637.606	8.088E-02	0.2146	0.005	67.84	8.26E-01	1.482E-01
2837.241	7.519E-02	0.2192	0.0046	69.28	8.73E-01	1.462E-01
3039.521	7.018E-02	0.2234	0.0042	70.63	9.13E-01	1.435E-01
3243.547	6.577E-02	0.2274	0.004	71.88	9.51E-01	1.408E-01
3449.867	6.183E-02	0.231	0.0036	73.02	9.87E-01	1.384E-01
3658.683	5.831E-02	0.2344	0.0034	74.1	1.03E+00	1.369E-01
3869.395	5.513E-02	0.2377	0.0033	75.12	1.08E+00	1.359E-01
4082.901	5.225E-02	0.2407	0.003	76.09	1.12E+00	1.344E-01
4299.051	4.962E-02	0.2437	0.003	77.02	1.17E+00	1.330E-01
4517.348	4.722E-02	0.2465	0.0029	77.92	1.21E+00	1.314E-01
4737.09	4.503E-02	0.2493	0.0028	78.81	1.26E+00	1.306E-01
4959.079	4.302E-02	0.252	0.0027	79.66	1.32E+00	1.304E-01
5183.662	4.115E-02	0.2545	0.0024	80.43	1.37E+00	1.301E-01
5410.141	3.943E-02	0.2568	0.0024	81.18	1.43E+00	1.300E-01
5639.465	3.783E-02	0.259	0.0022	81.88	1.48E+00	1.295E-01
5870.334	3.634E-02	0.2612	0.0022	82.58	1.53E+00	1.287E-01
6103.549	3.495E-02	0.2634	0.0022	83.27	1.58E+00	1.272E-01
6338.111	3.366E-02	0.2656	0.0021	83.95	1.62E+00	1.257E-01
6574.57	3.245E-02	0.2676	0.0021	84.6	1.67E+00	1.250E-01
6812.675	3.131E-02	0.2696	0.002	85.22	1.72E+00	1.241E-01
7053.074	3.025E-02	0.2715	0.0019	85.81	1.77E+00	1.235E-01
7295.67	2.924E-02	0.2732	0.0017	86.36	1.81E+00	1.222E-01
7540.361	2.829E-02	0.2749	0.0017	86.9	1.84E+00	1.199E-01
7787.098	2.739E-02	0.2766	0.0017	87.43	1.86E+00	1.175E-01

Appendix Table 3 (Continued)

Pressure	Pore Diameter	Volume Intruded	Delta Volume	% Volume Intruded	Dv(d)	-dV/d(log d)
[PSI]	[μm]	[cc/g]	[cc/g]	%	[cc/(μm-g)]	[cc/g]
8035.881	2.655E-02	0.2782	0.0016	87.94	1.88E+00	1.153E-01
8285.86	2.575E-02	0.2798	0.0016	88.43	1.90E+00	1.128E-01
8538.187	2.498E-02	0.2812	0.0015	88.89	1.92E+00	1.104E-01
8792.059	2.426E-02	0.2825	0.0013	89.31	1.94E+00	1.084E-01
9048.575	2.358E-02	0.2838	0.0013	89.72	1.96E+00	1.064E-01
9306.639	2.292E-02	0.2851	0.0013	90.12	1.97E+00	1.039E-01
9567.196	2.230E-02	0.2863	0.0012	90.5	1.98E+00	1.016E-01
9829.352	2.170E-02	0.2875	0.0011	90.86	1.98E+00	9.918E-02
10093.652	2.113E-02	0.2886	0.0011	91.22	1.99E+00	9.724E-02
10359.749	2.059E-02	0.2897	0.0011	91.56	2.01E+00	9.566E-02
10627.79	2.007E-02	0.2907	0.001	91.89	2.02E+00	9.347E-02
10897.879	1.957E-02	0.2917	0.001	92.2	2.01E+00	9.050E-02
11170.363	1.910E-02	0.2927	0.001	92.51	2.00E+00	8.779E-02
11444.992	1.864E-02	0.2936	0.001	92.81	1.99E+00	8.515E-02
11721.467	1.820E-02	0.2945	0.0009	93.1	1.97E+00	8.228E-02
12006.375	1.777E-02	0.2954	0.0008	93.36	1.94E+00	7.907E-02
12293.178	1.735E-02	0.2961	0.0007	93.59	1.91E+00	7.617E-02
12582.178	1.695E-02	0.2968	0.0007	93.82	1.88E+00	7.293E-02
12873.272	1.657E-02	0.2975	0.0007	94.03	1.83E+00	6.961E-02
13166.413	1.620E-02	0.2981	0.0006	94.23	1.78E+00	6.596E-02
13461.548	1.585E-02	0.2987	0.0006	94.42	1.72E+00	6.268E-02
13758.631	1.550E-02	0.2993	0.0006	94.6	1.68E+00	6.003E-02
14064.146	1.517E-02	0.2998	0.0005	94.77	1.66E+00	5.808E-02
14378.69	1.484E-02	0.3003	0.0005	94.94	1.65E+00	5.631E-02
14695.581	1.452E-02	0.3008	0.0005	95.09	1.64E+00	5.501E-02
15014.568	1.421E-02	0.3013	0.0005	95.24	1.64E+00	5.375E-02
15328.915	1.392E-02	0.3018	0.0005	95.38	1.64E+00	5.282E-02
15645.706	1.363E-02	0.3022	0.0005	95.52	1.64E+00	5.159E-02
15963.744	1.336E-02	0.3026	0.0004	95.66	1.65E+00	5.103E-02
16283.929	1.310E-02	0.3031	0.0005	95.81	1.67E+00	5.076E-02
16605.908	1.285E-02	0.3035	0.0004	95.95	1.73E+00	5.143E-02
16937.969	1.259E-02	0.304	0.0004	96.09	1.78E+00	5.194E-02
17271.924	1.235E-02	0.3044	0.0004	96.22	1.83E+00	5.259E-02
17601.592	1.212E-02	0.3048	0.0004	96.35	1.89E+00	5.326E-02
17926.516	1.190E-02	0.3052	0.0004	96.47	1.96E+00	5.403E-02

Appendix Table 3 (Continued)

Pressure	Pore Diameter	Volume Intruded	Delta Volume	% Volume Intruded	Dv(d)	-dV/d(log d)
[PSI]	[µm]	[cc/g]	[cc/g]	%	[cc/(µm-g)]	[cc/g]
18252.635	1.169E-02	0.3057	0.0005	96.62	2.00E+00	5.423E-02
18581.002	1.148E-02	0.3061	0.0004	96.76	2.05E+00	5.453E-02
18911.316	1.128E-02	0.3065	0.0004	96.89	2.10E+00	5.496E-02
19243.127	1.109E-02	0.307	0.0004	97.03	2.17E+00	5.578E-02
19577.381	1.090E-02	0.3074	0.0004	97.17	2.22E+00	5.588E-02
19913.184	1.071E-02	0.3078	0.0004	97.3	2.26E+00	5.584E-02
20250.932	1.053E-02	0.3082	0.0004	97.43	2.23E+00	5.417E-02
20578.75	1.037E-02	0.3086	0.0004	97.55	2.21E+00	5.263E-02
20908.363	1.020E-02	0.309	0.0004	97.68	2.16E+00	5.072E-02
21239.674	1.004E-02	0.3094	0.0004	97.79	2.10E+00	4.841E-02
21572.434	9.889E-03	0.3097	0.0003	97.9	2.04E+00	4.626E-02
21907.287	9.737E-03	0.31	0.0003	97.98	1.97E+00	4.402E-02
22244.035	9.590E-03	0.3102	0.0003	98.06	1.94E+00	4.263E-02
22582.383	9.446E-03	0.3105	0.0002	98.14	1.88E+00	4.080E-02
22923.074	9.306E-03	0.3107	0.0002	98.2	1.83E+00	3.930E-02
23265.312	9.169E-03	0.3109	0.0002	98.28	1.81E+00	3.829E-02
23609.549	9.035E-03	0.3111	0.0002	98.34	1.80E+00	3.779E-02
23955.977	8.905E-03	0.3114	0.0003	98.42	1.84E+00	3.812E-02
24308.094	8.776E-03	0.3116	0.0002	98.49	1.86E+00	3.788E-02
24662.508	8.650E-03	0.3118	0.0003	98.57	1.91E+00	3.837E-02
25018.617	8.527E-03	0.3121	0.0003	98.65	1.97E+00	3.901E-02
25376.773	8.406E-03	0.3124	0.0003	98.74	2.00E+00	3.890E-02
25737.523	8.288E-03	0.3126	0.0003	98.82	2.08E+00	3.992E-02
26099.717	8.173E-03	0.3129	0.0002	98.89	2.08E+00	3.924E-02
26464.211	8.061E-03	0.3131	0.0003	98.97	2.13E+00	3.975E-02
26830.949	7.951E-03	0.3133	0.0002	99.05	2.15E+00	3.950E-02
27199.682	7.843E-03	0.3135	0.0002	99.11	2.17E+00	3.925E-02
27570.461	7.737E-03	0.3138	0.0003	99.19	2.12E+00	3.780E-02
27943.283	7.634E-03	0.314	0.0002	99.25	2.07E+00	3.654E-02
28317.607	7.533E-03	0.3142	0.0002	99.32	2.09E+00	3.624E-02
28693.975	7.434E-03	0.3144	0.0002	99.39	2.08E+00	3.576E-02
29072.486	7.338E-03	0.3147	0.0002	99.46	2.08E+00	3.526E-02
29453.193	7.243E-03	0.3148	0.0002	99.51	2.13E+00	3.564E-02
29835.346	7.150E-03	0.315	0.0002	99.56	2.07E+00	3.422E-02
30219.5	7.059E-03	0.3152	0.0002	99.62	2.02E+00	3.289E-02

Appendix Table 3 (Continued)

Pressure	Pore Diameter	Volume Intruded	Delta Volume	% Volume Intruded	Dv(d)	-dV/d(log d)
[PSI]	[μm]	[cc/g]	[cc/g]	%	[cc/(μm-g)]	[cc/g]
30605.898	6.970E-03	0.3154	0.0002	99.69	2.05E+00	3.293E-02
30994.193	6.883E-03	0.3156	0.0002	99.75	2.01E+00	3.192E-02
31380.93	6.798E-03	0.3158	0.0002	99.81	2.01E+00	3.135E-02
31770.533	6.714E-03	0.3159	0.0001	99.86	2.06E+00	3.163E-02
32163.688	6.632E-03	0.316	0.0001	99.89	2.12E+00	3.193E-02
32558.537	6.552E-03	0.3162	0.0002	99.96	2.14E+00	3.165E-02
32959.203	6.472E-03	0.3164	0.0001	100	2.13E+00	3.085E-02

Appendix Table 4 Pore Size Distribution By Volume – Intrusion for GS-30-Steam curing

Pressure	Pore Diameter	Volume Intruded	Delta Volume	% Volume Intruded	Dv(d)	-dV/d(log d)
[PSI]	[µm]	[cc/g]	[cc/g]	%	[cc/(µm-g)]	[cc/g]
1.157	1.844E+02	0.0000	0.0000	0.00	1.018E-05	6.785E-03
1.491	1.431E+02	0.0013	0.0013	0.40	1.312E-05	7.322E-03
1.930	1.105E+02	0.0023	0.0010	0.71	2.098E-05	7.487E-03
2.354	9.062E+01	0.0029	0.0006	0.90	3.117E-05	7.444E-03
2.702	7.896E+01	0.0033	0.0004	1.03	4.074E-05	7.233E-03
3.030	7.041E+01	0.0036	0.0003	1.12	4.941E-05	7.060E-03
3.361	6.347E+01	0.0041	0.0005	1.26	6.348E-05	7.525E-03
3.687	5.785E+01	0.0045	0.0003	1.37	5.863E-05	6.887E-03
4.005	5.326E+01	0.0047	0.0003	1.45	5.811E-05	6.546E-03
4.317	4.942E+01	0.0049	0.0002	1.50	6.020E-05	6.378E-03
4.607	4.630E+01	0.0050	0.0002	1.55	6.466E-05	6.502E-03
4.879	4.372E+01	0.0052	0.0001	1.59	7.009E-05	6.714E-03
5.151	4.141E+01	0.0053	0.0001	1.62	6.833E-05	6.417E-03
5.422	3.934E+01	0.0054	0.0001	1.66	6.878E-05	6.274E-03
5.694	3.746E+01	0.0055	0.0001	1.69	7.217E-05	6.360E-03
5.949	3.586E+01	0.0057	0.0002	1.74	7.907E-05	6.698E-03
6.203	3.439E+01	0.0058	0.0002	1.78	8.668E-05	7.073E-03
6.458	3.303E+01	0.0059	0.0001	1.82	9.482E-05	7.429E-03
6.732	3.169E+01	0.0061	0.0001	1.86	1.045E-04	7.834E-03
7.005	3.045E+01	0.0062	0.0001	1.91	1.144E-04	8.191E-03
7.279	2.931E+01	0.0064	0.0002	1.95	1.258E-04	8.628E-03
7.551	2.825E+01	0.0065	0.0002	2.00	1.293E-04	8.501E-03
7.823	2.727E+01	0.0067	0.0001	2.04	1.322E-04	8.362E-03
8.095	2.635E+01	0.0068	0.0001	2.08	1.394E-04	8.520E-03
8.384	2.544E+01	0.0069	0.0001	2.13	1.488E-04	8.776E-03
8.672	2.460E+01	0.0071	0.0002	2.17	1.556E-04	8.854E-03
8.961	2.381E+01	0.0072	0.0001	2.20	1.566E-04	8.586E-03
9.249	2.306E+01	0.0073	0.0001	2.23	1.561E-04	8.264E-03
9.555	2.233E+01	0.0074	0.0001	2.27	1.564E-04	7.993E-03
9.842	2.167E+01	0.0075	0.0001	2.31	1.529E-04	7.544E-03
10.111	2.110E+01	0.0076	0.0001	2.34	1.493E-04	7.155E-03
10.380	2.055E+01	0.0077	0.0001	2.36	1.403E-04	6.560E-03
10.665	2.000E+01	0.0078	0.0001	2.38	1.437E-04	6.542E-03
10.950	1.948E+01	0.0078	0.0001	2.40	1.464E-04	6.479E-03

Appendix Table 4 (Continued)

Pressure	Pore Diameter	Volume Intruded	Delta Volume	% Volume Intruded	Dv(d)	-dV/d(log d)
[PSI]	[µm]	[cc/g]	[cc/g]	%	[cc/(µm-g)]	[cc/g]
11.217	1.902E+01	0.0079	0.0000	2.42	1.368E-04	5.886E-03
11.466	1.860E+01	0.0079	0.0000	2.43	1.235E-04	5.206E-03
11.715	1.821E+01	0.008	0.0000	2.44	1.113E-04	4.609E-03
11.965	1.783E+01	0.008	0.0001	2.46	1.101E-04	4.493E-03
12.231	1.744E+01	0.0081	0.0001	2.48	1.097E-04	4.408E-03
12.495	1.707E+01	0.0081	0.0000	2.48	1.086E-04	4.295E-03
12.774	1.670E+01	0.0081	0.0000	2.49	1.120E-04	4.341E-03
13.069	1.632E+01	0.0081	0.0000	2.50	1.148E-04	4.361E-03
13.362	1.597E+01	0.0082	0.0000	2.51	1.205E-04	4.471E-03
13.653	1.563E+01	0.0082	0.0000	2.53	1.135E-04	4.125E-03
13.958	1.528E+01	0.0083	0.0000	2.54	1.072E-04	3.823E-03
14.264	1.496E+01	0.0083	0.0000	2.56	1.149E-04	3.998E-03
14.568	1.464E+01	0.0084	0.0000	2.57	1.235E-04	4.187E-03
14.887	1.433E+01	0.0084	0.0000	2.58	1.329E-04	4.392E-03
15.206	1.403E+01	0.0084	0.0000	2.59	1.276E-04	4.102E-03
15.506	1.376E+01	0.0085	0.0000	2.60	1.215E-04	3.812E-03
15.790	1.351E+01	0.0085	0.0000	2.61	1.200E-04	3.703E-03
16.074	1.327E+01	0.0085	0.0000	2.62	1.174E-04	3.569E-03
16.357	1.304E+01	0.0086	0.0000	2.63	1.138E-04	3.411E-03
16.624	1.283E+01	0.0086	0.0000	2.63	1.153E-04	3.429E-03
16.875	1.264E+01	0.0086	0.0000	2.64	1.244E-04	3.649E-03
17.125	1.246E+01	0.0086	0.0000	2.64	1.326E-04	3.837E-03
17.391	1.227E+01	0.0086	0.0000	2.65	1.308E-04	3.734E-03
17.671	1.207E+01	0.0087	0.0000	2.66	1.295E-04	3.647E-03
17.948	1.189E+01	0.0087	0.0000	2.67	1.300E-04	3.617E-03
18.241	1.169E+01	0.0087	0.0000	2.68	1.328E-04	3.605E-03
18.546	1.150E+01	0.0088	0.0000	2.69	1.336E-04	3.534E-03
18.850	1.132E+01	0.0088	0.0000	2.70	1.275E-04	3.307E-03
19.137	1.115E+01	0.0088	0.0000	2.71	1.240E-04	3.202E-03
19.393	1.100E+01	0.0088	0.0000	2.71	1.488E-04	4.418E-03
20.132	1.060E+01	0.0089	0.0000	2.72	2.129E-04	8.255E-03
21.303	1.001E+01	0.0089	0.0000	2.73	3.036E-04	1.401E-02
23.889	8.930E+00	0.0089	0.0001	2.74	4.213E-04	2.023E-02
29.037	7.346E+00	0.0091	0.0002	2.80	6.445E-04	2.711E-02

Appendix Table 4 (Continued)

Pressure	Pore Diameter	Volume Intruded	Delta Volume	% Volume Intruded	Dv(d)	-dV/d(log d)
[PSI]	[µm]	[cc/g]	[cc/g]	%	[cc/(µm-g)]	[cc/g]
38.346	5.563E+00	0.0112	0.0020	3.42	1.121E-03	3.478E-02
50.916	4.190E+00	0.0170	0.0058	5.21	2.053E-03	4.352E-02
68.694	3.105E+00	0.0259	0.0089	7.93	3.893E-03	5.388E-02
96.022	2.222E+00	0.0365	0.0107	11.20	7.757E-03	6.595E-02
135.258	1.577E+00	0.0483	0.0118	14.81	1.594E-02	7.989E-02
188.500	1.132E+00	0.0609	0.0127	18.69	3.222E-02	9.576E-02
256.608	8.313E-01	0.0744	0.0135	22.82	5.855E-02	1.108E-01
339.835	6.277E-01	0.0885	0.0141	27.14	9.043E-02	1.206E-01
438.629	4.863E-01	0.1033	0.0148	31.69	1.254E-01	1.266E-01
551.844	3.866E-01	0.1187	0.0154	36.42	1.671E-01	1.317E-01
678.930	3.142E-01	0.1346	0.0159	41.30	2.165E-01	1.369E-01
818.340	2.607E-01	0.1494	0.0147	45.82	2.730E-01	1.418E-01
970.923	2.197E-01	0.1609	0.0116	49.37	3.354E-01	1.466E-01
1135.431	1.879E-01	0.1700	0.0091	52.17	4.021E-01	1.510E-01
1307.074	1.632E-01	0.1780	0.0079	54.60	4.679E-01	1.546E-01
1483.607	1.438E-01	0.1855	0.0075	56.89	5.263E-01	1.572E-01
1663.932	1.282E-01	0.1925	0.0071	59.06	5.718E-01	1.581E-01
1847.001	1.155E-01	0.1995	0.0069	61.19	6.132E-01	1.590E-01
2031.517	1.050E-01	0.2062	0.0068	63.27	6.745E-01	1.628E-01
2217.480	9.620E-02	0.2128	0.0066	65.30	7.565E-01	1.685E-01
2405.639	8.868E-02	0.2193	0.0064	67.27	8.498E-01	1.746E-01
2594.995	8.221E-02	0.2255	0.0062	69.17	9.454E-01	1.797E-01
2786.148	7.657E-02	0.2314	0.0059	70.98	1.045E+00	1.845E-01
2979.396	7.160E-02	0.2371	0.0057	72.74	1.139E+00	1.874E-01
3174.291	6.720E-02	0.2425	0.0054	74.41	1.226E+00	1.889E-01
3372.030	6.326E-02	0.2477	0.0052	75.99	1.305E+00	1.887E-01
3572.463	5.971E-02	0.2525	0.0048	77.47	1.373E+00	1.870E-01
3774.892	5.651E-02	0.2572	0.0046	78.90	1.436E+00	1.848E-01
3979.666	5.360E-02	0.2614	0.0042	80.20	1.492E+00	1.820E-01
4187.383	5.094E-02	0.2654	0.0040	81.42	1.534E+00	1.778E-01
4397.746	4.851E-02	0.2691	0.0036	82.54	1.569E+00	1.731E-01
4610.354	4.627E-02	0.2724	0.0034	83.57	1.596E+00	1.680E-01
4826.056	4.420E-02	0.2757	0.0033	84.57	1.620E+00	1.629E-01
5044.601	4.229E-02	0.2787	0.0031	85.51	1.627E+00	1.567E-01
5265.243	4.052E-02	0.2815	0.0028	86.37	1.634E+00	1.507E-01

Appendix Table 4 (Continued)

Pressure	Pore Diameter	Volume Intruded	Delta Volume	% Volume Intruded	Dv(d)	-dV/d(log d)
[PSI]	[μm]	[cc/g]	[cc/g]	%	[cc/(μm-g)]	[cc/g]
5487.979	3.887E-02	0.2842	0.0026	87.18	1.637E+00	1.449E-01
5712.912	3.734E-02	0.2866	0.0025	87.93	1.641E+00	1.396E-01
5939.740	3.591E-02	0.2889	0.0023	88.64	1.648E+00	1.348E-01
6168.614	3.458E-02	0.2910	0.0021	89.27	1.642E+00	1.294E-01
6399.833	3.333E-02	0.2929	0.0019	89.86	1.627E+00	1.237E-01
6632.948	3.216E-02	0.2947	0.0018	90.41	1.614E+00	1.184E-01
6868.458	3.106E-02	0.2964	0.0017	90.93	1.597E+00	1.132E-01
7106.165	3.002E-02	0.2981	0.0017	91.44	1.578E+00	1.082E-01
7345.866	2.904E-02	0.2996	0.0015	91.90	1.557E+00	1.034E-01
7587.264	2.812E-02	0.3009	0.0014	92.32	1.545E+00	9.931E-02
7830.907	2.724E-02	0.3022	0.0013	92.71	1.533E+00	9.553E-02
8076.996	2.641E-02	0.3034	0.0012	93.07	1.517E+00	9.170E-02
8324.730	2.563E-02	0.3045	0.0011	93.42	1.500E+00	8.799E-02
8574.610	2.488E-02	0.3056	0.0011	93.75	1.466E+00	8.354E-02
8826.486	2.417E-02	0.3066	0.0010	94.06	1.436E+00	7.945E-02
9079.760	2.349E-02	0.3076	0.0010	94.35	1.406E+00	7.553E-02
9335.528	2.285E-02	0.3085	0.0009	94.63	1.376E+00	7.184E-02
9592.843	2.224E-02	0.3093	0.0008	94.89	1.342E+00	6.812E-02
9852.353	2.165E-02	0.3100	0.0007	95.11	1.306E+00	6.445E-02
10113.859	2.109E-02	0.3107	0.0007	95.32	1.265E+00	6.077E-02
10377.762	2.056E-02	0.3113	0.0006	95.50	1.221E+00	5.720E-02
10643.808	2.004E-02	0.3119	0.0006	95.68	1.175E+00	5.372E-02
10911.801	1.955E-02	0.3124	0.0005	95.84	1.134E+00	5.065E-02
11181.740	1.908E-02	0.3129	0.0005	95.98	1.090E+00	4.763E-02
11453.624	1.862E-02	0.3133	0.0004	96.12	1.064E+00	4.550E-02
11727.405	1.819E-02	0.3137	0.0004	96.25	1.040E+00	4.346E-02
12003.431	1.777E-02	0.3141	0.0004	96.38	1.021E+00	4.176E-02
12281.053	1.737E-02	0.3145	0.0004	96.50	1.006E+00	4.031E-02
12567.406	1.697E-02	0.3149	0.0004	96.62	1.004E+00	3.938E-02
12861.494	1.659E-02	0.3153	0.0004	96.74	1.003E+00	3.851E-02
13164.466	1.620E-02	0.3157	0.0004	96.85	1.017E+00	3.819E-02
13475.818	1.583E-02	0.3161	0.0004	96.96	1.036E+00	3.806E-02
13796.004	1.546E-02	0.3164	0.0004	97.07	1.059E+00	3.802E-02
14118.281	1.511E-02	0.3168	0.0004	97.19	1.090E+00	3.828E-02

Appendix Table 4 (Continued)

Pressure	Pore Diameter	Volume Intruded	Delta Volume	% Volume Intruded	Dv(d)	-dV/d(log d)
[PSI]	[μm]	[cc/g]	[cc/g]	%	[cc/(μm-g)]	[cc/g]
14442.657	1.477E-02	0.3172	0.0004	97.30	1.128E+00	3.880E-02
14769.079	1.444E-02	0.3175	0.0004	97.41	1.157E+00	3.892E-02
15097.994	1.413E-02	0.3179	0.0004	97.53	1.203E+00	3.959E-02
15428.656	1.383E-02	0.3183	0.0004	97.65	1.252E+00	4.030E-02
15761.616	1.353E-02	0.3187	0.0004	97.77	1.300E+00	4.091E-02
16089.934	1.326E-02	0.3191	0.0004	97.89	1.338E+00	4.116E-02
16414.508	1.300E-02	0.3194	0.0004	98.00	1.382E+00	4.159E-02
16734.492	1.275E-02	0.3198	0.0004	98.11	1.398E+00	4.116E-02
17049.686	1.251E-02	0.3202	0.0004	98.22	1.387E+00	3.997E-02
17359.791	1.229E-02	0.3205	0.0003	98.32	1.372E+00	3.872E-02
17671.992	1.207E-02	0.3208	0.0003	98.42	1.327E+00	3.669E-02
17986.689	1.186E-02	0.3211	0.0003	98.51	1.269E+00	3.441E-02
18303.080	1.165E-02	0.3214	0.0003	98.59	1.227E+00	3.261E-02
18620.670	1.146E-02	0.3216	0.0002	98.65	1.157E+00	3.018E-02
18940.605	1.126E-02	0.3218	0.0002	98.71	1.088E+00	2.790E-02
19261.986	1.107E-02	0.3219	0.0002	98.76	1.020E+00	2.574E-02
19585.512	1.089E-02	0.3221	0.0001	98.80	9.468E-01	2.353E-02
19910.787	1.071E-02	0.3222	0.0002	98.85	8.738E-01	2.144E-02
20236.758	1.054E-02	0.3223	0.0001	98.88	8.297E-01	2.012E-02
20561.383	1.037E-02	0.3225	0.0001	98.92	8.114E-01	1.942E-02
20888.305	1.021E-02	0.3226	0.0001	98.96	7.974E-01	1.884E-02
21216.320	1.005E-02	0.3227	0.0001	99.00	8.066E-01	1.879E-02
21545.686	9.901E-03	0.3228	0.0001	99.03	8.097E-01	1.856E-02
21877.199	9.751E-03	0.3229	0.0001	99.07	8.117E-01	1.835E-02
22211.006	9.604E-03	0.3231	0.0001	99.11	8.331E-01	1.854E-02
22545.908	9.462E-03	0.3232	0.0001	99.15	8.396E-01	1.840E-02
22883.057	9.322E-03	0.3233	0.0001	99.19	8.391E-01	1.810E-02
23221.803	9.186E-03	0.3234	0.0001	99.22	8.661E-01	1.840E-02
23562.693	9.053E-03	0.3235	0.0001	99.26	8.791E-01	1.839E-02
23905.877	8.923E-03	0.3237	0.0001	99.30	8.913E-01	1.839E-02
24254.205	8.795E-03	0.3238	0.0001	99.33	9.258E-01	1.888E-02
24604.227	8.670E-03	0.3239	0.0001	99.36	9.460E-01	1.905E-02
24956.494	8.548E-03	0.3240	0.0001	99.39	9.664E-01	1.920E-02
25310.457	8.428E-03	0.3241	0.0001	99.43	9.961E-01	1.950E-02
25666.619	8.311E-03	0.3242	0.0001	99.46	1.002E+00	1.931E-02
26024.674	8.197E-03	0.3244	0.0002	99.51	1.007E+00	1.912E-02

Appendix Table 4 (Continued)

Pressure	Pore Diameter	Volume Intruded	Delta Volume	% Volume Intruded	Dv(d)	-dV/d(log d)
[PSI]	[µm]	[cc/g]	[cc/g]	%	[cc/(µm-g)]	[cc/g]
26384.873	8.085E-03	0.3245	0.0001	99.55	1.029E+00	1.927E-02
26747.221	7.975E-03	0.3246	0.0001	99.59	1.062E+00	1.957E-02
27111.857	7.868E-03	0.3247	0.0001	99.62	1.067E+00	1.939E-02
27478.000	7.763E-03	0.3248	0.0001	99.65	1.081E+00	1.935E-02
27846.482	7.661E-03	0.3249	0.0001	99.68	1.067E+00	1.881E-02
28217.314	7.560E-03	0.3250	0.0001	99.72	1.002E+00	1.742E-02
28589.689	7.462E-03	0.3251	0.0001	99.75	9.641E-01	1.653E-02
28964.561	7.365E-03	0.3252	0.0001	99.78	9.233E-01	1.563E-02
29341.477	7.270E-03	0.3253	0.0001	99.81	9.024E-01	1.510E-02
29720.287	7.178E-03	0.3254	0.0001	99.83	9.110E-01	1.506E-02
30100.596	7.087E-03	0.3255	0.0001	99.85	9.174E-01	1.499E-02
30483.201	6.998E-03	0.3255	0.0001	99.87	9.064E-01	1.465E-02
30867.455	6.911E-03	0.3256	0.0001	99.89	8.540E-01	1.362E-02
31250.604	6.826E-03	0.3257	0.0001	99.91	8.465E-01	1.327E-02
31636.139	6.743E-03	0.3258	0.0001	99.94	8.320E-01	1.283E-02
32024.387	6.661E-03	0.3258	0.0001	99.96	8.414E-01	1.275E-02
32413.818	6.581E-03	0.3259	0.0001	99.99	8.872E-01	1.319E-02
32806.617	6.502E-03	0.3260	0.0000	100.00	9.207E-01	1.343E-02

Appendix Table 5 Pore Size Distribution By Volume – Intrusion for GS-50/2-Normal curing

Pressure	Pore Diameter	Volume Intruded	Delta Volume	% Volume Intruded	Dv(d)	-dV/d(log d)
[PSI]	[µm]	[cc/g]	[cc/g]	%	[cc/(µm-g)]	[cc/g]
1.157	1.844E+02	0.0000	0.0000	0.00	6.321E-07	6.394E-04
1.491	1.431E+02	0.0000	0.0000	0.00	1.000E-06	8.078E-04
1.93	1.105E+02	0.0000	0.0000	0.00	1.891E-06	9.614E-04
2.354	9.062E+01	0.0000	0.0000	0.01	3.252E-06	1.108E-03
2.702	7.896E+01	0.0001	0.0000	0.02	4.865E-06	1.249E-03
3.03	7.041E+01	0.0002	0.0002	0.06	6.670E-06	1.399E-03
3.361	6.347E+01	0.0003	0.0001	0.09	9.606E-06	1.698E-03
3.687	5.785E+01	0.0004	0.0001	0.11	1.301E-05	1.962E-03
4.005	5.326E+01	0.0005	0.0001	0.14	1.709E-05	2.241E-03
4.317	4.942E+01	0.0005	0.0001	0.16	2.148E-05	2.510E-03
4.607	4.630E+01	0.0006	0.0001	0.19	2.400E-05	2.467E-03
4.879	4.372E+01	0.0007	0.0001	0.21	2.260E-05	2.184E-03
5.151	4.141E+01	0.0008	0.0001	0.23	2.261E-05	2.019E-03
5.422	3.934E+01	0.0008	0.0001	0.25	2.214E-05	1.834E-03
5.694	3.746E+01	0.0009	0.0001	0.28	2.107E-05	1.626E-03
5.949	3.586E+01	0.0009	0.0000	0.28	1.932E-05	1.397E-03
6.203	3.439E+01	0.0009	0.0000	0.28	1.661E-05	1.134E-03
6.476	3.294E+01	0.0009	0.0000	0.28	1.292E-05	8.345E-04
6.75	3.160E+01	0.0009	0.0000	0.28	9.377E-06	5.709E-04
7.023	3.037E+01	0.0009	0.0000	0.28	5.074E-06	2.920E-04
7.297	2.924E+01	0.0009	0.0000	0.28	0.000E+00	0.000E+00
7.569	2.818E+01	0.0009	0.0000	0.28	0.000E+00	0.000E+00
7.842	2.720E+01	0.0009	0.0000	0.28	0.000E+00	0.000E+00
8.113	2.629E+01	0.0009	0.0000	0.28	0.000E+00	0.000E+00
8.402	2.539E+01	0.0009	0.0000	0.28	0.000E+00	0.000E+00
8.691	2.455E+01	0.0009	0.0000	0.28	0.000E+00	0.000E+00
8.979	2.376E+01	0.0009	0.0000	0.28	0.000E+00	0.000E+00
9.267	2.302E+01	0.0009	0.0000	0.28	0.000E+00	0.000E+00
9.555	2.233E+01	0.0009	0.0000	0.28	0.000E+00	0.000E+00
9.86	2.163E+01	0.0009	0.0000	0.28	0.000E+00	0.000E+00
10.165	2.099E+01	0.0009	0.0000	0.28	0.000E+00	0.000E+00
10.468	2.038E+01	0.0009	0.0000	0.28	0.000E+00	0.000E+00
10.771	1.981E+01	0.0009	0.0000	0.28	0.000E+00	0.000E+00
11.073	1.926E+01	0.0009	0.0000	0.28	0.000E+00	0.000E+00

Appendix Table 5 (Continued)

Pressure	Pore Diameter	Volume Intruded	Delta Volume	% Volume Intruded	Dv(d)	-dV/d(log d)
[PSI]	[µm]	[cc/g]	[cc/g]	%	[cc/(µm-g)]	[cc/g]
11.358	1.878E+01	0.0009	0.0000	0.28	0.000E+00	0.000E+00
11.625	1.835E+01	0.0009	0.0000	0.28	0.000E+00	0.000E+00
11.892	1.794E+01	0.0009	0.0000	0.28	0.000E+00	0.000E+00
12.177	1.752E+01	0.0009	0.0000	0.28	0.000E+00	0.000E+00
12.477	1.710E+01	0.0009	0.0000	0.28	0.000E+00	0.000E+00
12.774	1.670E+01	0.0009	0.0000	0.28	0.000E+00	0.000E+00
13.069	1.632E+01	0.0009	0.0000	0.28	0.000E+00	0.000E+00
13.362	1.597E+01	0.0009	0.0000	0.28	0.000E+00	0.000E+00
13.653	1.563E+01	0.0009	0.0000	0.28	0.000E+00	0.000E+00
13.958	1.528E+01	0.0009	0.0000	0.28	0.000E+00	0.000E+00
14.264	1.496E+01	0.0009	0.0000	0.28	0.000E+00	0.000E+00
14.568	1.464E+01	0.0009	0.0000	0.28	0.000E+00	0.000E+00
14.887	1.433E+01	0.0009	0.0000	0.28	0.000E+00	0.000E+00
15.206	1.403E+01	0.0009	0.0000	0.28	0.000E+00	0.000E+00
15.506	1.376E+01	0.0009	0.0000	0.28	0.000E+00	0.000E+00
15.79	1.351E+01	0.0009	0.0000	0.28	0.000E+00	0.000E+00
16.074	1.327E+01	0.0009	0.0000	0.28	0.000E+00	0.000E+00
16.357	1.304E+01	0.0009	0.0000	0.28	0.000E+00	0.000E+00
16.624	1.283E+01	0.0009	0.0000	0.28	0.000E+00	0.000E+00
16.875	1.264E+01	0.0009	0.0000	0.28	0.000E+00	0.000E+00
17.125	1.246E+01	0.0009	0.0000	0.28	0.000E+00	0.000E+00
17.391	1.227E+01	0.0009	0.0000	0.28	0.000E+00	0.000E+00
17.671	1.207E+01	0.0009	0.0000	0.28	0.000E+00	0.000E+00
17.948	1.189E+01	0.0009	0.0000	0.28	0.000E+00	0.000E+00
18.241	1.169E+01	0.0009	0.0000	0.28	0.000E+00	0.000E+00
18.546	1.150E+01	0.0009	0.0000	0.28	0.000E+00	0.000E+00
18.85	1.132E+01	0.0009	0.0000	0.28	0.000E+00	0.000E+00
19.153	1.114E+01	0.0009	0.0000	0.28	0.000E+00	0.000E+00
19.456	1.096E+01	0.0009	0.0000	0.28	0.000E+00	0.000E+00
19.773	1.079E+01	0.0009	0.0000	0.28	0.000E+00	0.000E+00
20.09	1.062E+01	0.0009	0.0000	0.28	0.000E+00	0.000E+00
20.389	1.046E+01	0.0009	0.0000	0.28	1.563E-06	4.573E-05
20.687	1.031E+01	0.0009	0.0000	0.28	6.405E-06	2.067E-04
20.964	1.018E+01	0.0009	0.0000	0.28	2.562E-05	1.011E-03
21.659	9.849E+00	0.0009	0.0000	0.28	7.172E-05	3.502E-03

Appendix Table 5 (Continued)

Pressure	Pore Diameter	Volume Intruded	Delta Volume	% Volume Intruded	Dv(d)	-dV/d(log d)
[PSI]	[µm]	[cc/g]	[cc/g]	%	[cc/(µm-g)]	[cc/g]
23.022	9.266E+00	0.0009	0.0000	0.28	1.339E-04	7.433E-03
25.85	8.252E+00	0.0009	0.0000	0.28	2.185E-04	1.240E-02
32.006	6.665E+00	0.0011	0.0002	0.33	3.755E-04	1.837E-02
43.168	4.942E+00	0.0022	0.0011	0.69	7.313E-04	2.528E-02
60.436	3.530E+00	0.0062	0.0040	1.91	1.549E-03	3.342E-02
86.205	2.475E+00	0.0129	0.0067	3.95	3.388E-03	4.295E-02
122.985	1.735E+00	0.0214	0.0084	6.53	7.431E-03	5.429E-02
173.371	1.230E+00	0.0311	0.0098	9.52	1.584E-02	6.754E-02
238.895	8.930E-01	0.0417	0.0106	12.76	3.202E-02	8.297E-02
320.026	6.666E-01	0.0531	0.0114	16.23	5.853E-02	9.918E-02
417.074	5.115E-01	0.0651	0.0121	19.92	9.267E-02	1.127E-01
529.640	4.028E-01	0.0781	0.0129	23.88	1.337E-01	1.234E-01
657.125	3.246E-01	0.0918	0.0137	28.07	1.831E-01	1.326E-01
797.932	2.673E-01	0.1063	0.0145	32.49	2.413E-01	1.409E-01
950.565	2.244E-01	0.1205	0.0142	36.84	3.094E-01	1.492E-01
1113.975	1.915E-01	0.1326	0.0121	40.55	3.856E-01	1.568E-01
1286.516	1.658E-01	0.1426	0.0100	43.62	4.679E-01	1.639E-01
1465.344	1.456E-01	0.1515	0.0088	46.32	5.498E-01	1.691E-01
1648.663	1.294E-01	0.1595	0.0081	48.78	6.257E-01	1.723E-01
1834.477	1.163E-01	0.1673	0.0077	51.15	6.864E-01	1.726E-01
2022.635	1.055E-01	0.1746	0.0074	53.4	7.345E-01	1.710E-01
2212.590	9.641E-02	0.1817	0.0071	55.57	7.882E-01	1.701E-01
2404.142	8.873E-02	0.1883	0.0066	57.58	8.537E-01	1.705E-01
2598.588	8.209E-02	0.1944	0.0061	59.46	9.247E-01	1.711E-01
2794.880	7.633E-02	0.2	0.0055	61.14	9.948E-01	1.709E-01
2993.716	7.126E-02	0.205	0.0051	62.7	1.058E+00	1.696E-01
3195.596	6.676E-02	0.2097	0.0047	64.13	1.116E+00	1.678E-01
3399.472	6.275E-02	0.2142	0.0044	65.49	1.165E+00	1.652E-01
3605.743	5.916E-02	0.2183	0.0042	66.76	1.211E+00	1.626E-01
3814.210	5.593E-02	0.2221	0.0038	67.92	1.255E+00	1.601E-01
4025.321	5.300E-02	0.2257	0.0036	69.01	1.304E+00	1.581E-01
4238.877	5.033E-02	0.2291	0.0034	70.07	1.356E+00	1.566E-01
4454.329	4.789E-02	0.2325	0.0033	71.08	1.409E+00	1.551E-01
4672.924	4.565E-02	0.2356	0.0032	72.06	1.461E+00	1.535E-01
4893.666	4.359E-02	0.2387	0.0031	73	1.518E+00	1.527E-01

Appendix Table 5 (Continued)

Pressure	Pore Diameter	Volume Intruded	Delta Volume	% Volume Intruded	Dv(d)	-dV/d(log d)
[PSI]	[µm]	[cc/g]	[cc/g]	%	[cc/(µm-g)]	[cc/g]
5116.901	4.169E-02	0.2417	0.0030	73.91	1.583E+00	1.524E-01
5342.033	3.993E-02	0.2446	0.0029	74.78	1.653E+00	1.526E-01
5568.861	3.831E-02	0.2473	0.0027	75.61	1.722E+00	1.526E-01
5797.386	3.680E-02	0.2498	0.0026	76.39	1.785E+00	1.519E-01
6027.956	3.539E-02	0.2524	0.0026	77.19	1.847E+00	1.512E-01
6260.523	3.407E-02	0.2549	0.0025	77.96	1.908E+00	1.503E-01
6494.836	3.284E-02	0.2574	0.0025	78.71	1.968E+00	1.494E-01
6731.244	3.169E-02	0.2598	0.0024	79.44	2.028E+00	1.487E-01
6970.397	3.060E-02	0.262	0.0022	80.12	2.098E+00	1.486E-01
7211.246	2.958E-02	0.2642	0.0021	80.78	2.172E+00	1.486E-01
7453.392	2.862E-02	0.2662	0.0021	81.41	2.226E+00	1.473E-01
7697.634	2.771E-02	0.2682	0.0020	82.02	2.279E+00	1.460E-01
7943.872	2.685E-02	0.2702	0.0020	82.63	2.322E+00	1.442E-01
8192.056	2.604E-02	0.2722	0.0020	83.23	2.365E+00	1.424E-01
8442.685	2.527E-02	0.2741	0.0019	83.82	2.414E+00	1.410E-01
8695.209	2.453E-02	0.2759	0.0018	84.37	2.460E+00	1.394E-01
8949.530	2.384E-02	0.2776	0.0017	84.9	2.500E+00	1.375E-01
9206.146	2.317E-02	0.2793	0.0017	85.41	2.542E+00	1.359E-01
9464.660	2.254E-02	0.2809	0.0016	85.9	2.571E+00	1.336E-01
9724.669	2.194E-02	0.2825	0.0015	86.37	2.578E+00	1.303E-01
9986.724	2.136E-02	0.2839	0.0015	86.82	2.572E+00	1.266E-01
10251.274	2.081E-02	0.2853	0.0014	87.25	2.578E+00	1.235E-01
10517.970	2.028E-02	0.2867	0.0014	87.68	2.577E+00	1.203E-01
10786.761	1.978E-02	0.288	0.0013	88.08	2.584E+00	1.177E-01
11057.447	1.929E-02	0.2892	0.0012	88.45	2.593E+00	1.153E-01
11329.980	1.883E-02	0.2904	0.0011	88.79	2.603E+00	1.131E-01
11610.996	1.837E-02	0.2915	0.0011	89.13	2.612E+00	1.108E-01
11893.758	1.794E-02	0.2926	0.0011	89.46	2.631E+00	1.090E-01
12178.866	1.752E-02	0.2937	0.0011	89.8	2.639E+00	1.070E-01
12466.068	1.711E-02	0.2948	0.0011	90.13	2.658E+00	1.054E-01
12755.416	1.672E-02	0.2958	0.0011	90.46	2.695E+00	1.045E-01
13053.597	1.634E-02	0.2969	0.0010	90.77	2.742E+00	1.039E-01
13353.473	1.598E-02	0.2979	0.0010	91.08	2.782E+00	1.029E-01
13655.347	1.562E-02	0.2989	0.0010	91.39	2.825E+00	1.022E-01
13965.700	1.527E-02	0.2999	0.0010	91.7	2.835E+00	1.001E-01

Appendix Table 5 (Continued)

Pressure	Pore Diameter	Volume Intruded	Delta Volume	% Volume Intruded	Dv(d)	-dV/d(log d)
[PSI]	[µm]	[cc/g]	[cc/g]	%	[cc/(µm-g)]	[cc/g]
14284.885	1.493E-02	0.3009	0.0010	92	2.836E+00	9.784E-02
14613.303	1.460E-02	0.3019	0.0010	92.3	2.838E+00	9.557E-02
14937.528	1.428E-02	0.3028	0.0009	92.58	2.845E+00	9.361E-02
15264.100	1.398E-02	0.3036	0.0009	92.85	2.841E+00	9.142E-02
15592.418	1.368E-02	0.3044	0.0008	93.09	2.830E+00	8.914E-02
15922.530	1.340E-02	0.3052	0.0007	93.32	2.808E+00	8.658E-02
16255.140	1.312E-02	0.3059	0.0007	93.54	2.776E+00	8.388E-02
16582.906	1.286E-02	0.3066	0.0007	93.76	2.743E+00	8.126E-02
16913.020	1.261E-02	0.3073	0.0007	93.97	2.707E+00	7.865E-02
17245.279	1.237E-02	0.308	0.0007	94.17	2.684E+00	7.653E-02
17573.248	1.214E-02	0.3086	0.0006	94.35	2.697E+00	7.550E-02
17896.176	1.192E-02	0.3091	0.0006	94.53	2.714E+00	7.465E-02
18214.215	1.171E-02	0.3097	0.0005	94.69	2.732E+00	7.391E-02
18534.549	1.151E-02	0.3102	0.0005	94.85	2.759E+00	7.346E-02
18856.830	1.131E-02	0.3107	0.0005	95.01	2.796E+00	7.329E-02
19180.955	1.112E-02	0.3113	0.0005	95.18	2.862E+00	7.387E-02
19506.729	1.094E-02	0.3118	0.0005	95.34	2.934E+00	7.453E-02
19834.049	1.076E-02	0.3123	0.0005	95.5	3.026E+00	7.565E-02
20160.070	1.058E-02	0.3129	0.0005	95.67	3.108E+00	7.640E-02
20486.691	1.041E-02	0.3134	0.0005	95.83	3.218E+00	7.781E-02
20815.258	1.025E-02	0.314	0.0006	96.01	3.297E+00	7.838E-02
21145.369	1.009E-02	0.3145	0.0006	96.18	3.341E+00	7.809E-02
21476.730	9.933E-03	0.3151	0.0006	96.35	3.383E+00	7.774E-02
21809.986	9.781E-03	0.3156	0.0005	96.52	3.417E+00	7.720E-02
22144.443	9.633E-03	0.3162	0.0005	96.68	3.434E+00	7.635E-02
22480.693	9.489E-03	0.3167	0.0005	96.84	3.447E+00	7.544E-02
22818.689	9.349E-03	0.3171	0.0005	96.98	3.385E+00	7.292E-02
23159.180	9.211E-03	0.3176	0.0004	97.11	3.341E+00	7.089E-02
23501.320	9.077E-03	0.318	0.0004	97.24	3.282E+00	6.864E-02
23848.750	8.945E-03	0.3184	0.0004	97.37	3.295E+00	6.801E-02
24199.268	8.815E-03	0.3189	0.0004	97.5	3.269E+00	6.660E-02
24551.387	8.689E-03	0.3192	0.0004	97.61	3.267E+00	6.569E-02
24905.000	8.565E-03	0.3196	0.0004	97.72	3.319E+00	6.585E-02
25261.113	8.445E-03	0.32	0.0004	97.84	3.382E+00	6.621E-02
25618.969	8.327E-03	0.3204	0.0004	97.97	3.435E+00	6.634E-02

Appendix Table 5 (Continued)

Pressure	Pore Diameter	Volume Intruded	Delta Volume	% Volume Intruded	Dv(d)	-dV/d(log d)
[PSI]	[µm]	[cc/g]	[cc/g]	%	[cc/(µm-g)]	[cc/g]
25979.068	8.211E-03	0.3208	0.0004	98.1	3.492E+00	6.653E-02
26341.312	8.098E-03	0.3212	0.0004	98.22	3.540E+00	6.653E-02
26705.855	7.988E-03	0.3216	0.0004	98.35	3.641E+00	6.742E-02
27071.795	7.880E-03	0.3221	0.0004	98.48	3.723E+00	6.791E-02
27440.080	7.774E-03	0.3225	0.0004	98.61	3.785E+00	6.800E-02
27810.457	7.671E-03	0.3229	0.0004	98.73	3.734E+00	6.614E-02
28182.486	7.569E-03	0.3233	0.0004	98.85	3.747E+00	6.544E-02
28556.557	7.470E-03	0.3236	0.0004	98.96	3.746E+00	6.453E-02
28933.170	7.373E-03	0.324	0.0004	99.08	3.708E+00	6.303E-02
29312.086	7.278E-03	0.3244	0.0003	99.18	3.675E+00	6.170E-02
29692.545	7.184E-03	0.3246	0.0003	99.27	3.588E+00	5.940E-02
30075.299	7.093E-03	0.325	0.0003	99.37	3.541E+00	5.790E-02
30459.850	7.003E-03	0.3253	0.0003	99.47	3.552E+00	5.745E-02
30845.998	6.916E-03	0.3256	0.0003	99.56	3.520E+00	5.624E-02
31231.336	6.830E-03	0.3259	0.0003	99.66	3.530E+00	5.542E-02
31618.969	6.747E-03	0.3261	0.0002	99.73	3.558E+00	5.487E-02
32009.240	6.664E-03	0.3264	0.0003	99.81	3.650E+00	5.525E-02
32402.844	6.583E-03	0.3268	0.0003	99.91	3.678E+00	5.470E-02
32797.840	6.504E-03	0.327	0.0003	100.00	3.715E+00	5.428E-02

Appendix Table 6 Pore Size Distribution By Volume – Intrusion for GS-50/2-Steam curing

Pressure	Pore Diameter	Volume Intruded	Delta Volume	% Volume Intruded	Dv(d)	-dV/d(log d)
[PSI]	[µm]	[cc/g]	[cc/g]	%	[cc/(µm-g)]	[cc/g]
1.198	1.780E+02	0	0	0	7.647E-06	4.295E-03
1.53	1.395E+02	0.0014	0.0014	0.57	9.554E-06	4.536E-03
1.889	1.129E+02	0.0018	0.0004	0.72	1.364E-05	4.260E-03
2.26	9.438E+01	0.002	0.0002	0.82	1.847E-05	4.044E-03
2.56	8.332E+01	0.0022	0.0002	0.88	2.314E-05	3.884E-03
2.88	7.406E+01	0.0023	0.0001	0.94	2.763E-05	3.777E-03
3.218	6.629E+01	0.0026	0.0003	1.05	3.562E-05	4.007E-03
3.569	5.978E+01	0.0027	0.0001	1.1	2.422E-05	2.970E-03
3.909	5.457E+01	0.0028	0.0001	1.13	2.420E-05	2.770E-03
4.261	5.006E+01	0.0029	0.0001	1.17	2.533E-05	2.665E-03
4.607	4.630E+01	0.003	0.0001	1.21	2.618E-05	2.534E-03
4.949	4.311E+01	0.003	0.0001	1.24	2.757E-05	2.464E-03
5.306	4.020E+01	0.0031	0.0001	1.26	2.262E-05	1.976E-03
5.678	3.757E+01	0.0031	0.0001	1.28	2.263E-05	1.824E-03
6.049	3.527E+01	0.0032	0.0001	1.31	2.242E-05	1.675E-03
6.4	3.333E+01	0.0032	0	1.32	2.097E-05	1.453E-03
6.734	3.168E+01	0.0033	0	1.34	1.848E-05	1.207E-03
7.068	3.018E+01	0.0033	0	1.34	1.574E-05	9.775E-04
7.402	2.882E+01	0.0033	0	1.35	1.403E-05	8.203E-04
7.736	2.758E+01	0.0033	0	1.35	1.192E-05	6.586E-04
8.052	2.649E+01	0.0033	0	1.35	9.213E-06	4.853E-04
8.35	2.555E+01	0.0033	0	1.35	6.742E-06	3.398E-04
8.65	2.466E+01	0.0033	0	1.35	3.621E-06	1.781E-04
8.95	2.384E+01	0.0033	0	1.35	2.589E-06	1.215E-04
9.249	2.306E+01	0.0033	0	1.35	1.384E-06	6.214E-05
9.565	2.230E+01	0.0033	0	1.35	0.000E+00	0.000E+00
9.897	2.156E+01	0.0033	0	1.35	0.000E+00	0.000E+00
10.244	2.082E+01	0.0033	0	1.35	0.000E+00	0.000E+00
10.572	2.018E+01	0.0033	0	1.35	0.000E+00	0.000E+00
10.883	1.960E+01	0.0033	0	1.35	2.215E-06	1.161E-04
11.192	1.906E+01	0.0033	0	1.35	4.685E-06	2.347E-04
11.502	1.855E+01	0.0033	0	1.35	7.436E-06	3.566E-04
11.827	1.804E+01	0.0033	0	1.35	1.311E-05	6.061E-04
12.135	1.758E+01	0.0033	0	1.35	1.941E-05	8.626E-04

Appendix Table 6 (Continued)

Pressure	Pore Diameter	Volume Intruded	Delta Volume	% Volume Intruded	Dv(d)	-dV/d(log d)
[PSI]	[µm]	[cc/g]	[cc/g]	%	[cc/(µm-g)]	[cc/g]
12.424	1.717E+01	0.0033	0	1.36	2.627E-05	1.125E-03
12.715	1.678E+01	0.0033	0	1.36	3.368E-05	1.393E-03
13.004	1.640E+01	0.0034	0	1.37	4.171E-05	1.668E-03
13.293	1.605E+01	0.0034	0	1.38	5.003E-05	1.934E-03
13.58	1.571E+01	0.0034	0	1.39	5.936E-05	2.222E-03
13.866	1.538E+01	0.0034	0	1.4	8.052E-05	2.957E-03
14.152	1.507E+01	0.0035	0	1.41	9.566E-05	3.441E-03
14.438	1.478E+01	0.0035	0	1.42	1.119E-04	3.936E-03
14.738	1.447E+01	0.0035	0	1.43	1.294E-04	4.442E-03
15.021	1.420E+01	0.0035	0	1.45	1.394E-04	4.673E-03
15.303	1.394E+01	0.0036	0.0001	1.47	1.497E-04	4.907E-03
15.585	1.369E+01	0.0037	0.0001	1.49	1.604E-04	5.145E-03
15.866	1.344E+01	0.0037	0.0001	1.51	1.717E-04	5.386E-03
16.146	1.321E+01	0.0038	0.0001	1.54	1.835E-04	5.633E-03
16.424	1.299E+01	0.0038	0	1.55	1.963E-04	5.898E-03
16.701	1.277E+01	0.0038	0	1.57	2.091E-04	6.150E-03
16.978	1.256E+01	0.0039	0	1.58	1.881E-04	5.415E-03
17.254	1.236E+01	0.0039	0	1.6	1.712E-04	4.814E-03
17.529	1.217E+01	0.004	0	1.62	1.527E-04	4.201E-03
17.802	1.198E+01	0.004	0	1.63	1.326E-04	3.573E-03
18.075	1.180E+01	0.004	0	1.65	1.174E-04	3.093E-03
18.347	1.163E+01	0.004	0	1.65	1.010E-04	2.602E-03
18.635	1.145E+01	0.004	0	1.65	8.346E-05	2.102E-03
18.907	1.128E+01	0.004	0	1.65	6.466E-05	1.592E-03
19.178	1.112E+01	0.004	0	1.65	4.444E-05	1.072E-03
19.433	1.098E+01	0.004	0	1.65	2.287E-05	5.406E-04
19.673	1.084E+01	0.004	0	1.65	0.000E+00	0.000E+00
19.928	1.070E+01	0.004	0	1.65	8.670E-06	2.291E-04
20.197	1.056E+01	0.004	0	1.65	1.786E-05	4.625E-04
20.465	1.042E+01	0.004	0	1.65	2.710E-05	6.873E-04
20.718	1.030E+01	0.004	0	1.65	3.685E-05	9.167E-04
20.97	1.017E+01	0.004	0	1.65	4.708E-05	1.150E-03
21.222	1.005E+01	0.004	0	1.65	5.738E-05	1.376E-03
21.473	9.934E+00	0.0041	0	1.66	6.347E-05	1.493E-03
21.736	9.814E+00	0.0041	0	1.66	6.839E-05	1.582E-03

Appendix Table 6 (Continued)

Pressure	Pore Diameter	Volume Intruded	Delta Volume	% Volume Intruded	Dv(d)	-dV/d(log d)
[PSI]	[µm]	[cc/g]	[cc/g]	%	[cc/(µm-g)]	[cc/g]
21.997	9.698E+00	0.0041	0	1.67	7.644E-05	1.775E-03
22.257	9.584E+00	0.0041	0	1.68	8.308E-05	1.962E-03
22.529	9.469E+00	0.0041	0	1.68	8.915E-05	2.185E-03
23.567	9.052E+00	0.0041	0	1.69	8.662E-05	2.265E-03
26.471	8.059E+00	0.0042	0	1.71	9.255E-05	2.478E-03
32.688	6.526E+00	0.0044	0.0002	1.79	1.175E-04	2.955E-03
45.325	4.706E+00	0.0047	0.0003	1.91	1.838E-04	3.755E-03
68.325	3.122E+00	0.0051	0.0004	2.09	3.494E-04	5.075E-03
104.582	2.040E+00	0.0057	0.0006	2.35	7.234E-04	6.949E-03
156.525	1.363E+00	0.0066	0.0009	2.7	1.640E-03	9.679E-03
224.605	9.498E-01	0.0078	0.0012	3.19	3.598E-03	1.326E-02
309.221	6.899E-01	0.0094	0.0016	3.84	6.828E-03	1.749E-02
410.787	5.193E-01	0.0115	0.0021	4.7	1.254E-02	2.292E-02
529.241	4.031E-01	0.014	0.0025	5.74	2.208E-02	2.960E-02
664.061	3.212E-01	0.0171	0.0031	7	3.712E-02	3.749E-02
814.248	2.620E-01	0.0207	0.0036	8.46	5.989E-02	4.687E-02
978.257	2.181E-01	0.0246	0.0039	10.05	9.216E-02	5.742E-02
1153.393	1.850E-01	0.029	0.0044	11.86	1.360E-01	6.905E-02
1335.515	1.597E-01	0.0338	0.0048	13.83	1.919E-01	8.152E-02
1521.977	1.402E-01	0.0389	0.0051	15.93	2.611E-01	9.475E-02
1710.984	1.247E-01	0.0444	0.0055	18.17	3.426E-01	1.083E-01
1901.537	1.122E-01	0.0501	0.0057	20.49	4.371E-01	1.224E-01
2092.890	1.019E-01	0.0559	0.0058	22.87	5.455E-01	1.367E-01
2285.389	9.334E-02	0.0618	0.0059	25.28	6.633E-01	1.504E-01
2479.835	8.602E-02	0.0678	0.006	27.72	7.916E-01	1.639E-01
2674.780	7.975E-02	0.0737	0.0059	30.15	9.290E-01	1.769E-01
2871.071	7.430E-02	0.0797	0.006	32.6	1.069E+00	1.886E-01
3069.159	6.951E-02	0.0857	0.006	35.04	1.215E+00	1.996E-01
3269.043	6.526E-02	0.0915	0.0058	37.43	1.365E+00	2.098E-01
3470.923	6.146E-02	0.0974	0.0058	39.82	1.514E+00	2.184E-01
3674.649	5.805E-02	0.1031	0.0058	42.18	1.663E+00	2.259E-01
3880.023	5.498E-02	0.1087	0.0056	44.47	1.814E+00	2.328E-01
4087.791	5.219E-02	0.1143	0.0056	46.74	1.959E+00	2.383E-01
4298.703	4.962E-02	0.1198	0.0055	48.98	2.103E+00	2.428E-01
4511.959	4.728E-02	0.125	0.0052	51.12	2.246E+00	2.466E-01

Appendix Table 6 (Continued)

Pressure	Pore Diameter	Volume Intruded	Delta Volume	% Volume Intruded	Dv(d)	-dV/d(log d)
[PSI]	[µm]	[cc/g]	[cc/g]	%	[cc/(µm-g)]	[cc/g]
4726.463	4.513E-02	0.1301	0.0051	53.19	2.377E+00	2.487E-01
4943.911	4.315E-02	0.1351	0.0050	55.24	2.502E+00	2.500E-01
5163.504	4.131E-02	0.1399	0.0048	57.21	2.623E+00	2.506E-01
5385.493	3.961E-02	0.1446	0.0047	59.12	2.723E+00	2.490E-01
5609.577	3.803E-02	0.1491	0.0045	60.97	2.809E+00	2.462E-01
5835.706	3.655E-02	0.1533	0.0042	62.7	2.893E+00	2.434E-01
6064.181	3.518E-02	0.1575	0.0041	64.4	2.965E+00	2.396E-01
6294.752	3.389E-02	0.1614	0.0039	66	3.012E+00	2.342E-01
6527.667	3.268E-02	0.165	0.0036	67.48	3.052E+00	2.287E-01
6761.731	3.155E-02	0.1684	0.0034	68.86	3.077E+00	2.224E-01
6998.089	3.048E-02	0.1716	0.0032	70.18	3.093E+00	2.160E-01
7236.942	2.948E-02	0.1747	0.0031	71.43	3.103E+00	2.096E-01
7478.291	2.853E-02	0.1775	0.0028	72.58	3.092E+00	2.022E-01
7721.934	2.763E-02	0.1802	0.0027	73.68	3.079E+00	1.951E-01
7967.573	2.677E-02	0.1827	0.0026	74.73	3.083E+00	1.895E-01
8215.158	2.597E-02	0.1852	0.0024	75.73	3.089E+00	1.843E-01
8464.839	2.520E-02	0.1875	0.0023	76.67	3.089E+00	1.790E-01
8716.864	2.447E-02	0.1896	0.0021	77.53	3.092E+00	1.742E-01
8970.486	2.378E-02	0.1916	0.0021	78.38	3.110E+00	1.704E-01
9226.005	2.312E-02	0.1937	0.002	79.2	3.112E+00	1.658E-01
9484.069	2.249E-02	0.1956	0.002	80	3.114E+00	1.614E-01
9744.129	2.189E-02	0.1975	0.0019	80.77	3.111E+00	1.569E-01
10006.582	2.132E-02	0.1993	0.0018	81.51	3.106E+00	1.525E-01
10271.133	2.077E-02	0.2011	0.0018	82.23	3.115E+00	1.489E-01
10537.978	2.024E-02	0.2027	0.0016	82.88	3.119E+00	1.452E-01
10806.919	1.974E-02	0.2042	0.0015	83.5	3.105E+00	1.410E-01
11078.005	1.926E-02	0.2056	0.0015	84.1	3.076E+00	1.362E-01
11351.236	1.879E-02	0.207	0.0014	84.65	3.045E+00	1.316E-01
11632.103	1.834E-02	0.2083	0.0013	85.2	3.004E+00	1.267E-01
11915.812	1.790E-02	0.2096	0.0013	85.74	2.950E+00	1.215E-01
12201.419	1.748E-02	0.2109	0.0012	86.24	2.910E+00	1.170E-01
12496.006	1.707E-02	0.212	0.0011	86.71	2.871E+00	1.127E-01
12792.790	1.668E-02	0.2131	0.0011	87.16	2.828E+00	1.084E-01
13091.368	1.629E-02	0.2142	0.001	87.58	2.795E+00	1.047E-01
13391.794	1.593E-02	0.2151	0.001	87.98	2.751E+00	1.007E-01

Appendix Table 6 (Continued)

Pressure	Pore Diameter	Volume Intruded	Delta Volume	% Volume Intruded	Dv(d)	-dV/d(log d)
[PSI]	[µm]	[cc/g]	[cc/g]	%	[cc/(µm-g)]	[cc/g]
13700.652	1.557E-02	0.216	0.0009	88.36	2.711E+00	9.720E-02
14011.655	1.522E-02	0.2169	0.0009	88.72	2.693E+00	9.457E-02
14331.241	1.489E-02	0.2178	0.0009	89.07	2.698E+00	9.282E-02
14660.006	1.455E-02	0.2187	0.0009	89.43	2.712E+00	9.134E-02
14992.017	1.423E-02	0.2195	0.0008	89.76	2.729E+00	8.997E-02
15326.069	1.392E-02	0.2203	0.0008	90.09	2.766E+00	8.922E-02
15662.422	1.362E-02	0.2211	0.0008	90.44	2.803E+00	8.848E-02
15994.181	1.334E-02	0.222	0.0008	90.78	2.848E+00	8.804E-02
16327.938	1.306E-02	0.2228	0.0008	91.12	2.905E+00	8.796E-02
16664.188	1.280E-02	0.2236	0.0008	91.44	2.956E+00	8.762E-02
17002.385	1.255E-02	0.2244	0.0008	91.76	3.014E+00	8.746E-02
17336.490	1.230E-02	0.2251	0.0007	92.05	3.042E+00	8.641E-02
17672.889	1.207E-02	0.2258	0.0007	92.35	3.042E+00	8.465E-02
18004.900	1.185E-02	0.2265	0.0007	92.64	3.028E+00	8.263E-02
18331.920	1.164E-02	0.2272	0.0007	92.91	3.006E+00	8.053E-02
18654.100	1.144E-02	0.2278	0.0006	93.16	2.987E+00	7.862E-02
18978.027	1.124E-02	0.2283	0.0006	93.39	2.974E+00	7.701E-02
19303.549	1.105E-02	0.2289	0.0005	93.6	2.967E+00	7.558E-02
19631.117	1.087E-02	0.2294	0.0005	93.81	2.939E+00	7.364E-02
19960.482	1.069E-02	0.2299	0.0005	94.01	2.904E+00	7.162E-02
20291.246	1.051E-02	0.2303	0.0005	94.21	2.882E+00	6.995E-02
20620.262	1.035E-02	0.2308	0.0005	94.41	2.853E+00	6.820E-02
20950.076	1.018E-02	0.2313	0.0005	94.61	2.854E+00	6.715E-02
21281.637	1.002E-02	0.2318	0.0004	94.79	2.871E+00	6.651E-02
21614.545	9.869E-03	0.2322	0.0004	94.97	2.880E+00	6.567E-02
21949.498	9.719E-03	0.2326	0.0004	95.15	2.893E+00	6.495E-02
22285.752	9.572E-03	0.2331	0.0004	95.32	2.918E+00	6.454E-02
22623.998	9.429E-03	0.2335	0.0004	95.49	2.935E+00	6.399E-02
22964.439	9.289E-03	0.2339	0.0004	95.65	2.948E+00	6.339E-02
23306.877	9.153E-03	0.2343	0.0004	95.81	2.992E+00	6.343E-02
23651.010	9.020E-03	0.2347	0.0004	95.97	3.028E+00	6.326E-02
23997.488	8.889E-03	0.2351	0.0004	96.13	3.071E+00	6.327E-02
24349.557	8.761E-03	0.2355	0.0004	96.3	3.139E+00	6.375E-02
24704.270	8.635E-03	0.2359	0.0004	96.47	3.209E+00	6.425E-02
25060.877	8.512E-03	0.2363	0.0004	96.63	3.262E+00	6.438E-02

Appendix Table 6 (Continued)

Pressure	Pore Diameter	Volume Intruded	Delta Volume	% Volume Intruded	Dv(d)	-dV/d(log d)
[PSI]	[µm]	[cc/g]	[cc/g]	%	[cc/(µm-g)]	[cc/g]
25419.482	8.392E-03	0.2367	0.0004	96.79	3.343E+00	6.504E-02
25780.082	8.275E-03	0.2371	0.0004	96.96	3.453E+00	6.625E-02
26143.477	8.160E-03	0.2375	0.0004	97.12	3.529E+00	6.675E-02
26508.318	8.047E-03	0.2379	0.0004	97.29	3.607E+00	6.731E-02
26875.250	7.937E-03	0.2383	0.0004	97.45	3.727E+00	6.863E-02
27244.188	7.830E-03	0.2387	0.0004	97.61	3.810E+00	6.921E-02
27614.967	7.725E-03	0.2391	0.0004	97.79	3.935E+00	7.052E-02
27987.293	7.622E-03	0.2395	0.0004	97.96	4.063E+00	7.185E-02
28361.914	7.521E-03	0.2399	0.0004	98.12	4.163E+00	7.264E-02
28738.680	7.423E-03	0.2404	0.0004	98.31	4.253E+00	7.321E-02
29117.045	7.326E-03	0.2408	0.0004	98.48	4.356E+00	7.395E-02
29497.904	7.232E-03	0.2412	0.0004	98.65	4.492E+00	7.527E-02
29880.551	7.139E-03	0.2417	0.0004	98.84	4.561E+00	7.544E-02
30264.852	7.049E-03	0.2421	0.0004	99.01	4.595E+00	7.491E-02
30651.801	6.960E-03	0.2425	0.0004	99.18	4.572E+00	7.345E-02
31040.242	6.872E-03	0.2429	0.0004	99.34	4.343E+00	6.865E-02
31427.156	6.788E-03	0.2433	0.0004	99.52	4.400E+00	6.827E-02
31817.420	6.705E-03	0.2438	0.0004	99.69	4.416E+00	6.728E-02
32210.119	6.623E-03	0.2441	0.0003	99.83	4.389E+00	6.569E-02
32605.922	6.542E-03	0.2444	0.0003	99.95	4.365E+00	6.416E-02
33002.562	6.464E-03	0.2445	0.0001	100	4.323E+00	6.242E-02

CURRICULUM VITAE

NAME : Mr. Muhammad Ilyas

BIRTH DATE : March 8, 1978

BIRTH PLACE : Quetta, Pakistan

EDUCATION	**: YEAR**	**INSTITUTE**	**DEGREE/DIPLOMA**
	2003	NWFP Univ. of Engg & Techn. Pakistan.	B. in Civil Engineering

POSITION/TITLE **: Assistant Engineer**

WORK PLACE **: Communication and Works Department, Government of Baluchistan, Pakistan**

SCHOLARSHIP/AWARDS **: Royal Thai Government Scholarship 2009**